Wilfrid Laurier University

Scholars Commons @ Laurier

Theses and Dissertations (Comprehensive)

2016

Partitioning Evapotranspiration in Forested Peatlands within the Western Boreal Plain, Fort McMurray, Alberta, Canada

Elise C. Gabrielli
gabr3950@mylaurier.ca

Follow this and additional works at: https://scholars.wlu.ca/etd

 Part of the Hydrology Commons

Recommended Citation

Gabrielli, Elise C., "Partitioning Evapotranspiration in Forested Peatlands within the Western Boreal Plain, Fort McMurray, Alberta, Canada" (2016). *Theses and Dissertations (Comprehensive)*. 1820.
https://scholars.wlu.ca/etd/1820

This Thesis is brought to you for free and open access by Scholars Commons @ Laurier. It has been accepted for inclusion in Theses and Dissertations (Comprehensive) by an authorized administrator of Scholars Commons @ Laurier. For more information, please contact scholarscommons@wlu.ca.

Partitioning Evapotranspiration in Forested Peatlands within the Western Boreal Plain, Fort McMurray, Alberta, Canada

by

Elise Catherine Gabrielli
Honours B.A. with Administration Option,
Wilfrid Laurier University, 2012

THESIS
Submitted to the Department of Geography and Environmental Studies
in partial fulfillment of the requirements for
Degree in Masters of Science
Wilfrid Laurier University

© Elise Catherine Gabrielli 2016

Author's Declaration

I hereby declare that I am the sole author of this thesis. This is a true copy of the thesis, including any required final revisions, as accepted by my examiners.

I understand that my thesis may be made electronically available to the public.

Abstract

Forested peatlands in the Western Boreal Plain (WBP) represent hydrologically sensitive ecosystems that often support an open-crown forest of *Picea mariana* and/or *Larix laricina*. These systems store globally significant soil carbon, containing one-fourth to one-third of the world's soil organic carbon pool (Turunen *et al*., 2002), serving a critical role in regulating atmospheric CO_2. Recent studies indicate that the hydrological conditions are the critical determinant of a peatland's carbon budget (Price *et al*., 2005; Aurela *et al*., 2007). To understand current hydrological conditions, it is essential to accurately estimate the rate of *ET*, due to its dominance within a peatland's water balance (Price and Maloney, 1994; Fraser *et al*., 2001; Lafleur, 2008). The mechanism by which peatlands retain and exchange water with the atmosphere is important to maintain the stability of these systems. However, this stability is threatened by the impacts of both warmer and drier conditions associated with climate change, and altered hydroclimatic cycles as a result of landscape disturbance. Increasing drought (frequency and severity) has the potential to increase tree growth, modifying density, size and spatial arrangement of the trees (Kettridge *et al*., 2013). This expansion impedes incoming solar radiation from reaching the peat surface, potentially limiting surface evapotranspiration (*ET*), which at present, represents the main flux water loss from these systems. A reduction in surface *ET* (ET_{surf}) could further produce a reduction in total fen *ET*, despite predicted increases in canopy transpiration (*T*) attributed to the higher stem density.

This research partitions *ET* between the canopy and understory between two typical fens, under current climate conditions, within the oil sands region of Fort McMurray, Alberta. The effects of climate, tree canopy and surface vegetation on the energy balance and *ET* processes were analyzed using a micrometeorology (MET) and eddy-covariance (EC) data in two typical Western Boreal Plain (WBP) fens during the growing 2013 season. Flux data were partitioned through the application of the stem heat balance (SHB) method and dynamic closed chambers. The two fens are distinguished as a poor fen with an open canopy composed of *Picea mariana*, and a rich fen, with a dense *Larix laricina* canopy. Additionally, the two fens are distinguished by differences in localized climate, with the poor fen subjected to significantly cooler air (T_a) and soil (T_g) temperatures.

The energy balance of both fens was regulated by the latent heat flux (Q_E). The seasonal pattern of *ET* was closely linked with growing season net radiation (Q^*), vapour pressure deficit

(*VPD*), T_a and precipitation (*P*) events, averaging 2.3 mm d^{-1} and 3.5 mm d^{-1} between the poor, open canopy fen and rich, dense canopy fen, respectively. A strong, positive linear correlation was exhibited between the control parameters Q^*, T_a, and daily transpiration (*T*). Seasonal mean *T* rates varied over the four month growing season at the *Picea mariana* poor fen, averaging 0.3 mm d^{-1}, while *T* rates at the *Larix laricina* rich fen supplied a higher contribution to the fen's total *ET* flux, averaging 2.7 mm d^{-1}. Both *ET* and *T* reached maxima in conditions of high Q^*, T_a, and moderate to high *VPD*, that coincided with lower relative humidity (*RH*) and moderate windspeed (*u*). Neither *ET* nor *T* demonstrated a direct relationship with volumetric moisture content (*VMC*), due to the consistently high water table, generally at or above the peat surface, maintained at both sites.

The poor fen's discontinuous *Picea mariana* canopy permitted a larger degree of incoming radiation to reach the underlying peat surface, while the rich fen's higher tree density composed of the *Larix laricina*, limited incoming radiation due to shading. Subsequently, surface vegetation of the former was dominated by *Sphagnum* moss, while the latter was composed of a variety of feather moss and the brown moss, *Tomenthypnum nitens*. The poor fen's open canopy and dominant *Sphagnum* moss resulted in the dominance of the ET_{surf}, with a mean of 0.8 mm d^{-1}, contributing approximately > 80% to the daily *ET* budget. Conversely, the rich fen's dense canopy diminished the impact of ET_{surf} to 0.5 mm d^{-1}, contributing < 20% to the total *ET* flux. Increased tree density from a *Picea mariana* open-canopy, to a *Larix laricina* dense canopy, reduced average *PAR* reaching the underlying surface to < 500 μmol m^{-2} s^{-1} and < 300 μmol m^{-2} s^{-1}. Although the presence of an overstory did not produce a microclimate that was statistically different between open and covered plot conditions, it did generally support cooler, wet conditions that inhibited ET_{surf}.

Acknowledgements

First and foremost I would like to extend my sincerest gratitude to my supervisor, Dr. Richard Petrone for your patient support, guidance and invaluable mentorship over the past few years.

It started with one simple slide at the beginning of an undergraduate hydrology class with Dr. Fereidoun Rezanezhad, detailing an oil sands project in Fort McMurray, Alberta. Little known to me, how one simple inquiry would dramatically alter the next several years, pushing myself to new limits, reshaping me as an academic and on an individual level.

I could not have achieved this without the incredible support of the staff and students of the Fort Mac team. I cannot express enough thanks to George Sutherland for continually solving all my data problems, seemingly using just a little 'black magic' to resolve any issue I threw his way. Many thanks for the tremendous guidance in data collection from Justin Straker and Trevor Baker at IEG Consulting, as you navigated me through the world of sapflow. And a very special thanks to the incredible assistance from Laura Chasmer, generously sharing your knowledge of LiDAR and classification methodologies.

I cannot express enough thanks to my colleagues that not only spent long days in the field assisting in data collection, but provided countless laughs while creating so many fond memories. Tahni Phillips, Meagan Wood and Carolina Spagnuolo, you kindly and patiently showed me the ropes as I started my first summer in Fort Mac. My sincere thanks to Josh Feener and Tristan Gingras-Hill for keeping me sane with countless burritos, allowing me to blast my old-school country music and conveniently keeping chocolate in the truck for those especially trying days.

It goes without saying, I wouldn't be where I am today without the constant emotional support of my friends and family. To my parents who have been my biggest cheerleaders throughout all my educational purists. I cannot express how grateful I am for all your guidance and unwavering support. Whether it was just a simple pep talk or calm words of encouragement, you've always believed in me and in turn, taught me to believe in myself. To my sister Olivia, you were my port in the storm. Gestures big or small, you were there with constant words of encouragement, food when I was harnessed to my desk, and to accompany me on numerous late night drives. Living in Waterloo would not have been nearly as much fun without you. Last but not least, I would like to thank my patient best friend and partner in crime, Martin Schroder, who has been by my side from early undergrad days, through my seemingly endless academic career.

I am forever humbled to have met and worked with so many amazing individuals and express my sincere gratitude.

Table of Contents

List of Figures

List of Tables

Chapter One
Introduction

Canada's Western Boreal Plains (WBP) ecozone represents an extremely diverse landscape consisting of coniferous and mixed-wood forests and a variety of wetland types (Vitt *et al*., 2003), extending across Alberta to Manitoba (National Working Group, 1988). In this region wetlands account for 65% of the landscape, with bog and fen peatlands representing the dominant wetland class despite a sub-humid climate (Woynillowicz *et al*., 2005). From a global perspective, although only covering 3% of the terrestrial land surface (Yu, 2012), peatlands store approximately 30% of soil carbon (Limpens *et al*., 2014; Gorham, 1991; Limpens *et al*., 2008).

The WBP is composed of three common landforms including coarse-grained glaciofluvial outwash deposits, fine-grained disintegration moraines and low-lying glaciolacustrine plains (Devito *et al*., 2005a). Peatlands persist primarily in areas of poor drainage supported by enhanced groundwater flow from glacial deposits in addition to direct precipitation input (Devito and Mendoza, 2007). Moreover, it is the persistence of water-deficit conditions that shapes the unique hydrology of the WBP. Peatland hydrology, ecological functioning, and development are largely dependent on the local energy balance and whether precipitation (*P*) is balanced by evapotranspiration (*ET*) (Runkle *et al*., 2014). The WBP peatlands exist within a sub-humid climate where *P* is less than or equivalent to potential evapotranspiration (*PET*) (van der Kamp., 2003; Devito *et al.*, 2005b; Brown *et al.*, 2010), therefore *ET* constitutes a dominant hydrological flux (Bridgham *et al.*, 1999; Eaton *et al.*, 2001; Johnson and Miyanishi, 2008). It is the dominance of *ET* and persistence of a sub-humid climate that suggest that these peatland systems may be the most sensitive to any climatic variability (Petrone *et al.*, 2011). Previous research has suggested that climate-induced expansion of trees and shrubs has the potential to turn these ecosystems from net carbon sinks into sources when associated with reduced water tables. Increased water loss

through canopy transpiration (*T*) could further draw down water tables, thus stimulating peat decomposition and carbon release (Limpens *et al*., 2014). It is evident that future climate change scenarios may have profound effects on the maintenance of these systems, altering their capacity to store carbon.

Further threatening these peatland systems, is the rapid development of natural resource based industries that affect vast areas of the WBP. Specifically, mining practices within the oil sands region of Fort McMurray, Alberta have caused significant disturbance and/or the complete removal of vast areas of wetland (Alberta Environmental Protection, 1998). The Athabasca deposit surrounds the city of Fort McMurray, and encompasses approximately 475,000 ha of boreal Alberta, of which 99% is already leased (Rooney *et al*., 2012). Open-pit mining involves the complete removal of peat layers, leaving landscapes with very large pits up to 100 m in depth (Johnson and Miyanishi, 2008). Constraints imposed by the post-mining landscape coupled with the sensitivity of peatland vegetation prevent the natural restoration of the pre-mined landscape (Rooney *et al*., 2012). Threats imposed by climate change will further complicate the future trajectories of these systems.

Previous hydrologic research has shown that temporal climate patterns exert a strong control on the hydrologic processes driving wetland sustainability, vegetation patterns and regional groundwater recharge (Ferone and Devito, 2004; Devito *et al*., 2005b; Smerdon *et al*., 2005; Petrone *et al*., 2007; Smerdon *et al*., 2007). Recent attention has focused on the interactions between hydrology and the carbon cycle within peatland environments, and there is a general consensus that the hydrological cycle is an important first-order control to carbon fluxes, changes in vegetation cover, and microtopographic patterning (Billett *et al*., 2004; Couwenberg and Joosten, 2005; Limpens *et al*., 2008). Thus, quantifying impacts caused by anthropogenic

development requires a detailed understanding of the natural variability of the hydrologic processes (especially *ET*) and water cycling unique to this region, under past, present and future climatic conditions (Comer *et al*., 2000; Cleugh *et al.*, 2007; Raddatz *et al*., 2009). This requires a better understanding of the driving factors and controls on *ET*. This study focuses on the processes controlling the surface energy and water budgets within two relatively undisturbed peatlands in the Fort McMurray region.

Peatland surface vegetation exerts a significant control on the hydrology and microclimate of the system (Oechel and Van Cleve, 1986; Bisbee *et al*., 2001; Heijmans *et al*., 2001), integrating a range of environmental controls that influence the spatial variability of carbon exchange processes (Waddington and Roulet, 1996; Swanson and Flanagan, 2001; Bubier *et al*., 2003). This is especially significant within black spruce (*Picea mariana*) dominated peatlands, which represent the most widespread boreal forest system in North America (Oechel and Van Cleve, 1986). Because black spruce cover is relatively open due to the narrow structure and low density of the trees (Heijmans *et al*., 2004), a substantial portion of incoming solar radiation is able to reach the underlying peat surface, often dominated by *Sphagnum* species. Thus, the understory/surface vegetation exerts a significant role on the system's CO_2 (Goulden *et al*., 1997; Waddington *et al*., 1998) and water exchange (Williams and Flanagan, 1996). As such, moss evaporation rates are strongly dependent on the openness of forest canopy (Heijmans *et al*., 2004).

This study seeks to characterize the typical partitioning of *ET* among ecosystem components within two typical WBP fens, and determine how the partitioning of *ET* varies with the density and spatial organization of the trees. Souch *et al*. (1996) conclude that our understanding of *ET* and the related physical processes are not well characterized for many wetland types. Drexler *et al*. (2004) further state that despite the numerous methods available to quantify

wetland *ET*, it remains insufficiently characterized due to the diversity and complexity of wetland types. Therefore, this research will not only reduce uncertainty surrounding wetland *ET*, but understanding how the components of these systems contribute to the overall *ET* flux is essential to understand how a peatland ecosystem may respond to both climate change and anthropogenic disturbance. Further, such information will form a baseline study for future fen reclamation projects. Specifically, the first objective is to quantify the ecosystem scale energy and *ET* budgets of each fen throughout the growing season. The second objective seeks to understand the climatic and vegetational controls governing ecosystem scale *ET* and *T* via a comparison of two fens with distinct differences in canopy cover. The third objective will examine how surface microclimate and ET_{surf} varies within varying degrees of canopy cover. Lastly, the fourth objective will partition *ET* flux components between peat surface and canopy.

This thesis follows the manuscript format and has been organized into seven chapters including this introduction, which provides a brief overview of the research objectives and questions. General background information on relevant research in the WBP, the nature of *ET* in the WBP and a future climate change scenario, as well as, study rationale and site description are provided in Chapter two. Chapter three details the applied field and lab methods including the use of micrometeorological (MET) measurements, and the eddy covariance (EC) technique to measure ecosystem scale energy balance and *ET* data. An estimation of canopy transpiration (*T*) was obtained through the application of the stem heat balance (SHB) method. The use of dynamic closed chambers was used to characterize ET_{surf}. Forest inventory surveys and LiDAR derived land surface classification was employed to scale flux data to the fen boundary. Chapter four summarizes the results, and Chapter five includes of discussion of results as they pertain to the

research objectives. Finally, chapter six provides a summary of results and elaborates on the applicability of this research to industry, and within the context of future climate change scenarios.

Chapter Two
Literature Review

2.1 Western Boreal Plain

Boreal forest ecosystems constitute the second largest biome on Earth, occupying 10% of the entire global land area (McGuire *et al*., 1995), containing an estimated 22% of the total terrestrial carbon pool and more freshwater resources than any other terrestrial ecosystem (Watson *et al*., 2000). Within Canada, the composition of boreal forest vegetation is strongly dictated by climate (Wieder *et al*., 2006; Johnson and Miyanishi, 2008). Limited by long, cold winters and short growing seasons, boreal peatlands are typically species poor, dominated by conifer forests and shrub vegetation (Walter, 1973; Vitt, 2006; Wieder *et al*., 2006). However, in much of the WBP, it is the sub-humid climate, thick overburden layer and gentle topographic grade, comprising hillslopes and poorly drained lowlands that supports a landscape with one of the highest densities of peatlands globally (Gorham, 1991; Kuhry *et al*., 1992; Johnson and Miyanishi, 2008). The systems provide unique ecosystem services including the regulation of globally significant carbon stocks (Frolking *et al*., 2006; Wieder *et al*., 2009), storing one-fourth to one-third of the world's soil organic carbon pool (Turunen *et al*., 2002). However, these ecosystems are threatened by climate-mediated warming and anthropogenic disturbance, of particular concern within the oil sands region of northern Alberta.

To minimize the impacts produced from oil and gas-based mining, Alberta's *Environmental Protection and Enhancement Act* (EPEA) requires that the impacted landscape be restored as a functioning ecosystem of equivalent capabilities to the pre-disturbed conditions (Chymko, 2000; Grant *et al.*, 2008), and that peatlands, specifically fens, be given primary consideration for reclamation projects within the region of Fort McMurray (Alberta Environment, 2008b; Trites and Bailey, 2009). It is essential that the reconstructed system be self-sustaining,

carbon-accumulating, capable of supporting a representative assemblages of boreal species, tolerant of normal, periodic stress and can maintain appropriate peat moisture dynamics (Price *et al.*, 2011). To successfully construct a fen with equivalent function, it is necessary to understand the dominant processes that sustained the pre-disturbed systems and incorporate them into design reclamation strategies. Therefore, it is recommended that these processes are first understood within naturally occurring peatlands within the area of reclamation (Guo and Sun, 2012).

2.2 Evapotranspiration in the WBP

Peatlands within the WBP operate within a sub-humid climate where *P* is generally less than or equivalent to potential evapotranspiration (*PET*), and *ET* constitutes a dominant hydrological flux (Bridgham *et al.*, 1999; Eaton *et al.*, 2001; Petrone *et al.*, 2007; Johnson and Miyanishi, 2008). It is the persistence of a sub-humid climate and the dominance of *ET* in summer hydrologic budgets that indicates that peatlands may be extremely sensitive to any climatic variability (Petrone *et al*., 2011). *ET* is controlled by atmospheric demand (*PET*), and surface water availability, which are in turn influenced by climate, vegetation and soil (Wang *et al*., 2015). Due to the persistence of a sub-humid climate and sensitive linkages between the soil, vegetation and atmosphere, peatlands are extremely susceptible to the slightest variability that may disturb the balance between *P* and actual evapotranspiration (*AET*) (Loiselle *et al*., 2001; Petrone *et al*., 2007; Matsumoto *et al*., 2008; Lafleur, 2008; Brown *et al*., 2010; Phillips, 2014). Therefore, to understand these systems it is crucial to understand *ET* and identify the processes by which different components of the system retain and exchange water vapour with the atmosphere (Brown *et al*., 2010). Previous studies have illustrated the importance of air and soil temperatures, position of water table and the atmospheric demand (*PET*) as the primary variables controlling evaporation and transpiration among the different layers or components of the peatland (Petrone *et al*., 2000; Admiral *et al*., 2006;

Overgaard *et al*., 2006; Admiral and Lafleur, 2007; Petrone *et al*., 2007, Lafleur, 2008; Brown *et al*., 2010). The cold subsurface exerts a direct thermal regulation on peatland plants, impedes drainage thus promoting peatland development and exerts a strong control on the availability of soil water (Rouse, 2000). The surface exchange and atmospheric fluxes further influence the temperature and wetness of the soil surface, which, by governing the conditions for biological and chemical processes are significant for soil carbon balance and methane emissions (Bubier and Moore, 1994). Since the process of *ET* determine both water and heat balance for a peatland surface, a detailed description of *ET* control is essential (Lafleur, 1990).

ET can fluctuate both spatially and temporally, according (but not limited) to the variability in vegetation cover and water availability. Topographic highs and lows influence the soil moisture gradient and the microclimate at the peatland surface, and thus the processes, interactions, and the exchange of energy and mass within the system (Raupach and Finnigan, 1997; Drexler *et al*., 2004; Petrone *et al*., 2007). Within treed peatlands, this interaction is multidimensional with cumulative effects occurring at both the canopy and sub-canopy interface. The multi-layer canopy of a typical peatland is often dominated by woody evergreen vegetation interspersed with deciduous shrubs, underlain by a relatively continuous surface cover of moss species (Sonnentag *et al*., 2007). The effects of canopy cover on the underlying surface energy exchange is dependent on the density of the tree species (Moore *et al*., 2002; Lafleur *et al*., 2005; Petrone *et al*., 2011). However, detailed studies focusing on peatland canopy *LAI*, associated controls and their interactions with *ET* processes are lacking (Sonnentag *et al*., 2007).

Within the WBP, black spruce dominated peatlands represent the most widespread boreal forest system (Oechel and Van Cleve, 1986). Because black spruce cover is relatively open due to the narrow structure and low density of the trees (Heijmans *et al*., 2004), a substantial portion of

incoming solar radiation is able to reach the underlying peat surface, and consequently provides a significant contribution to ecosystem's flux exchange (Petrone *et al*., 2011). Previous studies have shown that the water loss from the peat surface is strongly governed by canopy cover, which creates a microclimate that either boosts or impedes ground surface *ET* (Limpens *et al*., 2014). To analyze this interrelationship a stratification of *ET* and *T* within varying height and degrees of canopy cover is needed. Quantifying and characterizing the plant-atmosphere exchange has received increased focus within climate change research in order to clarify the potential response of specific species (Sellers *et al*., 1995a). Climate-mediated warming, and associated increase in drought conditions (frequency and severity) within the northern hemisphere have been linked to higher vascular plant cover (Weltzin *et al*., 2001; Breeuwer *et al*., 2009; Limpens *et al*., 2014), and reduced moss vitality (Robroek *et al*., 2009; Limpens *et al*., 2014).

2.3 Future Climate Change Scenario

It is anticipated, under future climate change scenarios, that changing *P* patterns and increasing air temperatures could limit the potential for an ecosystem to dissipate its incident energy via the sensible heat flux (Q_H) in favour of the soil (Q_G) and latent heat flux (Q_E) (Worrall *et al*., 2015). The effects of shrub and tree encroachment on peatland functioning and, ultimately, their successional pathways are complex (Limpens *et al*., 2014; Heijmans *et al*., 2013). Previous studies have examined the effects of tree shading on moss *ET* and species composition (Kettridge *et al*., 2013; Limpens *et al*., 2014; Thompson *et al*., 2015). Canopy *T* is generally limited by low stem density, and nutrient poor conditions that are typical of *Picea mariana* dominant fens (Wieder *et al*., 2009), as well as the persistence of anaerobic conditions (Clulow *et al*., 2013). Consequently, surface *ET* is maximized by the significant proportion of solar radiation reaching the often saturated understory (Kim and Verma, 1996; Heijmans *et al*., 2004; Brown *et al*., 2010). It has

been predicted that despite increased *T* rates that are associated with a warmer climate and higher stem density, it may still be insufficient to counteract the reduction in surface *ET* resulting from reduced available energy at the surface (Kettridge *et al*., 2013). Furthermore, an increase in the tree and/or shrub canopy can result in a shift in surface vegetation to be outcompeted by shade-tolerant species (Marschall and Proctor, 2004; Hájek *et al*., 2009). However, current understanding of the magnitude and form of this potentially significant feedback mechanism is limited (Moore *et al*., 1998; Waddington *et al*., 2014). The effect on surface *ET* cannot be considered in isolation and therefore must be examined in parallel with changes to microclimatic and surface species composition.

2.4 Study Objectives

The objective of this research is to understand the vegetational processes controlling the rates and variability of *ET* and *T* of two typical fens during the 2013 growing season, within the Athabasca oils sands region of Fort McMurray, Alberta. The first objective is of this study is to quantify and characterize the magnitude of ecosystem-scale energy partitioning and *ET* in two typical WBP treed fens throughout the growing season. The fens are generally characterized as a poor fen, black spruce (*Picea mariana*) dominant, and a rich fen, larch (*Larix laricina*) dominant. Canopy cover varies significantly between the two sites, with the larch fen possessing a denser tree canopy. Due to the sensitivity of *ET* and *T* to environmental and physiological conditions (Brown *et al*., 2010), the second objective is to determine how the dominant controls governing site *ET* and *T* vary between the two fens. The third objective will quantify the spatial pattern of surface vegetation and ET_{surf} within varying tree density. This relationship will be examined alongside the effects of overstory canopy cover on micro- and hydro-climatological controls that regulate ET_{surf}. Finally,

the four objective will partition *ET* vertically between the canopy and understory, and how it varies between the two fens. This research addresses the following research questions:

1. How does the magnitude of ecosystems-scale energy partitioning and *ET* temporally vary between the two fens with differing canopies (differing dominant species and densities)
2. What are the dominant controls governing site *ET* and canopy *T*?
3. What are the environmental and physiological controls that govern ET_{surf} and how do they vary in varying degrees of canopy cover? How does the magnitude of ET_{surf} differ within varying degrees of canopy cover?
4. How is *ET* partitioned vertically between the peat surface and the tree canopy?

2.5 Study Sites and Climate Characteristics

Two fens, Pauciflora and Poplar, are located in close proximity to Fort McMurray, Alberta. Pauciflora, an 8 ha, poor fen, is located approximately 40 km south of the city (56.2230N, 111.14296W), while Poplar, an 11 ha, rich fen, is located approximately 25 km north (56.56192N, 111.32550W) (Figure 1). Mean air temperatures within the region vary from -2 to +1°C, with summer and winter averages fluctuating between 10 and 16 °C and -18 and -14 °C, respectively (Environment Canada, 2013). Both sites reside within the sub-humid climate of the WBP, where annual precipitation is approximately 300 to 600 mm, of which 70% typically occurs as rainfall during the four month growing season (May to August) (Johnson and Miyanishi, 2008).

Figure 1: Map of research sites Poplar and Pauciflora fens within the Western Boreal Plain (WBP) in the Fort McMurray region, Alberta, Canada.

Pauciflora Fen is characterized as a poor (groundwater pH ~ 4.5), treed fen located on a regional topographic high (Stoney Mountain, ~740 masl). During the period of data collection, *P* was higher, and temperatures were cooler than the averages collected by Environment Canada at the Fort McMurray airport (Environment Canada, 2015). Bocking (2015) reported Pauciflora fen as receiving > 50% *P* and mean T_a that was consistently a few degrees cooler than the Fort McMurray airport, between the study periods 2011 to 2014. Canopy cover is dominated by stunted *Picea mariana* with sparse occurrences of *Larix laricina*, with tree age ranging between 30 to 40 years. The canopy is discontinuous, consisting of densely treed plots to entirely open plots devoid

of any tree species. Average leaf area index (*LAI*) obtained from forestry inventory surveys conducted on 15 100 m^2 plots, delineated within the immediate vicinity of the micrometeorology (MET) tower at each site (Figure 2), displayed an average *LAI* value of 0.55 (IEG, 2014). Mean fen canopy closure is ≤ 35%. The understory is characterized by a microtopography of hummocks and hollows with an average peat depth of 2 m. Hummock vegetation is characterized by few shrub species, *Betula pumila*, dominated by *Rhododendron groenlandicum, Smilacena trifolia,* as well as *Carex aquatilis.* Other common species include *Andromeda polifolia, Rubus chamaemorus, Vaccinium vitis-idaea* and *Carex pauciflora* (few-flowered sedge). Groundcover was composed of *Sphagnum* moss, primarily *S. angustifolium, S. magellanicum, S. capillifolium*; hereinafter generalized as *Sphagnum* ssp. Hollow vegetation consisted of similar species with the addition of *Carex paupercula* and *Eriophorum vaginatum*¸ but was devoid of shrub species.

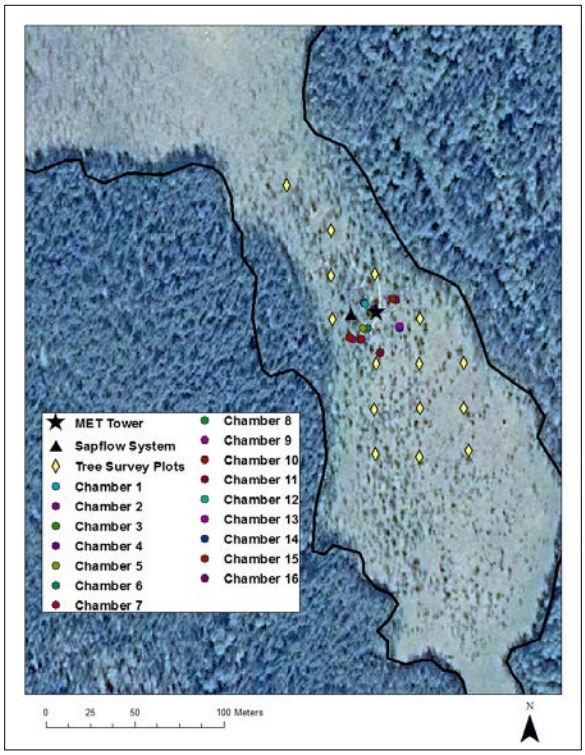

Figure 2: Map of Pauciflora fen study site instrumentation and forestry inventory sampling plots.

Poplar Fen, is a rich fen (groundwater pH ~ 6.6) dominated by a dense cover of *Larix laricina*, with sparse occurrences of *Picea mariana* within the immediate vicinity of the MET tower, which represents the focus of this study. *Picea mariana* is more prevalent within the fen and upland ecosites that surround this study area. In comparison to Pauciflora, Poplar supports a dense canopy with an average *LAI* of 2.82, obtained from 7 plots that surround the MET tower (Figure 3; IEG, 2014) and average tree age ranges from 25 to 35 yrs. Mean fen canopy closure is greater at ≥ 35%. The surface is composed of microtopographic highs and lows consisting of an average peat depth of 1 m. Understory vegetation consisted of a dense shrub layer of *Betula pumila*, *Equisetum fluviatile, Smilacena trifolia, Carex prairea,* and *Carex diandra.* Groundcover is composed of various moss species including the dominant *Tomenthypnum nitens* (Hedw.) Loeske and *Aulacomnium palustre* (Hedw.) with traces of traces of *Pleurozium schreberi* (Brid.) Mitt., *Hylocomium splendens* (Hedw.) BSG., *Sphagnum capillifolium* (Ehrh.) Hedw., *Bryum pseudotriquetrum* (Hedw.) and *Drepanocladus aduncus* (Hedw.) Warnst. (Goetz and Price, 2015).

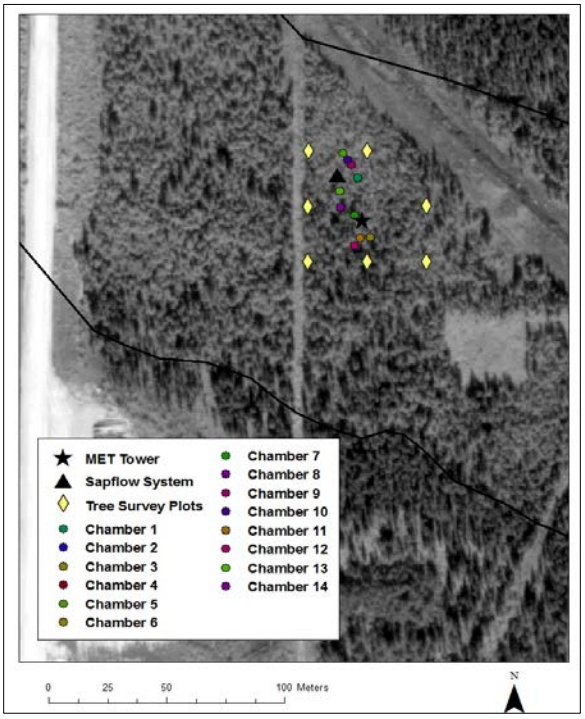

Figure 3: Map of Poplar fen study site instrumentation and forestry inventory sampling plots.

Chapter Three
Methods

3.1 Energy Balance

The surface energy balance can be estimated using,

$$Q^* = Q_E + Q_H + Q_G \quad (2.1)$$

where Q^* represents net radiation (W m^{-2}), Q_E is the latent heat flux (W m^{-2}), Q_H is the sensible heat flux (W m^{-2}), and Q_G is the ground heat flux (W m^{-2}).

To quantify the energy balance components, a MET tower was installed at each site. Measurements included wind and speed direction (Model 05103, R.M. Young Company, USA), net radiation (NR-Lite2, Campbell Scientific, Canada; installed 6 m above the surface at Pauciflora and 10 m at Poplar, with an additional sensor at 3 m at Poplar), relative humidity (*RH*) and temperature (HOBO U23 Pro v2, Onset Computer Corporation, Bourne, MA; installed at 6 and 1 m at Pauciflora, and 6, 3 and 1 m above the peatland surface at Poplar). Q_G was measured in both microforms at a 5 cm depth using soil heat flow transducers (Model HFT3.1, Campbell Scientific, Canada) and soil temperature profiles of 2, 5, 10 cm depths (Omega copper-constantin, Campbell Scientific Inc., USA). Precipitation (*P*) was measured in close proximity to the MET tower at each site using a tipping bucket rain gauge (HOBO U23 Pro v2, Onset Computer Corporation, Bourne, MA). Data were sampled every 60 s, and averaged over 30-minute intervals over 151 days (May through September). Quality control data filtering and gap filling were done according to Restrepo and Arain (2005), Falge *et al*. (2001), Phillips *et al.* (2014).

3.2 Eddy Covariance Theory

The eddy covariance (EC) technique was used to measure site-wide surface energy fluxes and *ET*, which requires a determination of turbulent fluxes of water vapour, momentum and sensible heat from the covariance of their respective eddies (Peixoto and Oort, 1992; Petrone *et al*., 2001). The mean vertical flux of the sensible and latent heat fluxes were calculated,

$$Q_H = \rho\ C_p\ w'T' \tag{2.2}$$

$$Q_E = L\rho\ w'q' \tag{2.3}$$

where ρ (kg m^{-3}) is the density of air, C_p (MJ kg^{-1} K^{-1}) is the heat capacity of the air, L (MJ kg^{-1} kPa^{-1}) is the latent heat of vaporization, w' (ms^{-1}), T' (K) and q' (kPa) are the instantaneous variance in the vertical windspeed, air temperature and specific humidity measured at the same height. The covariances between w', q' and T' were measured by an electronic analog computation consisting of a multiplication and averaging process on the CR23X datalogger. The CR23X sampled *w'*, *q'*, and *T'* at 20 Hz and averages calculated every 30 minutes. *ET* (mm d^{-1}) was then calculated from the product Q_E,

$$ET = \frac{Q_E}{L_V\ \rho_w} \tag{2.4}$$

where L_v is the latent heat of vaporization (J kg^{-1}) and ρ_w is the density of water (kg m^{-3}) (Oke, 1987).

EC systems were installed June 2013 on the pre-existing MET tower located at 5 and 10 m above the peat surface, at Pauciflora and Poplar, respectively, and consisted of LI-7200 closed path IRGAs and flow modules (Li-Cor Biosciences, Lincoln, NE, USA), and sonic anemometers (WindMaster Pro, Gill Instruments, Lymington, Hampshire, UK).

Prior to analysis, EC data were first filtered for periods of low turbulence ($u^* < 0.23$ m/s), then corrected for density effects (Webb *et al*., 1980; Leuning and Judd, 1996) and sensor separation (Blanford and Gay, 1992; Leuning and Judd, 1996). As a final correction to the flux data, the energy balance closure was calculated and forced to close for the study period (Petrone *et al*., 2015). Closure is most reasonably forced by assuming that the measured available energy is representative of the plot that the EC sensors are measuring (Petrone *et al*., 2015; Petrone *et al*., 2001), leaving Q_H and Q_E to be adjusted (Barr *et al*., 1994; Blanken *et al*., 1997; Twine *et al*., 2000; Petrone *et al*., 2001). To determine contributing areas of the measured EC fluxes, a footprint analysis was conducted for each site according to Schuepp *et al*. (1990). Results from the footprint model were used to filter-out data that originated outside the study area.

3.3 Sapflow Measurements of Transpiration

The theory of the stem heat balance (SHB) approach to measure sapflow has been described in detail by Sakuratani (1979) and Baker and Van Bavel (1987). The SHB method can be used to measure sapflow in both woody (Steinberg *et al*., 1989) and herbaceous (Baker and van Bavel, 1987) stems. Sapflow systems (Dynamax Flow32-1K, Houston, TX, USA) were installed at each site to estimate sapflow rates of selected trees throughout the months of May to September over two consecutive years, 2012 and 2013, using the steam heat balance (SHB) method. Continuous measurements were stored on a data logger (CR1000, Campbell Scientific Inc., UT, USA) installed at each site. Each system was additionally equipped with a 12 volt deep-cycle marine battery maintained by a 50-watt solar panel. To obtain a representative estimation of canopy *T* rates, each system was instrumented with seven separate sensors including five trees and two understory species. Sapflow systems were installed within close proximity to the MET tower, based on representative canopy species, size, and average height as well as proximity to each other due to

cable length limitations of the Flow32 monitoring system. System installation complied with size requirements outlined by the manufacturer (Dynamax Inc., 2007), with sensors adhering to recommended size specifications (Table 2.4.1). Each gauge consists of a flexible heater that is wrapped around the stem and enclosed by a layer of cork, insulation and an aluminum coated PVC weather shield (Figure 4a). Pairs of thermocouple junctions are embedded in the cork band to form a thermopile. Displayed in Figure 2.4.1b, one thermocouple junction is placed on the inner and outer surface of the cork to measure radial temperature gradients away from the heater (ΔT_r) (Steinberg *et al*., 1989). Additional junctions are positioned axially along the surface of the stem, with one junction from each pair staggered above and below the heater to measure temperature gradients ΔT_a and ΔT_b, which are used to calculate components of the heat balance of the stem (Figure 4c).

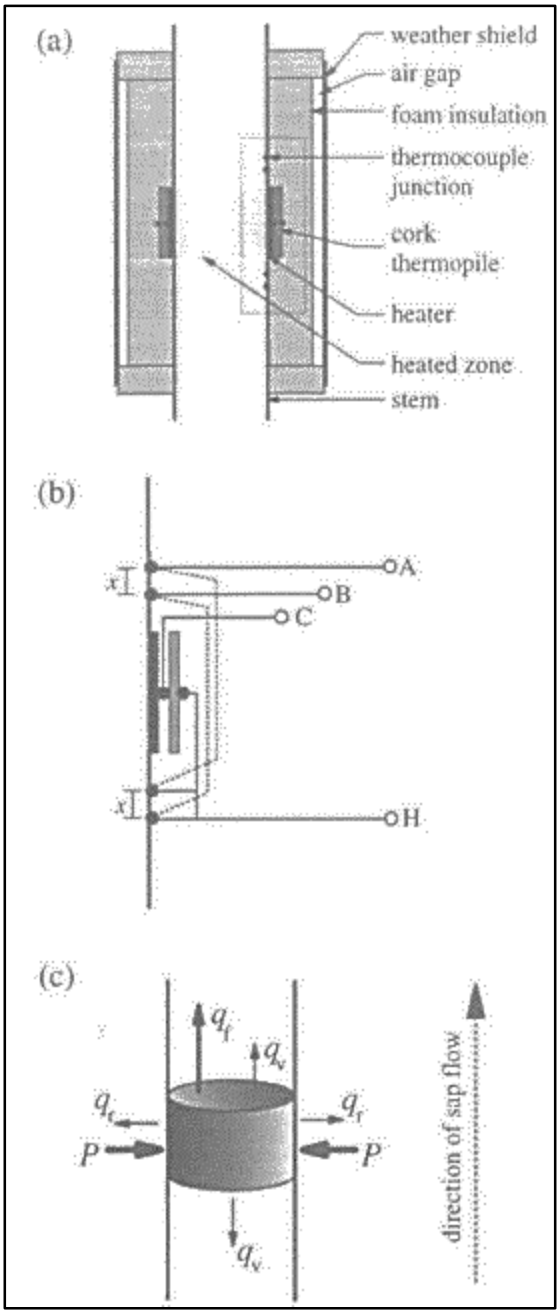

Figure 4: (a) Vertical cross-section through a stem heat balance (SHB) gauge. (b) Schematic of gauge thermocouples; copper wires shown as solid lines and constantan wires shown as dotted lines. For the determination of sapflow, the temperature differentials $\Delta T_a, \Delta T_b, \Delta T_r$ are obtained from measurements of voltages across AH, BH and CH, respectively. (c) Schematic of conductive heat fluxes within the heated stem segment, where P (P_{in}) is the applied heat to the stem, q_v is the rate of vertical heat loss, q_r is radial heat loss and q_f is heat uptake by the sap stream (Smith and Allen, 1996).

Site	Ref. No.	Sensor Size	Species	D_o (cm)	Height (cm)
PFLORA	**1**	SGA5	*Picea mariana sp.*	0.52	42
	2	SGA5	*Picea mariana sp.*	0.70	51
	4	SGB25	*Larix laricina*	3.24	222
	5	SGB35	*Picea mariana*	4.40	308
	6	SGB35	*Picea mariana*	4.40	294
	3	SGB50	*Larix laricina*	5.40	240
	7	SGB50	*Picea mariana*	6.32	440
POPLAR	**1**	SGA5	*Betula pumila var. glandulifera*	0.60	123
	2	SGA5	*Betula pumila var. glandulifera*	0.48	82
	3	SGB25	*Larix laricina*	2.70	266
	4	SGB35	*Larix laricina*	4.45	430
	5	SGB35	*Picea mariana*	4.45	445
	6	SGB50	*Larix laricina*	6.00	492
	7	SGB50	*Picea mariana*	6.30	500

Table 1: Sapflow monitored trees and understory species, including species size and sensor specifications, installed at Pauciflora (PFLORA) and Poplar fen. Sapling trees are denoted by (sp.) and tree diameter measured at peat surface (D_o).

The system requires a constant energy input that is balanced by heat flow out of the system (Figure 4c). Assuming no heat storage, P_{in} represents the power input to the stem from the heater, and the outward heat flow that is partitioned into conductive fluxes including vertical or axial heat conduction (q_v) (which has two components including an upward (q_u) and downward (q_d) heat flux (not shown)), radial conduction (q_r) away from the stem and mass heat transport by the sap stream (q_f). Through the measurement of P_{in}, q_r, q_u, q_d, heat convection carried by the sap (q_f) can be calculated as the residual of the energy balance expressed as (Sakuratani, 1981; Baker and van Bavel, 1987),

$$P_{in} = q_r + q_v + q_f \text{ (W)} \tag{2.5}$$

The value of P_{in} is calculated from the electrical resistance and voltage across the heater, while q_v and q_r are determined from measurements of ΔT_a, ΔT_b and ΔT_r. Finally, q_f is converted to a mass flow rate of sap.

The value of q_v is calculated using Fourier's Law for one-dimensional heat flow from the upward and downward temperature gradients (Sakuratani, 1981; Baker and van Bavel, 1987). The sum of these gradients is algebraically equivalent to (ΔT_b - ΔT_a) (K m^{-1}) (Steinberg *et al*., 1990b), and q_v is calculated,

$$q_v = A_{st} K_{st} \frac{(\Delta T_b - \Delta T_a)}{x} \tag{2.6}$$

where A_{st} is the cross-sectional area of the heated section (m^2), K_{st} is the stem thermal conductivity (W m^{-1} K^{-1}), and x is the distance between the two junctions positioned above and below the heater (m) obtained from Dynagage specifications. The value of K_{st} was taken from the literature as 0.42 W m^{-1} K^{-1} for woody stems (Steinberg *et al*., 1989). Additionally, the factor 0.040 mV C^{-1} is applied to convert the thermocouple differential signals to degrees C (Dynamax Flow32-1K, Houston, TX, USA).

Radial conduction, q_r, is determined from ΔT_r using,

$$q_r = K_{sh} \Delta T_r \tag{2.7}$$

where K_{sh} is the effective thermal conductance of the sheath of materials surrounding the heater (W mV^{-1}). The value is dependent on the thermal conductivity of the insulating sheath and stem. It generally changes for each new installation and therefore must be calculated from ΔT_r and additional components of SHB during periods when sapflow is known to be zero (Baker and van Bavel, 1987; Baker and Nieber, 1989).

Once all other components of the SHB are known, q_f is calculated from difference and mass flow rate of the sap per unit time (F_m) (g h^{-1}) is calculated using (Sakuratani, 1981; Baker and van Bavel, 1987; Steinberg *et al*., 1990b). This equation takes the residual of the energy balance (W), and converts it to a flow rate by dividing by the temperature increase of the sap and heat capacity of water,

$$F_m = \frac{2q_f}{c_s(\Delta T_a + \Delta T_b)} \quad (2.8)$$

where c_s is the specific heat capacity of water (4.186 J g^{-1} C) and $(\Delta T_a + \Delta T_b)/2$ is the increase in sap temperature across the heater, assuming the sap is radially uniform. Once more, the temperature increase of the sap (mV) is converted to degrees C by dividing by the thermocouple temperature conversion constant (0.040 mV C^{-1}).

Previous studies have reported errors in sapflow rates measured using the SHB method if changes in heat storage, within the heated section of the stem, are neglected. The size of these errors has been determine to increase with stem diameter (Groot and King, 1992; Shackel *et al*., 1992; Grime *et al*., 1995a). However, errors become less important when daily rates of transpiration (*T*) are determined, as the change in heat storage over a 24-hr period is generally zero (Weibel and Boersma, 1995), and provides a reasonable estimation of steady state sapflow even for larger stems (Perämäki *et al*., 2001). F_m was calculated for each of the monitored sapflow trees, and was then divided by the density of water (1 g $cm^{3\ -1}$), of which resulting sapflow velocities ($cm^3\ hr^{-1}$) were converted to litres (L hr^{-1}), and finally summed over a 24-hr period to derive the total volume of water transpired (F_s) per tree per day (L day^{-1}) (Clulow *et al*., 2013). Daily regression models were fitted to forest inventory mensuration data using sapwood area (*SA*) (cm^2) (at the height of the sensor) as the independent function (Ford *et al*., 2007).

To determine *SA*, 15 sample trees from each site were harvested between the studied periods 2012 and 2013, selected based on proximity to the monitored sapflow trees to maintain consistency imposed by environmental constraints. Additionally, samples were stratified by diameter and species to ensure a statistically significant representation of each the five monitored sapflow trees (three samples per monitored tree). Before harvesting, diameter at peat surface (D_o, cm), determined from the widest diameter flare separating stem from root (Fritts, 1976), height of

the live crown (m) and location were recorded. Recognized by Bond-Lamberty *et al*. (2002), the application of D_o as the primary, independent allometric variable for small trees and shrubs has been successfully used in previous studies (Smith and Brand, 1983). Additionally, D_o samples provide increased accuracy when estimating the number of growth years (Fraver *et al*., 2011).

Determining the extent of *SA* contained within the xylem requires a differentiation of the hydro-active from the inactive xylem. Located internal to the active *SA*, the heartwood represents primary or old growth rings incapable of water conduction or storage (Taylor *et al*., 2007). Often the heartwood can be determined through visual observation due to its dark pigmentation, however, this is not true for all species (Köstner *et al*., 1998). A commonly used method in estimating the hydro-active *SA* is to dye the xylem. For the purpose of this study, two separate dyeing techniques were applied to the harvested stem discs. Ferric nitrate ($F_e(NO_3)_3$) and Iodine-potassium iodide (Lugol's solution), a known indicator for starch (Vötter, 2005) were selected as effective indicator solutions in differentiating the heartwood-sapwood boundary for spruce and larch species (Kutscha and Sachs, 1962).

Sapwood cross-sectional area was determined on each sample disc by measuring xylem and heartwood diameters (cm), calculated as the mean diameter from two perpendicular measurements obtained from each sample disc. Measurements were recorded to the nearest 1 mm, from which xylem and heartwood cross-sectional areas (cm^2) were calculated using an ellipse formula (Maguire and Hann, 1987), and estimated *SA* by subtraction (Husch *et al*., 1972; Ryan, 1989). Total *SA* was estimated assuming a consistent cylindrical shape throughout the stem (Quiñonez-Piñó, 2007), with mean *SA*, obtained from three corresponding samples for each of the monitored sapflow trees at each site. Allometric correlations were established with a strong degree of confidence as the sample trees were subjected to same environmental constraints and growth

conditions as the monitored trees. *SA* (cm^2) at the height of the sensor was calculated from the ratio of *SA* to total stem cross-sectional area at crown base, Fractional Sapwood Area (*FSA*). The ratio was applied to the cross-sectional area measured at the height of the sapflow sensor. Due to the narrow structure of the tree stems, variation in *SA* were negligible.

Site	**Ref. No.**	**Species**	**AVG Sapwood Area (cm^2)**	**AVG No. Sapwood Rings**	**Percent of Stem Cross-section (%)**	**Fractional Sapwood Area (FSA)**
PFLORA	**4**	*Larix laricina*	7.8	20	62.1	
	5	*Picea mariana*	15.6	37	81.3	**0.8304**
	6	*Picea mariana*	11.1	29	84.8	
	3	*Larix laricina*	16.6	21	63.4	
	7	*Picea mariana*	27.6	39	85.0	
POPLAR	**3**	*Larix laricina*	8.3	14	66.2	**0.7271**
	4	*Larix laricina*	20.5	12	73.4	
	5	*Picea mariana*	15.5	28	89.4	**0.8938**
	6	*Larix laricina*	33.2	15	78.5	
	7	*Picea mariana*	23.8	27	89.4	

Table 2: Tree specific data required for calculation of sapflow. Fractional Sapwood Area (*FSA*) was determined for each tree species captured in forest mensuration data at each fen.

3.4 Calculating Tree Transpiration

A bottom-up scaling approach was used to scale sapflow (L day^{-1}) using *SA*. A sum sapflow of all trees within each forest mensuration plot was used to represent plot *T*, assuming the sum of the mass flow within the monitored tree stems is equivalent to total canopy *T* with a short time lag (Ford *et al*., 2007),

$$\hat{y} = \beta_o + \beta_1 (SA) \tag{2.9}$$

where β_o represents the linear regression model intercept and β_1 represents the linear regression model slope (Quiñonez-Piñón, 2007).

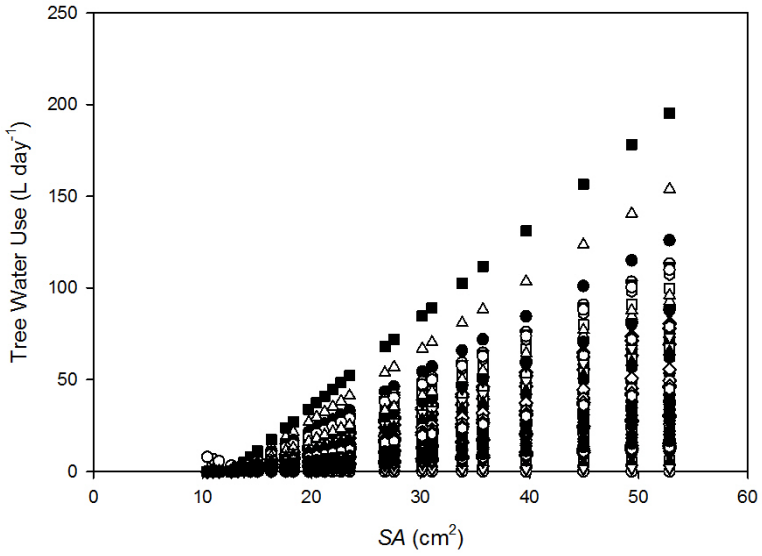

Figure 5: Example of diurnal regression model, stem sapwood area (*SA*) (cm^2) in relation to total tree water use (L day^{-1}).

Diurnal linear regression equations modeling diurnal *T* (L) against *SA* (cm^2) were developed for both species present at each site, *Picea mariana* and *Larix laricina* ($R^2 > 0.95$) (Vertessy *et al*., 1995) (specific equations provided in Appendix I, II, III). Total *T* (L day^{-1}) was averaged per plot, expressed per unit *LAI*, and then averaged across the fen study area (Ford *et al*., 2007). *T* was converted to mm d^{-1} following a series of conversions described in Allen *et al.* (1998).

3.5 Surface ET

ET_{surf} measurements were collected between the daylight hours of 08:00 and 16:00 MST using dynamic closed chambers, six times per month from May to September 2013 to acquire an adequate sample size and to ensure seasonal variation was captured (Brown *et al*., 2010; Solondz *et al*., 2008). 16 and 14 representative sites were selected at Pauciflora and Poplar, respectively, in both hummocks and hollows (Figure 2, 3). Additionally, sites were selected in varying degrees of overstory canopy closure. A canopy gap fraction was determined from the LiDAR land classification data, and was expressed as a mean percent canopy closure for each fen. Results coincided was previous research comparing canopy closure of tree peatlands of *Sphagnum* and

feathermoss-dominated plots (Solondz *et al*., 2008). Plots classified as covered were selected within immediate proximity to a cluster of trees or overstory, whereas plots classified as open had no immediate overstory. Due to Pauciflora's sparse canopy, covered plots were installed adjacent to a cluster of two to three trees, measuring ≥ 5 cm in *DBH* with a *LAI* of 0. 55 (fen overstory average). Covered plots at Poplar were installed in areas with approximately 20 trees, with a mean *DBH* of > 5 cm and an average *LAI* 2.51. Consequently, covered plots at Pauciflora maintained average *PAR* values ≤ 500 μmol m^{-2} s^{-1}, while a reduced threshold of ~300 μmol m^{-2} s^{-1} was demonstrated at Poplar. Both thresholds fell within the range of values presented by Solondz *et al*. (2008).

Collars constructed from polyvinyl chloride (PVC) plastic piping with a height of 16 cm and an inside diameter of 19 cm were installed 10 cm into the peat at each site (Brown *et al*., 2010). ET_{surf} was determined through changes in vapour pressure (*e*) over time, measured in a clear enclosed Plexiglas chamber (Waddington and Roulet, 2000; McLeod, *et al*. 2004; Brown *et al*., 2010), recorded over a two minute interval using a CIRAS-SC CO_2/H_2O Infrared Gas Analyzer (IRGA) (PP Systems, Amesbury, MA) (LeCain *et al*., 2002). The order of sampling sequence at each site was randomly varied throughout each sampling day to reduce confounding effects of the different light, temperature and moisture regimes that occur throughout the day, and to ensure sampling over a wide range of environmental conditions (LeCain *et al*., 2002; Brown *et al*., 2010; Phillips, 2014). Increases in *e* within the chamber is proportional to the instantaneous rate of *ET*, estimated using (McLeod *et al*., 2004),

$$ET_{surf} = 3.6 \frac{MVC}{A} \tag{2.10}$$

where ET_{surf} is the instantaneous rate of evaporation (mm hr^{-1}), 3.6 is a conversion coefficient to convert a volume of water into a flux rate (mm hr^{-1}), M is the constant slope of the vapour pressure for each interval over the time step (g m^{-3} s^{-1}), V is the volume inside the chamber (m^3), C is the calibration factor to account for vapour absorption by the chamber material (dimensionless) (described in Stannard, 1988; Brown *et al*., 2010), and A is the area of the fen surface that is covered by the chamber (m^2).

Environmental variables were sampled along with ET_{surf} at each site during the incubation period included air temperature (T_a) (thermocouple wire sealed in the chamber), photosynthetically active radiation (*PAR*) (Quantum Sensor LI-190SL, LI-COR, USA), peat temperature (2, 5, 10 and 20 cm; Omega, USA), and volumetric moisture content (*VMC*) at a depth of 12 cm (HydroSense, Campbell Scientific Inc., Canada). The HydroSense was calibrated for each site (specific equations and methods referenced in Goetz (2014)). Depth to water table was continuously monitored using the Odyssey™ capacitance water level loggers (Dataflow Systems PTY. Ltd., New Zealand) located in close proximity to each fen's MET tower, additional water tables measurements were manually recorded in wells installed adjacent to all sites. Finally, ET_{surf} values were classified using LiDAR land classification data following steps Phillips (2014), described in the following sections, and relative surface flux contributions were extrapolated over the daylight hour 08:00 and 16:00 to coincide with daily *ET* and *T*, and to assess the relative contribution of $ET_{surf.}$

3.6 Meteorological Tower Flux Footprint

The flux footprint was calculated to correctly identify the measurement signals recorded by the meteorological instruments to the original emission area. For this study it was measured using the methods described by Scheupp *et al*. (1990). Every source area will contribute to the flux profile downwind to a degree that varies with distance from the source (i.e. max length), elevation of observation (instrument elevation), characteristics of the turbulent boundary layer and atmospheric stability (Scheupp *et al*., 1990). Both the position of the peak footprint (x_{max}), the area to which the observation is most sensitive, and the position of 80% flux contribution (x_{frac}) were determined. Periods when fluxes originated from outside the calculated footprint were removed from analysis. (Measurements were omitted when > 80% of the flux measured at a height of 5 and 10 m above the peat surface were estimated to originate outside the fen boundary, approximately 45 m in the east or west direction and 80 m in the north or southward direction from the tower at Pauciflora and Poplar, respectively). Vegetation community distributions within each tower's footprint were determined with use of LiDAR land classification data, described in the preceding section.

3.7 Scaling T and ET Flux Data

To ensure that both canopy *T* and surface *ET* were representative of the larger fen boundary, two separate scaling techniques were employed. Canopy mensuration data were obtained through forest inventory surveys (IEG, 2014), and used to scale *T* data to the study area. Additionally, airborne light detection and ranging (LiDAR) data were used to classify groundcover within the fen boundary.

3.7.1 Forest Inventory Surveys

Survey plots, each measuring 100 m^2, were delineated within the immediate vicinity of the MET tower and sapflow system (Figure 2, 3). In 2013, 17 survey plots were selected for Pauciflora, and

8 plots allocated at Poplar. Sampling locations were constructed to ensure sufficient spatial coverage to capture the dominant species and size class at each site. The initial survey was conducted in August 2013, in which tree species, stem count and density, diameter at breast height (*DBH*, cm), total height (cm), and mean *LAI* per plot were measured (Table 3, 4). Centered within each 100 m^2 plot, a second 10 m^2 plot was delineated to include sapling species. Supplementary measurements included groundcover classification, slope and microtopography. A subsequent survey was conducted in 2014 within the original 25 plots; changes including stem count, size and species decay were recorded.

Canopy *LAI* values were attained with an *LAI*-2000 plant canopy analyzer (LI-COR, USA), and comprised of understory (LAI_U) and canopy (LAI_C) measurement, as well as a cumulative *LAI* (LAI_T) per plot, following similar techniques described in Vertessy *et al*. (1995). For a few select plots, LAI_C was estimated from a formulated regression between measured LAI_C and canopy cover (%). A conifer correction was applied to all LAI_C measurements. Additionally, a sun-scattering correction was applied using FV-2200 software (Gower *et al*., 1999). A bottom-up scaling approach was used to scale sapflow estimated *T* (L day^{-1}), summed for all trees within the forest survey plots using *SA* per tree. Previously described, *T* was then averaged per plot, expressed per unit *LAI*, and then averaged across the study area, expressed in mm day^{-1} (Vertessy *et al*., 1995; Ford *et al*., 2007).

PAUCIFLORA							
Plot	**Plot Size (m^2)**	***LAI*$_C$ (m^2)**	**Stem Count**	**AVG DBH (cm)**	**S.D.**	**AVG Height (cm)**	**S.D**
1	100	0.89	15	5.8	±1.7	480	±116
2		0.36	1				
3		0.45	3	5.4	±0.9	441	±6.6
4		2.61	16	5.8	±1.1	500	±87
5		0.30	5	5.2	±1.7	255	±247
6		0.18	2	5.9	±0.1	439	±64
7		0.41	1	4.8		377	
9		0.77	3	4.4	±0.4	412	±25
10		0.47	2	5.8	±1.1	430	±25
11		0.06	2	5.4	±0.3	427	±7.1
12		0.14	1				
13		0.29	1	4.8		407	
15		0.84	4	4.4	±0.3	355	±22
16		0.35	1	4.2		327	
17		0.15	1				
AVG		**0.55**		**5.5**	**±1.3**	**424**	**±148**

Table 3: Forest Inventory Survey data, including plot count, plot size (m^2), average canopy *LAI*$_C$ (m^2), stem count, average *DBH* (cm) and Height (cm) per plot, at Pauciflora fen. (S.D. represents standard deviation). Missing plots indicate no tree canopy. Missing values indicate presence of dead tree species.

POPLAR								
Plot	**Plot Size (m^2)**	***LAI*$_C$ (m^2)**	**Species**	**Stem Count**	**AVG DBH (cm)**	**S.D.**	**AVG Height (cm)**	**S.D**
1	100	3.76	***Lt***	**54**	**5.1**	**±1.0**	**592**	**±109**
			Sb	1				
2		1.46	***Lt***	**10**	**7.4**	**±5.2**	**562**	**±154**
			Sb	15	7.9	±2.4	623	±158
3		3.26	***Lt***	**26**	**6.7**	**±2.8**	**779**	**±220**
			Sb	14	9.1	4.5	746	±220
4		2.12	*Lt*	**23**	**5.7**	**±1.2**	**556**	**±125**
			Sb	7	6.1	±3.3	574	±178
5		2.53	***Lt***	**37**	**5.6**	**±1.2**	**556**	**±80**
			Sb					
6		2.44	***Lt***	**16**	**7.5**	**±5.5**	**718**	**±204**
			Sb	1	11.8		783	
7		4.17	*Lt*	**18**	**6.9**	**±4.2**	**747**	**±213**
			Sb	24	8.6	±3.0	726	±235
AVG		**2.82**			**6.5**	**±3.1**	**644**	**±190**

Table 4: Forest Inventory Survey data, including plot count, plot size (m^2), average canopy *LAI*$_C$ (m^2), tree species (*Lt*, Larch; *Sb*, Black Spruce), stem count, average *DBH* (cm) and Height (cm) per plot, at Poplar fen. (S.D. represents standard deviation). Missing values indicate presence of dead tree species.

3.7.2 Leaf Area Index and Biomass

Field measurements of *LAI* were obtained at each collar with a LP-80 *PAR*/*LAI* Ceptometer (Decagon, USA) in early August, the late period of peak plant growth (Solondz *et al.*, 2010; Brown *et al.*, 2010). Canopy mensuration data were obtained through forest inventory surveys (Figure 3.2.2, 3.2.3; IEG, 2014). Canopy *LAI* values were attained with an *LAI*-2000 plant canopy analyzer (LI-COR, USA), and comprised of understory (*LAI*$_U$) and canopy (*LAI*$_C$) measurement, as well as a cumulative *LAI* (*LAI*$_T$) per plot, following similar techniques described in Vertessy *et al*. (1995). For a few select plots, *LAI*$_C$ was estimated from a formulated regression between measured *LAI*$_C$ and canopy cover (%). A conifer correction was applied to all *LAI*$_C$ measurements. Additionally, a sun-scattering correction was applied using FV-2200 software. Supplementary collar measurements were obtained in the lab using the LI-3100C Area Meter (LI-COR, USA) with plant

material harvested from each collar in September 2013, which was then used to calculate *LAI* based on the area of the collars (Sims and Bradford, 2001). Following harvest and prior to *LAI* measurements, plants were removed at root depth, grouped by species, oven-dried (24 hours at 80°C), and weighed for total aboveground biomass (*AGB*) (Sims and Bradford, 2001). The roots were subsequently removed from the peat cores and then oven-dried (24 hours at 80°C), and weighed for below ground biomass (*BGB*) (Sims and Bradford, 2001).

3.7.3 LiDAR Land Cover Classification

Land cover classification employed methods described by Chasmer *et al*. (2016). Optical (spaceborne) and active (airborne) remote sensing data were used to characterize vegetation species types and structural characteristics as they are found in micro-topographic hummocks and hollows and with varying structural vegetation characteristics. Discrete return Airborne Light Detection and Ranging (LiDAR) data were acquired using an ALTM3100 on August 4, 2010 by Airborne Imaging Calgary and licensed for use by the Government of Alberta. LiDAR data were classified into ground and non-ground returns using TerraScan (TerraSolid, FI). Initial data products including a digital elevation model (DEM), digital surface model (DSM) and canopy height model (CHM = DSM – DEM) and gap fraction were created for an area of exceeding 2300 km^2 in Golden Software Surfer (Golden Software Inc. CO). The DEM was derived from ground returns using an inverse distance weighting (IDW) to a resolution of 1 m. The DSM was derived from all returns greater than 0.3 m above ground classified returns using the maximum return within a 1 x 1 m *x z* column. Canopy gap fraction at the Poplar site (in particularly due to dense shrub and tree vegetation) was rasterised based on the ratio of returns exceeding 1.3 m (often associated with DBH, represented by tree canopies) and returns exceeding 0.3 m to total returns within each 1 x 1 m *x z* column, representing canopy and canopy with understory gap fraction,

respectively. Hummocks and hollows were determined at Pauciflora and Poplar (but applied only to Pauciflora classification) sites using a 6 m radius search window, subtracted from the DEM at both sites for estimates of residual differences above and below the mean planar (normalized) surface.

Optical imagery data processing and analysis

WorldView2 multi-spectral and panchromatic data were acquired from Blackbridge Inc. (Lethbridge, AB) for Poplar fen on August 5, 2011. Digital numbers were converted to radiance and then converted to reflectance via atmospheric correction using Fast Line-of-sight Atmospheric Analysis of Hypercubes (FLAASH) in Exelis ENVI. Orthorectification was performed using the DEM derived from LiDAR data. Pleiades multi-spectral were also acquired from Blackbridge Inc. for Pauciflora fen on August 8, 2012. The same procedures were applied for conversion of digital numbers to radiance and reflectance in ENVI. Orthorectification was performed using the LiDAR DEM.

Classification of vegetation species types, vegetation structure and micro-topography

Poplar was classified with a support vector machine supervised classification based on visual assessment of vegetation optical characteristics and LiDAR structural data fusion based on a linear kernel. Input data included 8-band (WorldView-2), canopy height, and above and below canopy gap fraction. Approximately 15-25 training sets were created per species type. Four species classes were created and further aggregated based on a 3 pixel majority filter to remove speckle. Species classes were then divided into 2 m binned vegetation height characteristics. As a result of taller vegetation and occlusion of ground-cover vegetation, species distribution did not appear to be associated with micro-topography (hummocks and hollows), and therefore, micro-topography was excluded from the resulting classification.

Pauciflora was classified with a maximum likelihood classification (MLC) using similar methods of 4-band multi-spectral (Pleiades) and LiDAR data fusion based on visual examination of optical differences in species characteristics (and other land cover types within and adjacent to the fen). Between 15 and 25 training sets were created per species type, and 12 classes were created (including road). Species were further classified into hummocks, hollows and flat areas, and have naming conventions 1-5 that includes: conifer (*Larix laricina*), road, deciduous, conifer (*Picea mariana*), and other woody-shrub species, respectively. Numbers 106-312 refer to hummocks (100s), mid- or flat (200s) and hollows (300s) wetland ground cover and shrub species growing in these areas.

3.8 Statistical and Error Analysis

The data were delineated by month and by period of plant growth into Early Green (*EG*, DOY 121 to 158), Green (*G*, DOY 158 to 218) and Late Green (*LG*, DOY 219 to 260) to better understand temporal and seasonal trends. *EG* is generally defined as the period in which vascular species emerged but are immature, the *G* period corresponds with the stage vascular species were maturing, and the *LG* period represents the stage vascular species reached maturity and *LAI* reached a maximum (Solondz *et al*., 2008). Results were compared using a two-way analysis of variance (ANOVA) and independent sample *t*-tests, reported with the sample mean, if the data were normally distributed. If the data did not satisfy the test of normality, the Mann-Whitney or the Wilcoxon signed rank test was used to demine the statistical significance between variables. Differences were deemed to be statistically significant if they met a significance level of 0.05. Literature that has examined flux measurements has generally reported standard deviation (± S.D.) to access the daily uncertainty between and within sites (Kellner, 2001; McNeil and Waddington, 2003; Botting and Fredeen, 2006; Strack *et al*., 2006; Brown *et al*., 2014; Runkle *et al*., 2014). For

this study, standard deviation was used to describe the natural variability of the reported mean. Multiple regression equations were used to explain the relative contribution of control parameters in regulating both *ET* and *T* (Clulow *et al*., 2013). Error associated with EC flux measurements was determined following methods in Kroon *et al.* (2010). The accuracy of the SHB method and steady-state assumption was calculated using methods described in Skauratani (1982), Groot and King (1992) and Grime *et al.* (1995). Finally, ventilated chamber error, frequently associated with changes to Q^* and the underlying microclimate, was calculated following McLeod *et al*. (2004).

Chapter Four
Results

4.1 Climate

Over the study period the May to August monthly mean daytime T_a were 11.7 °C, 15.9 °C, 15.9 °C, and 18.0 °C at Pauciflora, and 13.9 °C, 19.6 °C, 20.5 °C, and 19.6 °C at Poplar, respectively (Figures 6). T_a varied significantly between the two sites (Z = -9.149, $p < 0.01$) (n=113); Poplar generally reported higher values with a seasonal mean of 18.4 °C compared to Pauciflora at 15.2 °C. However, mean T_a averaged between both sites were higher than climate normal for the region (1981-2010) (Environment Canada, 2015). Mean daily T_g at Pauciflora were below freezing (mean -0.04 °C) between DOY 121 – 131, while mean T_g at Poplar remained above freezing throughout the duration of the study period aside from the first two days in May (mean -0.87 °C) (DOY 121 – 122). The highest T_g recorded at a depth of 2 cm was 19.9 °C and 21.5 °C on DOY 183 at Pauciflora and Poplar, respectively. A comparison of T_g reported at both fens demonstrated a significant variation (Z = -3.491, $p < 0.01$) (n=123) between the seasonal means of 13.4 °C and 13.9 °C, at Pauciflora and Poplar respectively. *RH* tended to increase over the study period with both sites reporting a seasonal mean of approximately 67%; demonstrating spikes that corresponded with *P* events. *RH* did not significantly vary between the two fens (t = 0.130, $p > 0.05$) (n=113).

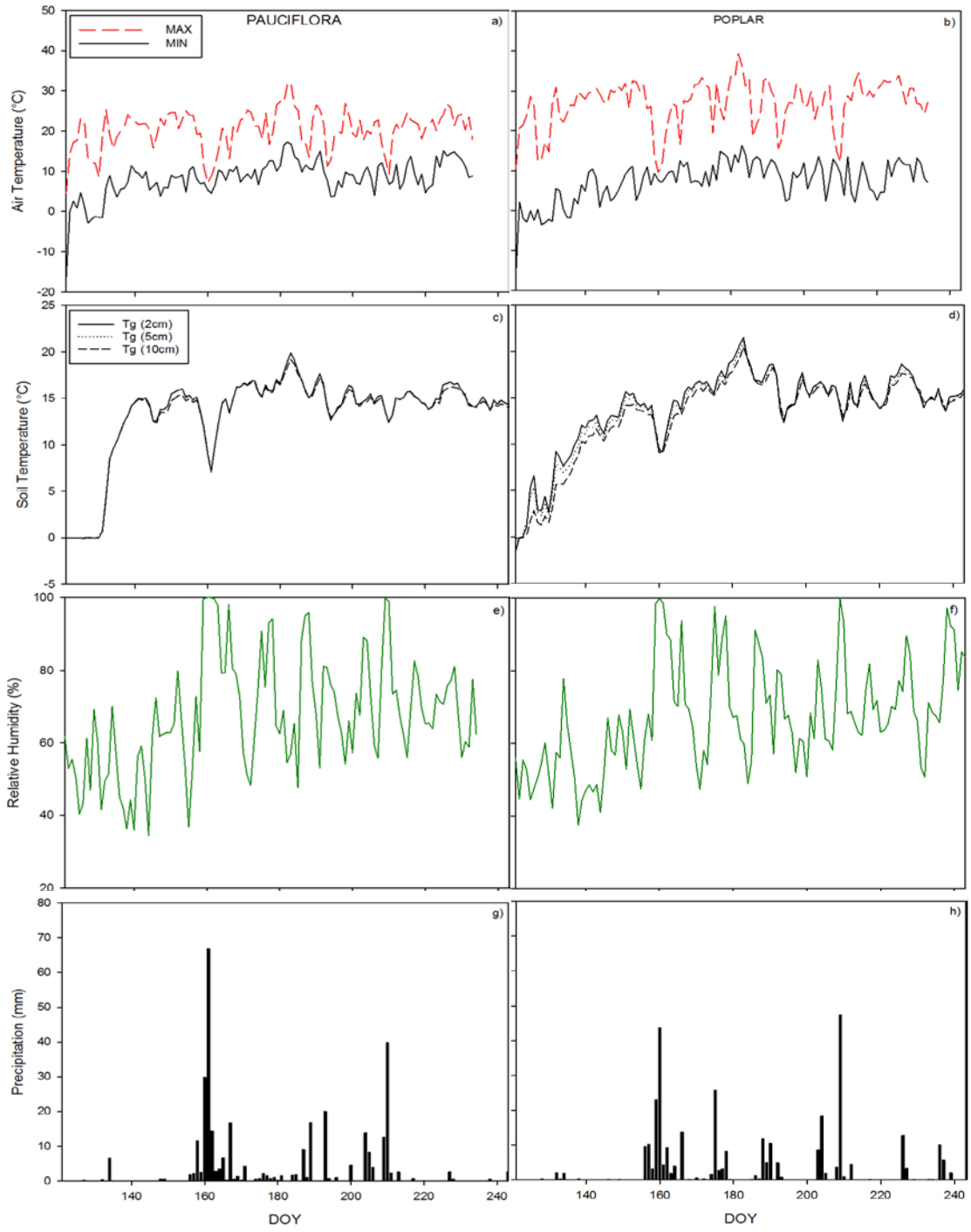

Figure 6: Daily (a)(b) maximum and minimum air temperatures (T_a, °C) (6m)(3m), (c)(d) mean soil temperatures (T_g, °C) (2,5,10 cm depths), (e)(f) mean relative humidity (*RH*, %) (6m)(3m) and (g)(h) total precipitation (*P*, mm) over the 2013 growing season at Pauciflora and Poplar fen, Fort McMurray, Alberta, Canada.

The majority of *P* fell midseason, with Pauciflora and Poplar receiving 327.1 and 320.8 mm of rain between May to August, respectively (Figure 7). Pauciflora and Poplar received 79.5 and 73.2 mm more *P* for this period, respectively, relative to the 30-year average of 247.6 mm for May to August (Environment Canada, 2015). Flooding conditions developed early in the season at both sites due to multiple high magnitude *P* events that occurred in early June. Maximum *P* events occurred on DOY 161 and 210 Pauciflora received 66.8 and 39.8 mm of rain, while Poplar received 43.8 and 47.4 mm respectively.

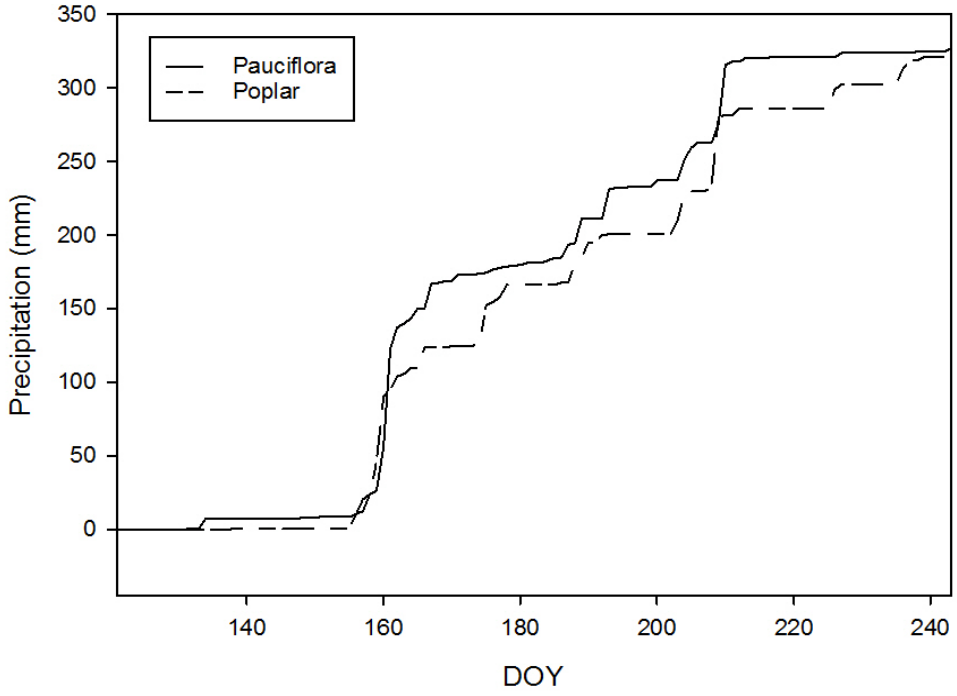

Figure 7: Cumulative precipitation recorded at the Pauciflora and Poplar fens over the 2013 growing season, Fort McMurray, Alberta, Canada.

Monthly average daytime vapor pressure deficits (*VPD*) ranged between 0.7 and 0.8 kPa at Pauciflora, and 1.0 to 1.2 kPa at Poplar. *VPD* reached maximum values when *Q** was also the largest, peaking at 2.1 and 3.0 kPa on DOY 182 at Pauciflora and Poplar, respectively. *VPD* fluctuated throughout the study period, generally demonstrating an inverse relationship to windspeed (u, m s^{-1}) (Figure 8); seasonal patterns are described in the following section.

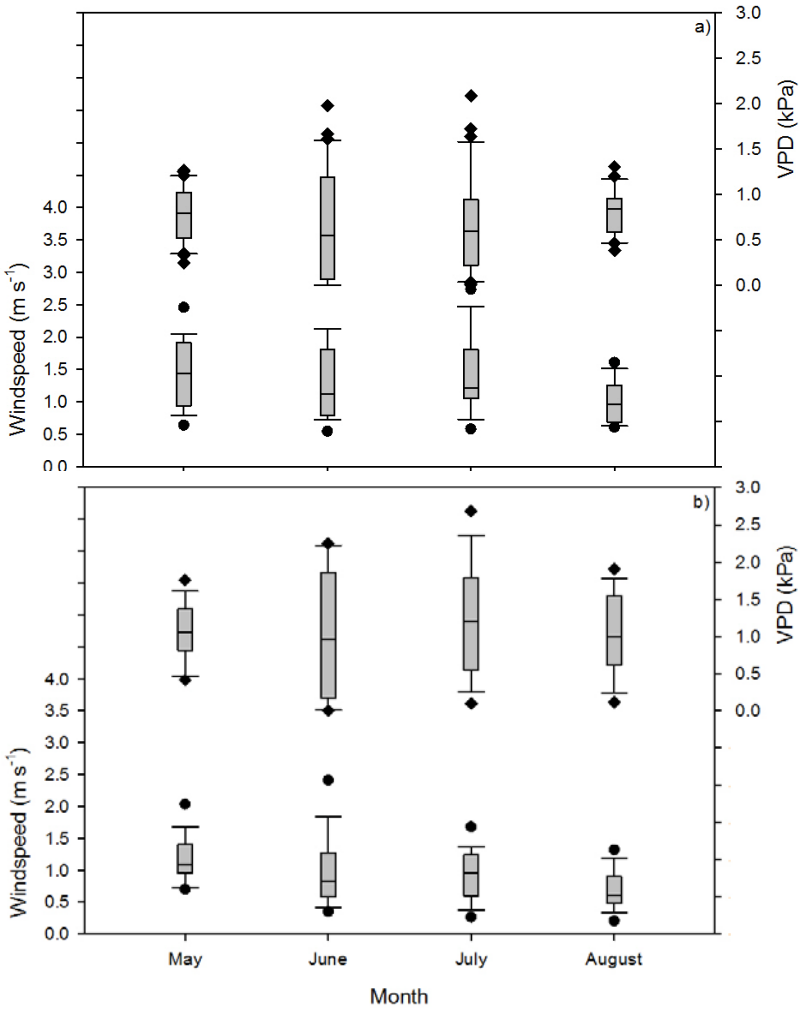

Figure 8: Monthly average windspeed (*u*, m s^{-1}) and vapour pressure deficit (*VPD*, kPa) with standard deviation error bars measured during the daylight hours at (a) Pauciflora and (b) Poplar fen, Fort McMurray, Alberta, Canada.

4.2 Meteorological Tower Flux Footprint

During the 2013 growing season the upwind location of the x_{frac} flux originated approximately 100 m and 120 m from an upwind distance (Table 5) at Pauciflora and Poplar, respectively. The upwind flux distance was largest in May, during the *EG* period of plant growth, at 112 m and 133 m, and smallest in August, the *LG* period, with averages dropping to 48 m and 109 m at Pauciflora and Poplar, respectively. Flux source areas are dependent on windspeed (u) (m s^{-1}) and wind direction (degrees), in conjunction with the upwind source vegetation and canopy structure. The mean u at Pauciflora was 1.7 m s^{-1}; reaching peak momentums throughout the months of June and July ranging between 3.0 and 4.6 m s^{-1}. Poplar reported a lower average of 1.0 m s^{-1}, with maxima occurring sporadically throughout May to July ranging between 1.8 and 3.0 m s^{-1}. Consistently higher u rates at Pauciflora contributed to the fen's smaller footprint. Frictional velocity (u*) (m s^{-1}) averaged 0.002 at Pauciflora and 0.39 at Poplar over the entire growing season. Results are dictated by roughness height; Pauciflora's sparse canopy measured at an average height of 4.2 m compared to 6.5 m at Poplar (Table 3, 4), while the understory reached a maximum height of ~ 0.4 m in contrast to Poplar at ~0.7 m.

Site	Month	u (m s^{-1})	u* (m s^{-1})	Wind Direction (degrees)	Footprint Length x_{max} (m)	Footprint Length x_{frac} (m)
PFLORA	MAY	1.88	0.002	194	24.9	112.0
	JUN	1.74	0.001	203	19.8	88.7
	JUL	1.85	0.002	186	22.0	98.6
	AUG	1.46	0.000	188	10.6	47.7
POPLAR	MAY	1.19	0.186	170	29.8	133.6
	JUN	1.00	0.142	179	26.5	118.7
	JUL	0.93	0.388	160	28.4	127.2
	AUG	0.69	0.233	176	24.5	109.8

Table 5: The 2013 growing season mean wind speed (u, m s^{-1}), mean frictional velocity (u*, m s^{-1}), wind direction (degrees) and averaged flux footprint length of the peak contributing area (x_{max}, m) and the 80 % contribution area (x_{frac}, m) for the EC tower installed at Pauciflora (PFLORA) and Poplar Fen, Fort McMurray, Alberta, Canada.

In addition, it is necessary to define the nature of the flux based on wind direction. The upwind source governs the direction of the fluxes and was estimated with a WindRose diagram (Figures 10) (Lakes Environmental Software). The results reveal that the majority of the flux footprint originated from the east and south-east portion of the fens, with Pauciflora tending towards the south and Poplar towards the east. The southern portion of Pauciflora consists of a sparse to completely bare canopy that includes the dominant tree species *Picea mariana*. The understory is composed of the dominant shrub species *Oxycoccus microcarpus*, *Rhododendron groenlandicum*, *Andromeda polifolia* as well as *Carex aquatilis*. The eastern portion of Poplar is composed of a dense canopy of the dominant tree species *Larix laricina*, with a dense understory consisting of *Betula pumila*, *Ledum groenlandicum,* and *Equisetum fluviatile*.

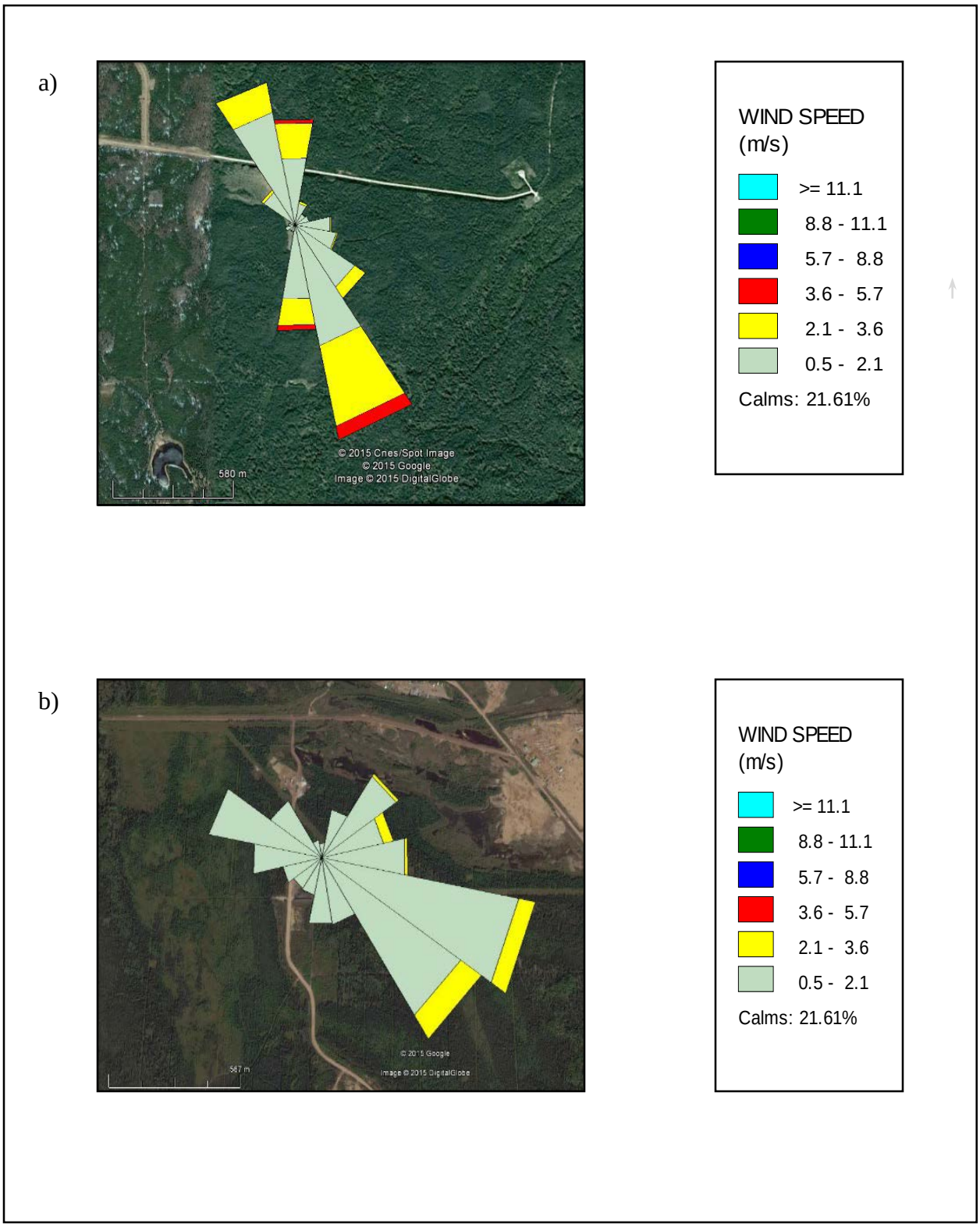

Figure 10: WindRose diagram partitioning wind direction and speed (m/s) over the 2013 growing season at (a) Pauciflora and (b) Poplar fen, Fort McMurray, Alberta, Canada.

4.3 LiDAR Land Cover Classification

Groundcover species captured within chamber plots, accurately classified ~ 50% and ~ 60% of the vegetation communities projected by the LiDAR land-cover classification within the entire fen boundary, at Pauciflora and Poplar, respectively. Table 6 and 7 display the results from the fusion-based spectral and airborne LiDAR derived land-cover classification. Four output maps for each fen are shown in Figure 10 and 11, which display classified vegetation cover (Figure 10a, 11a), microforms (hummocks, hollows, lawns and saturated areas) (Figure 10b, 11b), dominant vegetation cover captured by the flux footprint x_{frac} (Figure 10c, 11c) and x_{max} (Figure 10d, 11d).

Pauciflora is composed of 35% hummocks and 35% hollows, with remaining ground cover either consisting of lawn or saturated areas. In comparison, Poplar's microtopography is 47% hummocks and 53% hollows within the fen area. Poplar's dense canopy limited the degree of ground cover that could be detected and classified through airborne LiDAR, therefore identified chamber species were compared against additional vegetation surveys conducted within the fen (data not shown). The hummocks at Pauciflora are on average covered by 33% vascular vegetation with a mean height of 17 cm, while vascular vegetation cover within hollows are marginally lower with a mean of 30% and an average plant height of 16.5 cm. The hummocks at Poplar were on average covered by 25% vascular species and sustained a mean height of only a few centimeters. This does not account for the dominant *Betula pumila* sub-canopy that averages a few meters in height. Conversely, hollows were covered by < *10*% vascular vegetation with a mean height of < 1 cm. The hollows are concave features that occasionally contained pooling water at Pauciflora with a mean *VMC* of 80%**,** but a majority remained permanently flooded at Poplar. Conversely, hummocks were on average topographically higher than hollows, by 12 cm at Pauciflora and only 5 cm higher at Poplar.

Class	Species	Topography	Percent cover within fen boundary	Percent cover within the tower footprint (80% Contribution)
4	High cover *Rhododendron gro*., High cover *Sphagnum ang*.	Hummock Hollow	6.4	1.4
5	Medium cover *Rhododendron gro*., High cover *Sphagnum ang*.	Hummock Hollow	18.4	26.7
106	Low cover *Rhododendron gro.* High cover *Sphagnum ang.*	Hollow	4.0	1.5
111	Medium cover *Smilacena trifolia*, High cover *Sphagnum ang*.	Hollow	2.4	2.5
112	Medium cover *Carex aquatilis*, High cover *Sphagnum ang*.	Lawn	3.1	2.6
206	Low cover *Carex aquatilis*, High cover *Sphagnum ang*.	Hollow	3.9	2.1
210	High cover *Sphagnum ang.*	Lawn	1.7	3.2
211	Medium cover *Sphagnum ang*., Medium cover *Sphagnum mag*.	Lawn	1.8	2.5
308	High cover *Andromeda polifolia*, Medium cover *Sphagnum mag*.	Hummock	5.9	7.4
312	Medium cover *Rhododendro gro.*	Hummock	3.2	2.4

Table 6: Summary of results from the land-cover classification, derived from fusion-based spectral and airborne LiDAR data, Pauciflora fen, Fort McMurray, Alberta, Canada (2013). Associated with Figure 10.

Class	Species	Topography	Percent cover within fen boundary (%)	Percent cover within the tower footprint (80% Contribution)
41	Low cover *Larix laricina*	Hummock	8.4	5.8
42	Medium cover *Larix laricina*	Hummock	11.4	9.4
44	High cover *Larix laricina*	Hummock	10.8	10.8
70	Saturated area	Hollow	2.6	2.5
71	High cover *Betula pumila*	Hummock Hollow	6.0	5.5
72	Low cover *Picea mariana*, High cover *Tomenthypnum nitens*	Hummock	9.8	8.8
73	Medium cover *Picea mariana*, Medium cover *Tomenthypnum nitens*	Hummock	9.2	8.1
74	High cover *Picea mariana*, Low cover *Tomenthypnum nitens*	Hummock Hollow	8.0	6.6

Table 7: Summary of results from the land-cover classification derived from fusion-based spectral and airborne LiDAR data, Poplar fen, Fort McMurray, Alberta, Canada (2013). Associated with Figure 11.

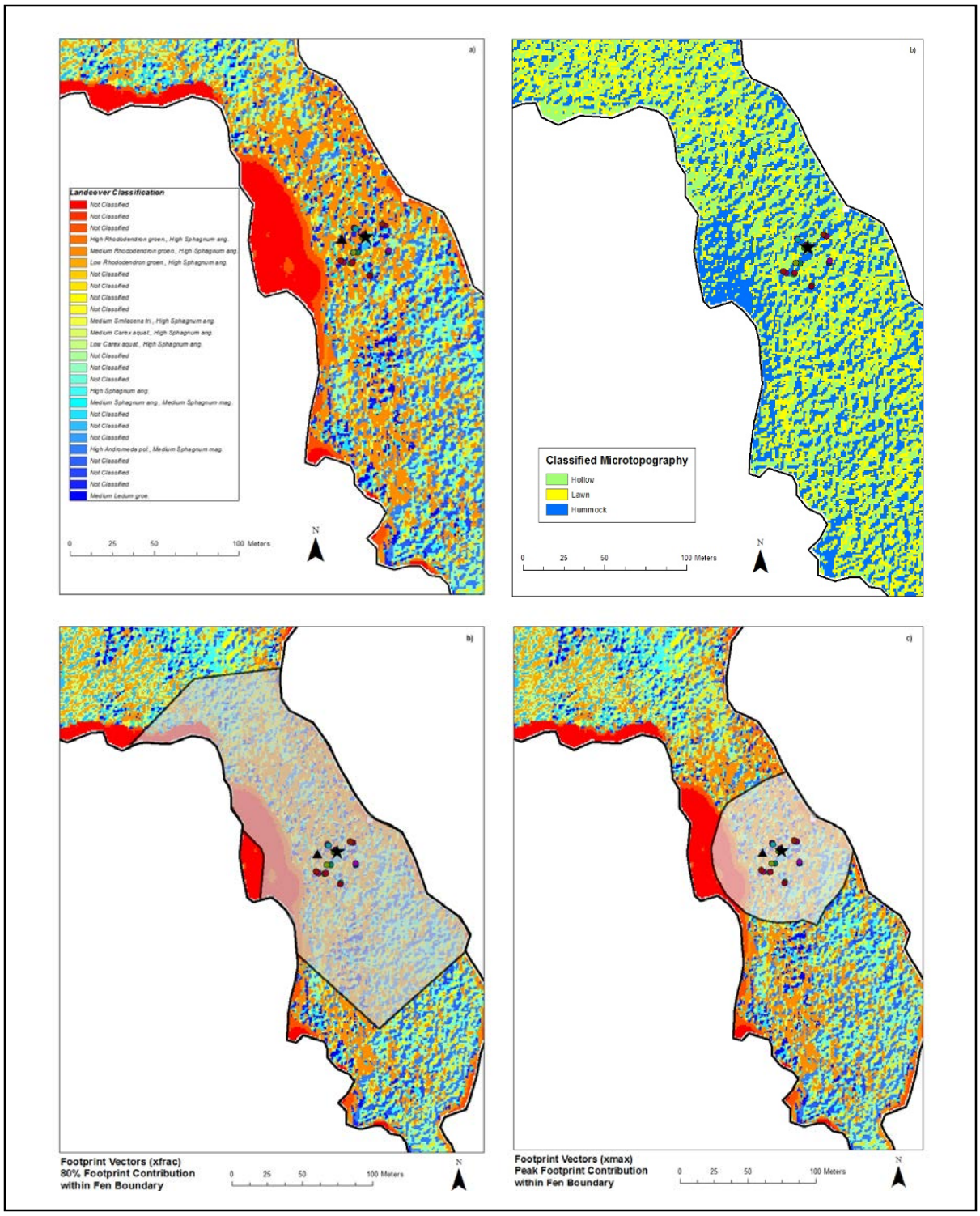

Figure 10: LiDAR output data, groundcover classification with applied maximum likelihood classification and fusion with topographic morphology and vegetation structure of species types and mixed vegetation cover within microforms, (b) classified microforms, (c) 80% contribution footprint vectors (x_{frac}) and (d) peak footprint vectors (x_{max}), Pauciflora fen, Fort McMurray

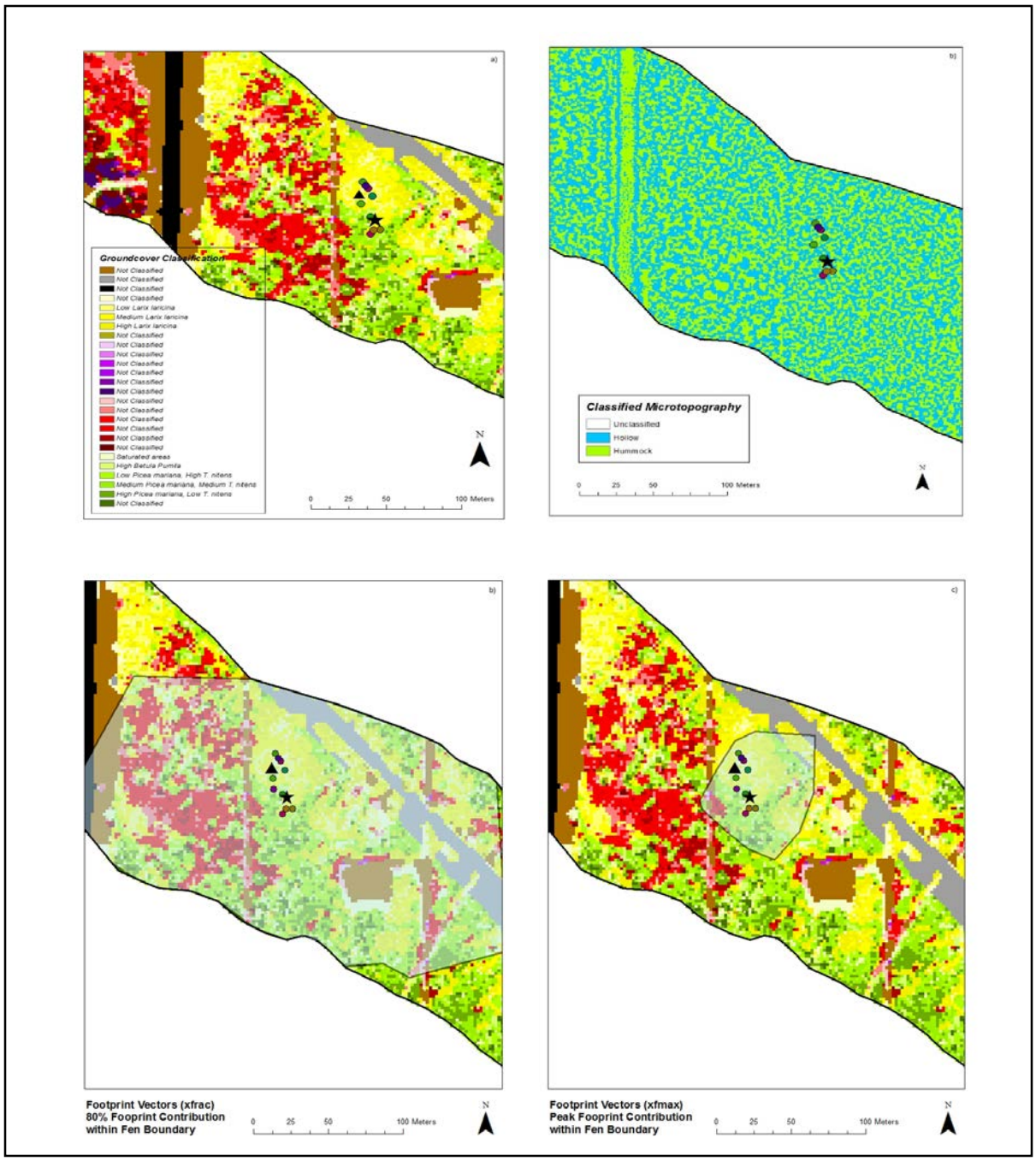

Figure 11: LiDAR output data (a) groundcover classification with a vector machine supervised classification and fusion with topographic morphology and vegetation structure of species types and mixed vegetation cover within microforms, and (b) classified microforms, cb) 80% contribution footprint vectors (x_{frac}), and (d) peak footprint vectors (x_{max}), Poplar fen, Fort McMurray, Alberta.

4.4 Energy Flux Densities

Q^* fluctuated throughout the season, peaking in mid-May through to early July, reaching a maximum of 201 W m^{-2} on DOY 172 and 215 W m^{-2} on DOY 154 at Pauciflora and Poplar, correspondingly. Q^* declined during the last month of the study period, mean August Q^* was 95 W m^{-2} compared to the seasonal mean of 111 W m^{-2} at Pauciflora, and 120 W m^{-2} compared to the seasonal mean of 137 W m^{-2} at Poplar. Throughout the growing season, mean Q^* remained significantly higher at Poplar compared to Pauciflora ($U = 4963$, $p < 0.01$). However, missing Q^* data, between DOY 234 and 243, is likely producing an inflated seasonal average. Both sites displayed similar seasonality in energy balance components with peaks generally occurring on the same DOY, reaching a maximum between 1200-1430 MST (Figure 13) and decreasing in intensity in the evening (1700-1900 MST) and early morning (0630-0830 MST). Energy fluxes Q^*, Q_E and Q_H were generally positive during the day and negative at night.

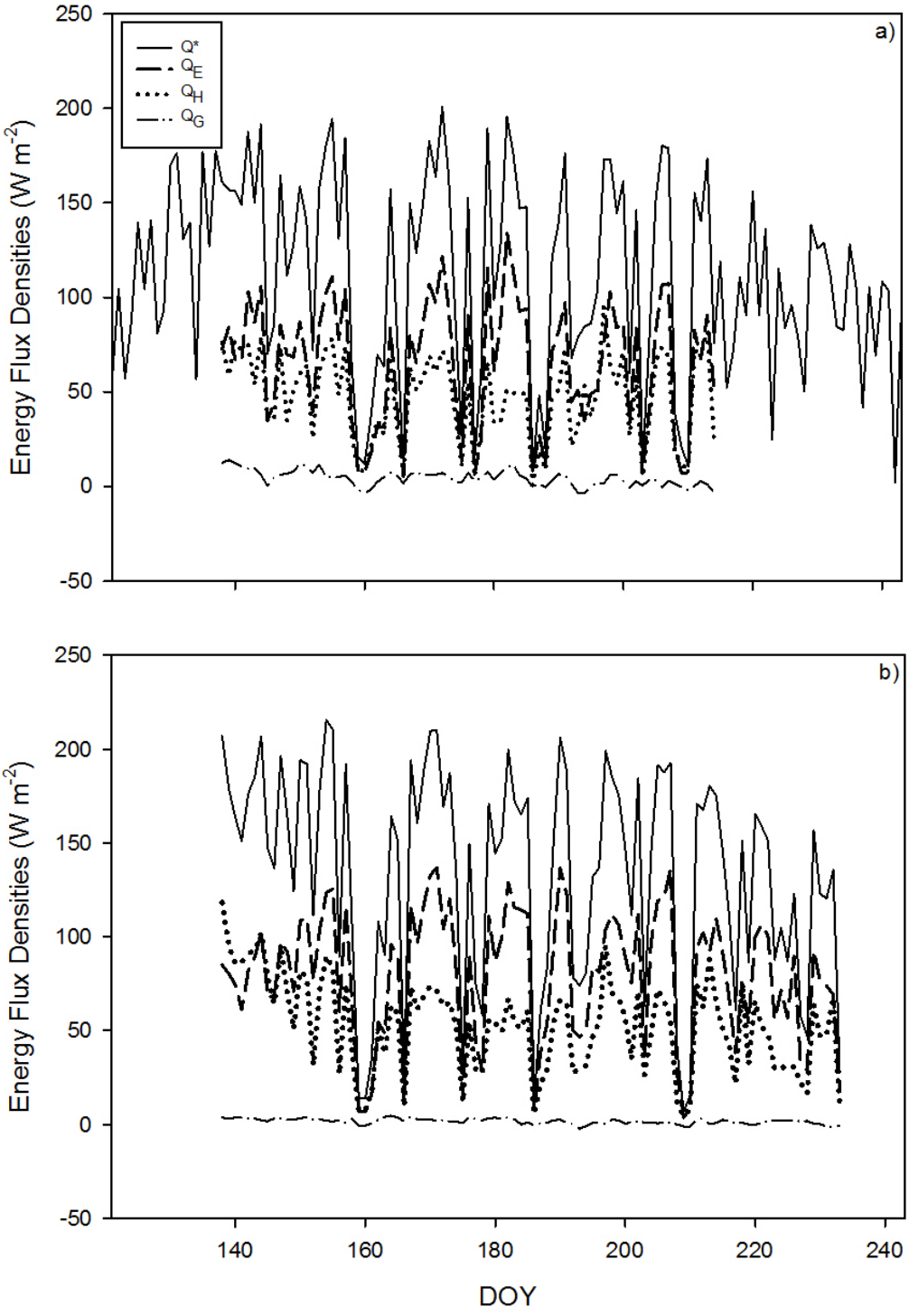

Figure 12: Mean daily wetland energy flux densities (W m^{-2}) for the 2013 growing season, at (a) Pauciflora, and (b) Poplar fen, Fort McMurray, Alberta, Canada.

Q_E represented the dominant flux at Pauciflora for a majority of the growing season, averaging 65 W m^{-2}. Q_E reached a seasonal maximum of 134 W m^{-2} on DOY 182, compared to Q_H that peaked later in the season at 95 W m^{-2} on DOY 197. Mean Q_H was 47 W m^{-2} (Figure 12a). Similarly, there was a marked dominance of Q_E over Q_H at Poplar throughout a majority of the growing season, with the exception of energy fluxes recorded during the early green period (Figure 12b). Q_E peaked at 137 W m^{-2} on DOY 171, 190 and 207, during the defined *G* period of plant growth. Peaks in Q_E generally followed periods of moderate *P* (events > 10 mm) and increasing Q^*. Mean Q_E was 80 W m^{-2} compared to the seasonal mean of Q_H of 53 W m^{-2}. As previously mentioned, Q_H peaked early in the season at 118 W m^{-2} on DOY 138.

Site	**Month**	Q^* **(W m^{-2})**	**S.D.**	Q_G **(W m^{-2})**	**S.D.**	Q_E **(W m^{-2})**	**S.D.**	Q_H **(W m^{-2})**	**S.D.**	$Q^* - Q_G$ **(W m^{-2})**	Q_E / Q^*-Q_g	Q_H / Q^*-Q_g
PFLORA	MAY	**143.7**	±34.8	**8.7**	±3.7	**74.4**	±19.7	**60.5**	±16.8	**135.0**	0.55	0.45
	JUN	**111.0**	±62.7	**4.7**	±3.2	**62.9**	±37.8	**43.5**	±23.3	**106.3**	0.57	0.43
	JUL	**110.4**	±60.5	**2.5**	±3.5	**63.2**	±36.7	**44.8**	±24.6	**107.9**	0.58	0.42
	AUG	**95.4**	±40.0	**- 1.0**	±2.9	**71.7**	±26.7	**54.0**	±39.5	**99.6**	0.60	0.40
POPLAR	MAY	**173.1**	±26.1	**3.0**	±0.6	**85.0**	±15.7	**85.1**	±16.7	**170.1**	0.50	0.50
	JUN	**133.2**	±64.7	**2.4**	±1.3	**81.0**	±41.1	**50.0**	±23.7	**130.8**	0.62	0.38
	JUL	**132.2**	±62.5	**1.0**	±1.4	**83.3**	±40.0	**48.0**	±23.1	**131.2**	0.64	0.36
	AUG	**117.0**	±44.2	**0.9**	±1.1	**71.6**	±26.5	**44.6**	±20.8	**116.1**	0.62	0.38

Table 8: The monthly mean net radiation (Q^*), soil heat flux (Q_G), latent heat flux (Q_E), sensible heat flux (Q_H) and available energy (Q^*-Q_G); relative latent heat flux (Q_E/Q^*-Q_G) and relative sensible heat flux (Q_H/Q^*-Q_G) for the 2013 growing season at Pauciflora (PFLORA) and Poplar Fen, Fort McMurray, Alberta, Canada. (Pauciflora August means contain missing data; instrument failure).

Energy flux components, expressed as a ratio of Q^*-Q_G, are shown in Table 8. Pauciflora was governed by the relative latent heat flux (Q_E/Q^*-Q_G), peaking following high magnitude *P* events, or multiple low magnitude *P* events. Conversely, at Poplar there was a shift from the early season green period that was equally governed by Q_H/Q^*-Q_G that switched with the onset of 'leaf out' to periods regulated by the relative latent heat flux (Q_E/Q^*-Q_G).

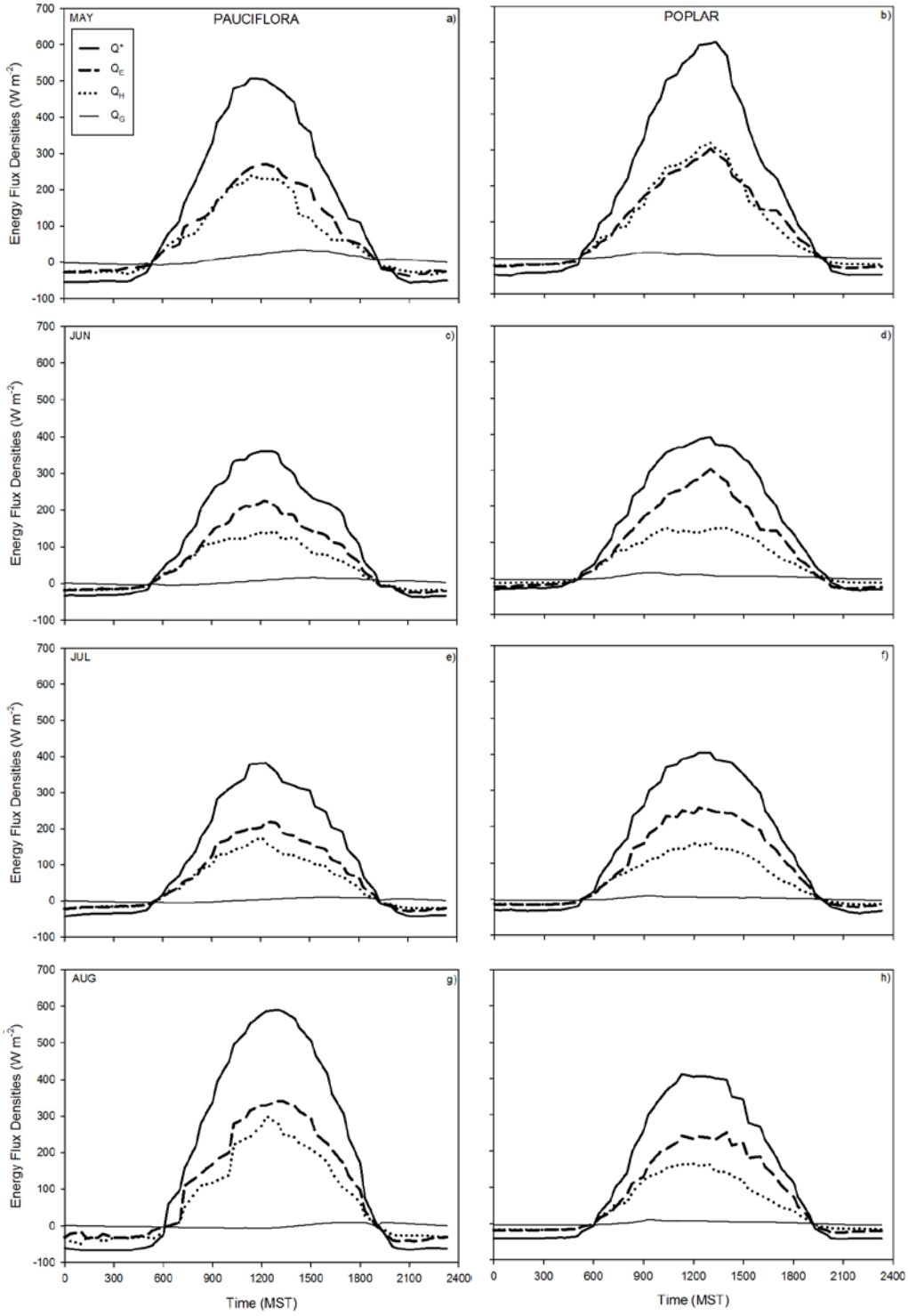

Figure 13: Hourly mean wetland energy flux densities (W m^{-2}) for each month in the 2013 growing season, at Pauciflora and Poplar fen, Fort McMurray, Alberta, Canada.

4.5 Total Evapotranspiration

Pauciflora *ET* fluctuated over the growing season, averaging 2.3 mm d^{-1} (± 1.2). Although missing data may be inflating the *ET* fluxes throughout August, as the late study period exhibited a notable reduction in *Q** and increase in *RH*. *ET* reached a maximum on DOY 182 at 4.6 mm d^{-1}. Conversely, daily *ET* at Poplar was less variable, averaging ~1 mm d^{-1} higher than Pauciflora with a seasonal mean of 3.6 mm d^{-1} (± 0.6). Daily *ET* demonstrated a noticeable decline throughout August with a mean of 3.3 mm d^{-1} (± 0.4). In contrast to Pauciflora, Poplar recorded multiple peak *ET* events (> 4.5 mm d^{-1}) throughout the green period of plant growth. Both sites displayed similar seasonality, peaking mid-season during the period of maximum 'leaf out.' Due to Poplar's dense canopy, *ET* was more reactive to the growth cycles of the vegetation. Overall, Pauciflora reported lower seasonal *ET* rates exhibiting greater variance (σ^2), 1.4 (n=77) from the mean, whereas *ET* recorded at Poplar was not only higher but exhibited lower σ^2, 0.33 (n=95), from the seasonal mean.

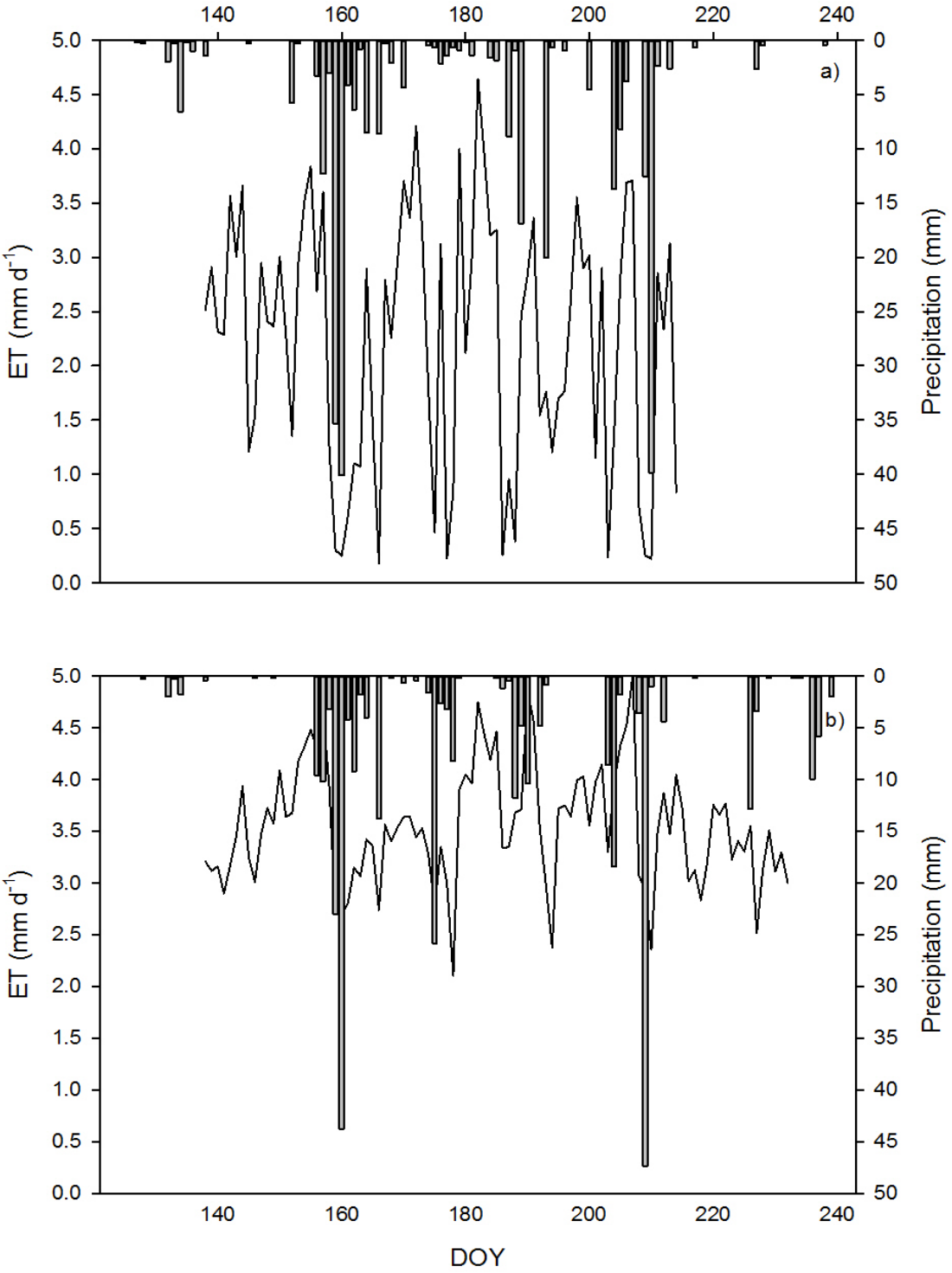

Figure 14: Daily evapotranspiration (*ET*) (mm d^{-1}) and precipitation (*P*) (bars) (mm) by DOY for the 2013 growing season, measured at (a) Pauciflora and (b) Poplar fen, Fort McMurray, Alberta, Canada.

Pauciflora *ET* was significantly correlated with available energy (Q^*-Q_G) ($F(1,75) = 21.981$, $p < 0.01$), and formed a strong linear relationship with daily *ET* ($R^2 = 0.95$) (n=56). *ET* demonstrated a similar response to *VPD* ($F(1,75) = 20.368$, $p < 0.01$; $R^2 = 0.60$) (n=56) but it was less responsive to mean daily T_a ($F(1,75) = 14.745$, $p < 0.01$; $R^2 = 0.47$) (n=56) (Figure 15). *ET* did not exhibit a distinguishable response to changes in *VMC*, because the water table remained at or above the surface, *VMC* was never limited. Daily *ET* at Poplar was significantly correlated with available energy *ET* ($F(1,93) = 73.349$, $p < 0.01$), however it provided a weak explanation for the variation in *ET* ($R^2 = 0.41$) (n=74). Daily *ET* demonstrated a similar response to *VPD* ($F(1,93) = 84.892$, $p < 0.01$; $R^2 = 0.48$) (n=74), and mean daily T_a ($F(1,93) = 67.992$, $p < 0.01$, $R^2 = 0.42$) (n=74) (Figure 15). Additionally, peak *ET* events at both fens generally followed large *P* events (Figure 14). Daily *ET* peaked between the daylight hours 1100-1300 MST, when Q^* reached a maximum, followed by a decline when *VPD* reached a daily maximum (Figure 16).

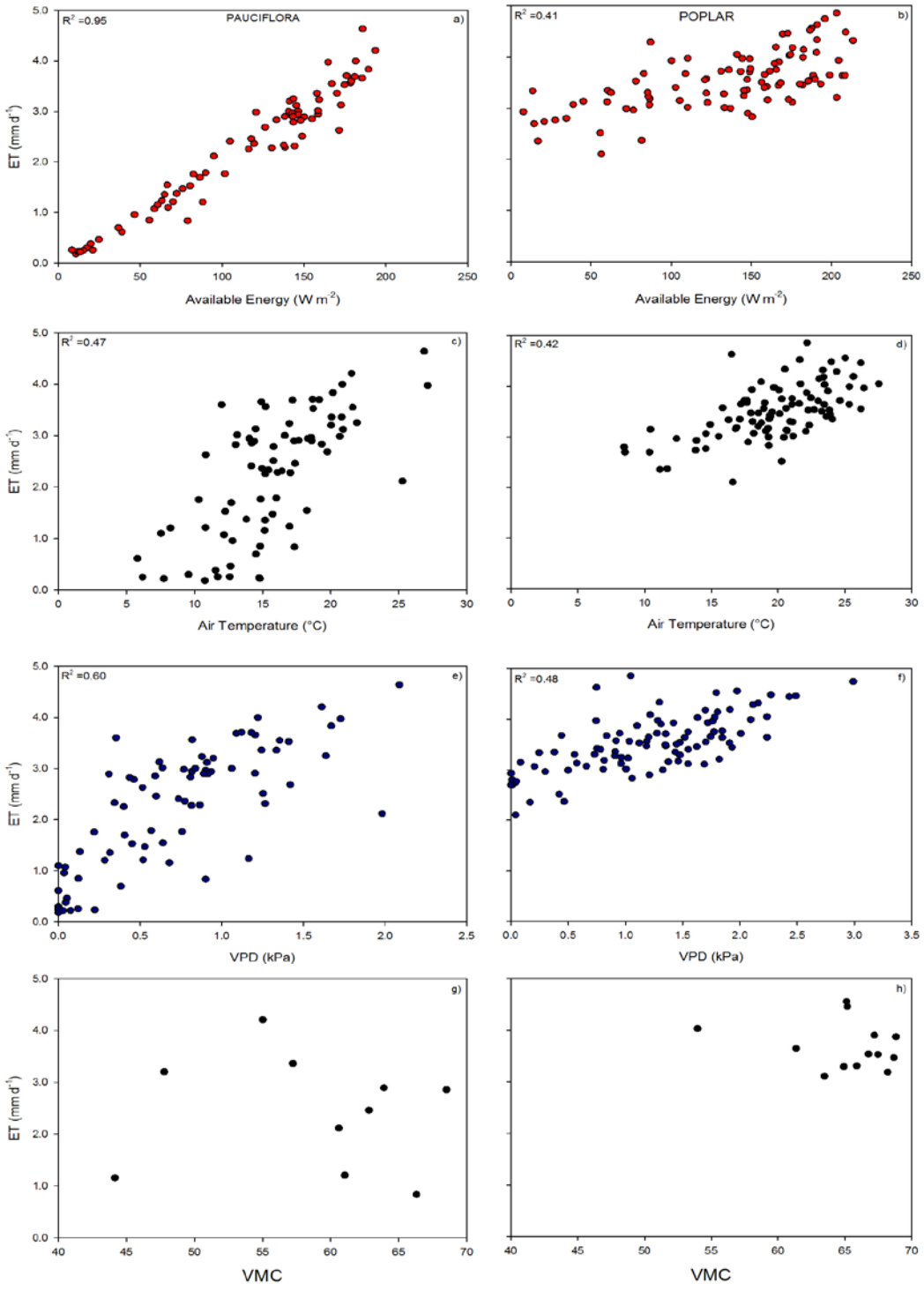

Figure 15: Relationship between *ET* (mm d^{-1}) and (a)(b) available Energy (W m^{-2}), (b)(c) air temperature (T_a)(°C), (d)(e) *VPD* (kPa), and (f)(g) volumetric moisture content (*VMC*), Pauciflora and Poplar fen, Fort McMurray, Alberta, Canada.

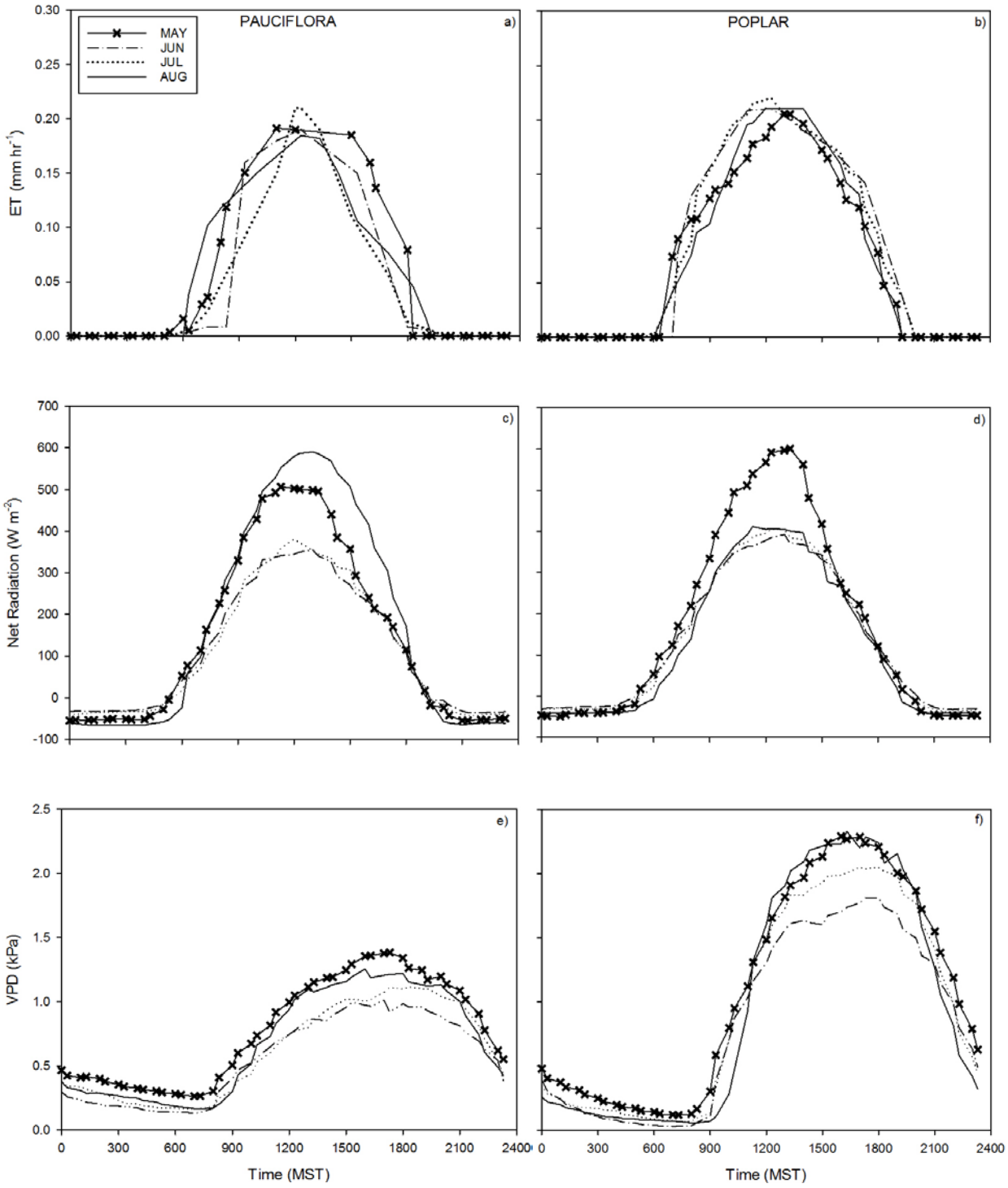

Figure 16: Hourly mean (a)(b) evapotranspiration (*ET*) (mm d^{-1}), (c)(d) net radiation (*Q**) (W m^{-2}) and (e)(f) vapour pressure deficit (*VPD*) (kPa)**,** Pauciflora and Poplar fen, Fort McMurray, Alberta, Canada.

4.6 Canopy Transpiration

Similar to *ET*, canopy transpiration (*T*) at Pauciflora remained fairly consistent over the duration of the study period, exhibiting a seasonal mean of 0.3 mm d^{-1}. Both *ET* and *T* demonstrated comparable seasonal trends that peaked during the *G* period of plant growth, followed by declining rates throughout August. *T* monthly mean was 0.6 mm d^{-1} (± 0.3), 0.3 mm d^{-1} (± 0.2) and 0.2 mm d^{-1} (± 0.1) in June, July and August, respectively (Figure 17a). Poplar *T* and *ET* displayed similar seasonality, with a seasonal mean considerably higher than Pauciflora, averaging 2.7 mm d^{-1}, with larch species contributing roughly 1.5 mm d^{-1} (± 0.5) and black spruce comprising the last 1.2 mm d^{-1} (± 0.3). Monthly means exhibited greater consistency at Poplar than at Pauciflora, with both June and July averaging 3.0 mm d^{-1} (± 0.6), followed by a decline to 2.0 mm d^{-1} (± 0.5) throughout August (Figure 17b).

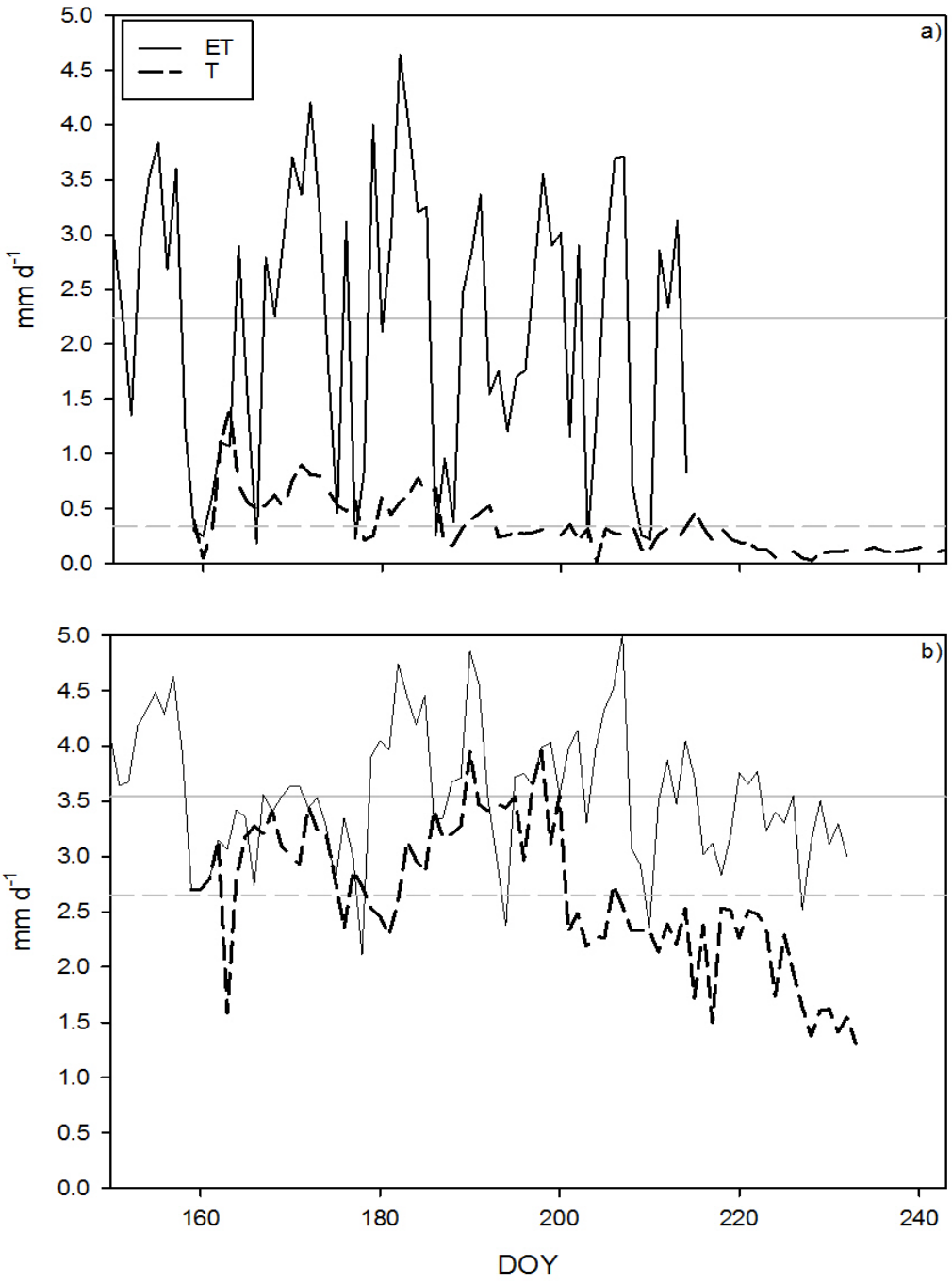

Figure 17: (a) Pauciflora and (b) Poplar fen, evapotranspiration (*ET*) (mm d^{-1}) (seasonal mean solid line) and canopy transpiration (*T*) (mm d^{-1}) (seasonal mean dashed line) by DOY for the 2013 growing season, Fort McMurray, Alberta, Canada.

Cumulative canopy transpiration measured between May and August was 29 mm at Pauciflora and approximately 202 mm at Poplar; not accounting for missing data between DOY 234 to 243 (Figure 18). Pauciflora was composed of a smaller stem density of 58 trees compared to Poplar that supported a substantially higher stem density of 237 trees that were captured in the forest inventory surveys (IEG, 2014).

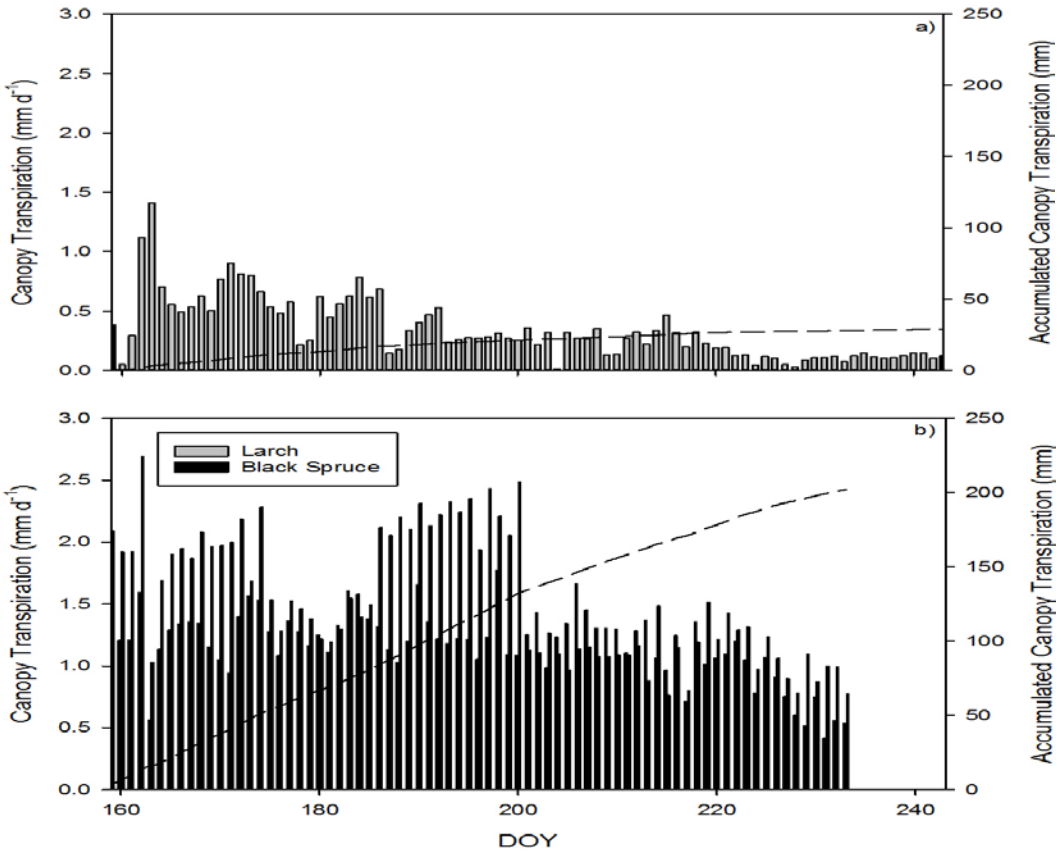

Figure 18: Daily canopy transpiration (mm d^{-1}) (bars) and accumulated water use (dashed line) (mm) at (a) Pauciflora and (b) Poplar fen, by DOY for the 2013 growing season, Fort McMurray, Alberta, Canada.

Canopy Stem Density and LAI

The tree canopy at Pauciflora is predominately *Picea mariana*; the only species captured within the forestry industry surveys (IEG, 2014). Tree growth was stunted, with the largest surveyed tree measuring 9.0 cm in diameter (*DBH*). Mean *DBH* was 5.5 cm (± 1.3) with a corresponding sapwood area of 20.7 cm^2 (*n*=43) (Figure 19a). In contrast, the canopy at Poplar is more diverse, consisting of both *Picea mariana* and *Larix laricina* across a larger size distribution. *Picea mariana* species were generally larger than those at Pauciflora, with the largest tree measuring 17.5 cm in stem diameter. Mean *DBH* of black spruce species was 8.4 cm (± 3.5) with a corresponding sapwood area of 50.0 cm^2 (*n*=51) (Figure 19b). However, within the immediate vicinity of the EC tower (x_{max} footprint), larch represents the dominant species that were on average slightly smaller, with a mean *DBH* of 6.0 cm (± 2.8), and sapwood area of 25.3 cm^2 (*n*=184).

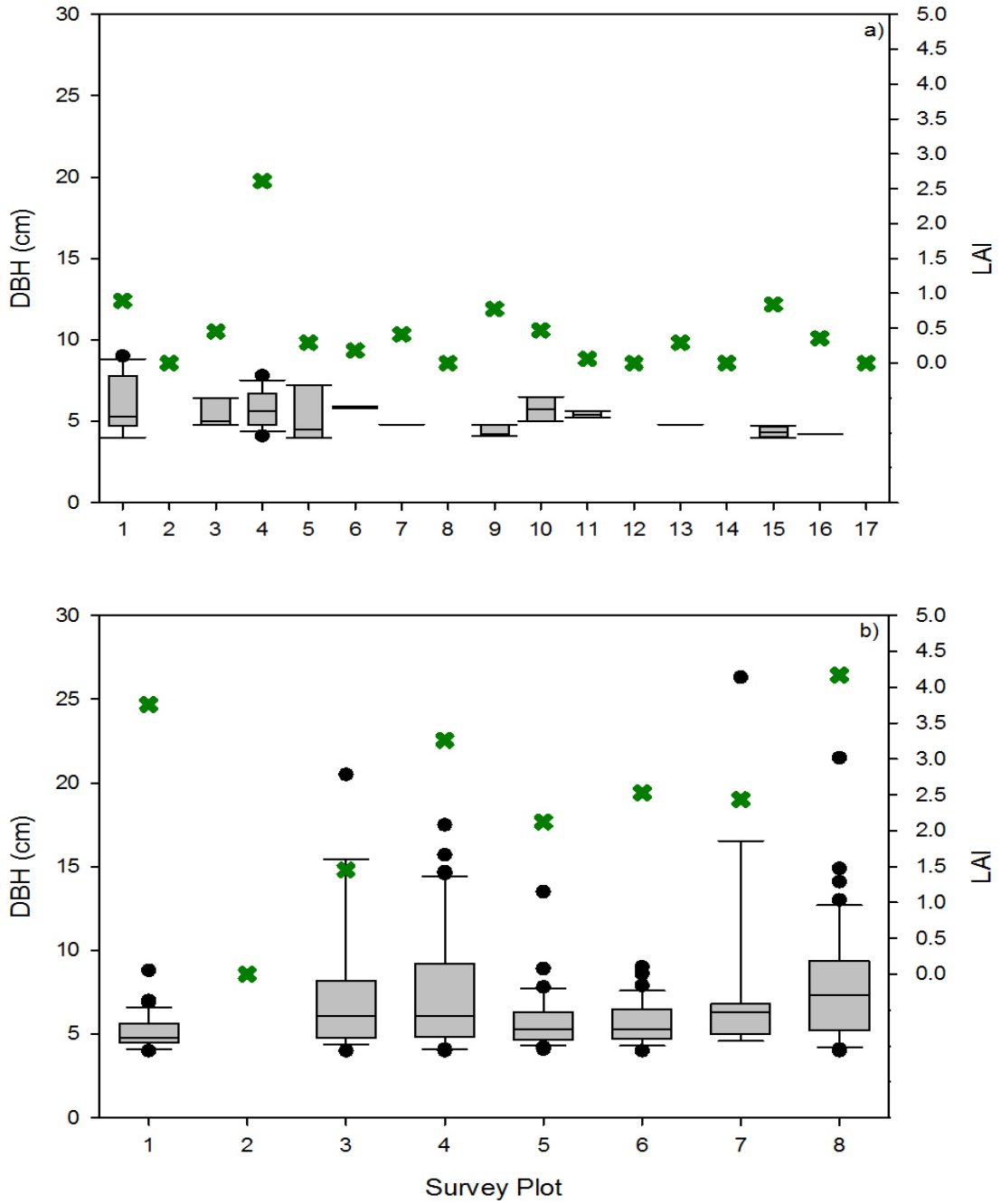

Figure 19: Average *DBH* (box-plot) and *LAI* (line) per plot, measured from Forest Inventory Surveys at (a) Pauciflora and (b) Poplar fen, during the 2013 growing season, Fort McMurray, Alberta, Canada. (Green symbol represent plot *LAI*)

LAI is the leaf material (m^2) per unit of ground area (m^2), and is a biophysical property closely linked to plant *ET* (Allen *et al.*, 1998). Pauciflora had a mean *LAI* of 0.55 (± 0.67) while the canopy at Poplar was significantly higher at 2.82 (± 0.96). However, of the 16 plots measured at Pauciflora, only one plot reported a *LAI* above 1.0. The remaining plots were significantly lower, with some plots completely devoid of tree cover. Removing the outlier plot reduced mean *LAI* to 0.41 (± 0.27). Cumulative monthly *T* at Pauciflora was significantly correlated with canopy *LAI* ($p < 0.01$) when analyzed against all 16 plots (Figure 20a). However, removing the outlier plot diminished the strength of the relationship and the correlation was not significant ($p > 0.01$). Similarly, cumulative monthly *T* at Poplar demonstrated a weak to moderate correlation with canopy *LAI*, with an average $R^2 = 0.30$ (Figure 20b).

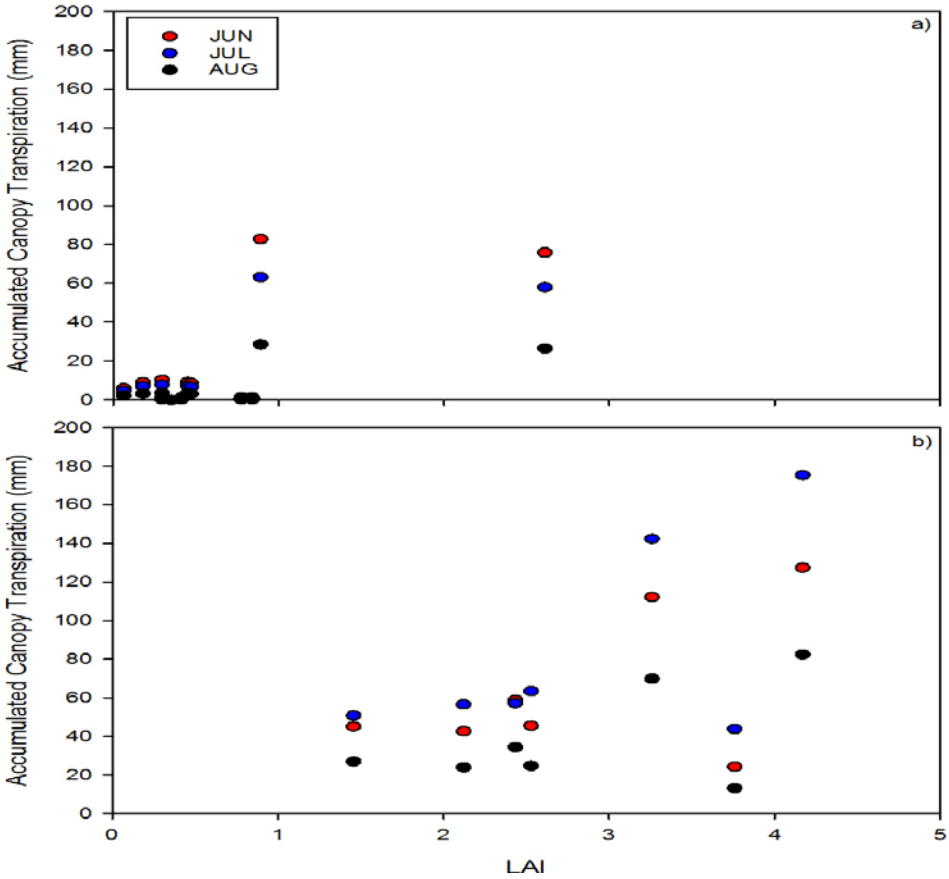

Figure 20: Accumulative monthly Transpiration (mm) plotted against plot *LAI*, for (a) Pauciflora and (b) Poplar fen, measured over the 2013 growing season, Fort McMurray, Alberta, Canada.

Micrometeorological and Climate Controls

T was compared to micrometeorological parameters including Q^*-Q_G, T_a *RH*, *P*, and *VMC* to determine the individual and combined drivers of *T* (Figure 21, Table 9). Additionally, *T* was compared by simple linear regression to *VPD* (Figure 22, 23). An analysis of the aforementioned variables produced a significantly correlated relationship with *T* ($p < 0.05$). An individual analysis of each variable revealed that Q^*-Q_G was the most significantly correlated with *T*. The multiple regression produced an $R^2 = 0.50$, moderately explaining variation in *T*; generally exhibiting an increase in *T* that corresponded with an increase in magnitude of the predictor variables. Residuals were normally distributed and an analysis of accumulated observed against accumulated predicted values produced a strong fit $R^2 = 0.96$. Conversely, Poplar *T* was not significantly correlated with the aforementioned variables. However, *T* was the most responsive to changes to Q^*-Q_G, demonstrating similarity between peak events, and moderately responsive to changes in T_a (Figure 21, Table 9).

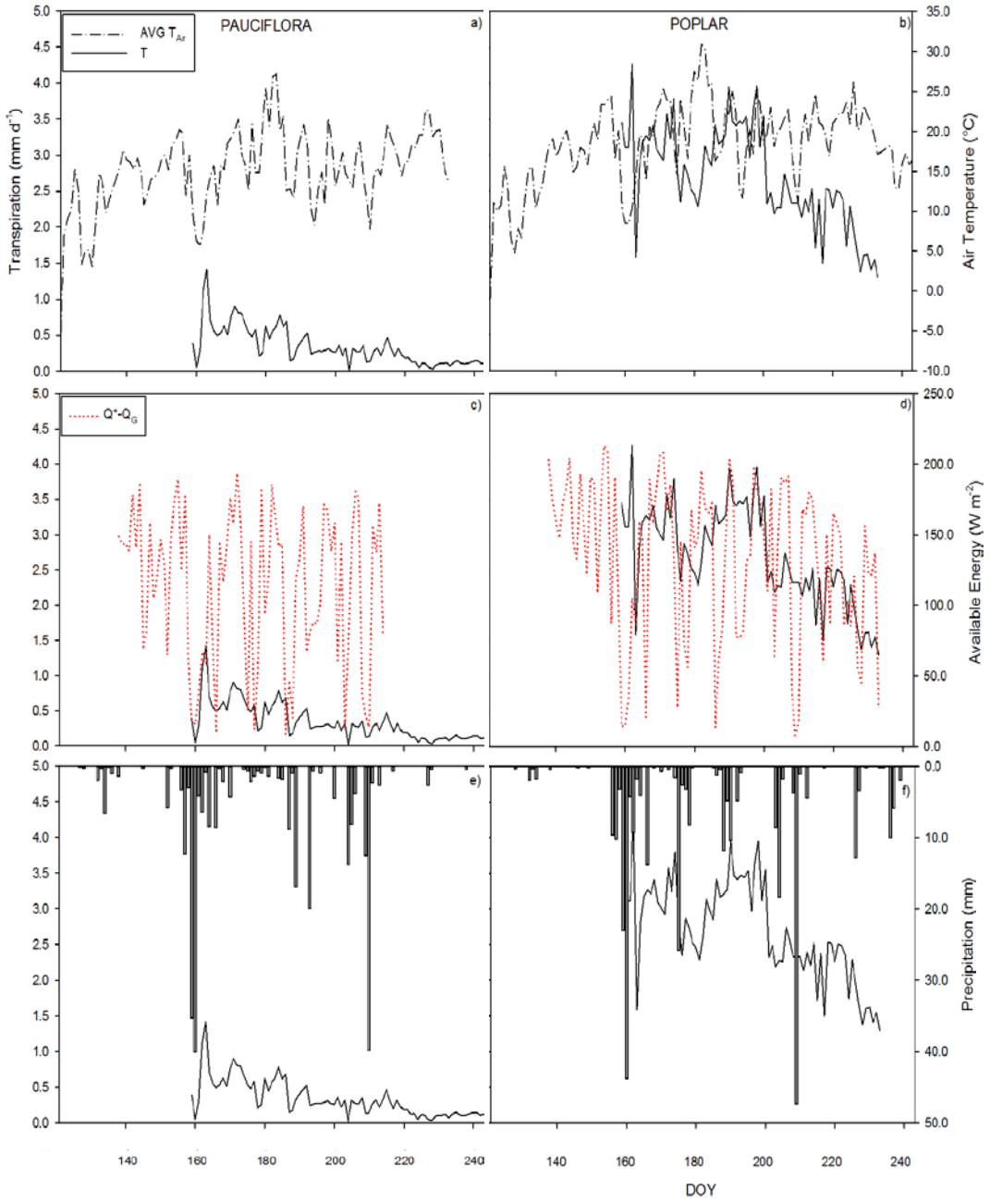

Figure 21: *T* (mm d^{-1}) plotted against (a)(b) max and min daily air temperature (°C), (c)(d) available energy (W m^{-2}), and (e)(f) precipitation (mm) by DOY at Pauciflora and Poplar fen, Fort McMurray, Alberta.

a) PAUCIFLORA										
Period	*ET*	*T*	Q^*-Q_G	*u*	*VPD*	T_a		*RH*	*P*	*VMC*
						MIN	MAX			
	(mm)	(mm)	(W m^{-2})	(m s^{-1})	(kPa)	(°C)		(%)	(mm)	(%)
EG	2.5		134.8	1.9	0.8	4.9	19.6	54.8	12.6	
G	2.5	0.4	104.4	1.7	0.7	9.6	20.2	75.0	308.4	57.0
LG	-	0.1	-	1.5	0.8	10.9	22.4	68.5	6.1	54.6

b) POPLAR										
Period	*ET*	*T*	Q^*-Q_G	*u*	*VPD*	T_a		*RH*	*P*	*VMC*
						MIN	MAX			
	(mm)	(mm)	(W m^{-2})	(m s^{-1})	(kPa)	(°C)		(%)	(mm)	(%)
EG	3.7	-	165.1	1.2	1.2	3.0	25.9	54.7	20.6	-
G	3.6	2.9	127.7	0.9	1.1	9.5	26.5	72.2	265.5	63.4
LG	3.3	1.9	108.1	0.7	1.0	9.1	29.8	73.7	34.6	66.7

Table 9: Average *ET*, *T* and associated predictor variables: available energy (Q^*-Q_G), windspeed (*u*), *VPD*, air temperature (T_a), *RH*, *P* and volumetric moisture content (*VMC*) by plant growth period (early green (*EG*) (DOY 121-158), green (*G*) (DOY 159-218) and late green (*LG*) (DOY 219-260), over the 2013 growing season, at (a) Paucifora and (b) Poplar fen, Fort McMurray, Alberta, Canada.

Canopy *T* was monitored at the beginning of the *G* through to the *LG* periods of plant growth. Q^*-Q_G peaked in the *EG* period at both sites at with a mean of 135 and 165 W m^{-2} at Pauciflora and Poplar, respectively. Q^*-Q_G was the lowest during the latter part of the growing season, Poplar reported a mean of 108 W m^{-2}. Despite missing data for the *LG* period at Pauciflora, Q^*-Q_G likely declined given the similar trends exhibited between the two fens. Although Q^*-Q_G was significantly correlated with T_a, air temperatures remained consistently high despite declining Q^* throughout August. Mean T_a was lowest during the *EG* period at 5 and 3 °C and peaked in the *LG* period at 22 and 30 °C at Pauciflora and Poplar, respectively. Average *RH* reached a maximum of ~ 75% mid-season at Pauciflora, and late season at Poplar reaching ~ 74%. However, *RH* was more variable at Pauciflora compared to Poplar. There is a notable spike in *RH* (*RH* ≥ 70%) at Poplar with the onset of 'leaf out,' which parallels a reduction in average windspeed (u < 1 m s^{-1}) that is maintained throughout the duration of the study period. Correspondingly, windspeed at Pauciflora exhibited greater irregularity, with no noticeable decline following 'leaf out.'

Two high magnitude *P* events (*P* > 40 mm) occurred at the beginning and end of the *G* period at both sites. The first event (DOY 160) was followed by a pronounced spike in *T*. The period was again marked by the onset of 'leaf out,' increasing *Q** and T_a. The second peak event (DOY 209) was, in contrast, followed by a gradual reduction of *T* that persisted into the *LG* period. The late growing season was marked by a decline in *Q**, less frequent *P* events, increased *RH*, and reduced *u*. However, it is late season increase in *RH* (Figure 6) and persistence of cooler T_a at Pauciflora that is likely driving the substantial reduction in late season *T* at Pauciflora, in comparison to Poplar. Finally, *VMC* and groundwater elevation did not fluctuate significantly over the study period. As previously shown, fluxes was not significantly correlated with *VMC* (Figure 15).

Finally, a comparison of *T* against *VPD* did not demonstrate a statistically significant correlation at either fen however Pauciflora *T* is more responsive to changes *VPD* compared to Poplar, generally increasing with increasing *VPD* until the threshold of approximately 1.5 kPa was surpassed (Figure 22). Poplar's *Picea mariana* displayed a negligible response to changes in *VPD*, whereas *Larix laricina* not only exhibited greater variability but it peaked in conditions of nearly 0 kPa, suggesting a log-normal curve (*T* was negatively correlated with *VPD*) (Figure 23). However, a closer examination for potential outlier variables would be necessary to confirm this response.

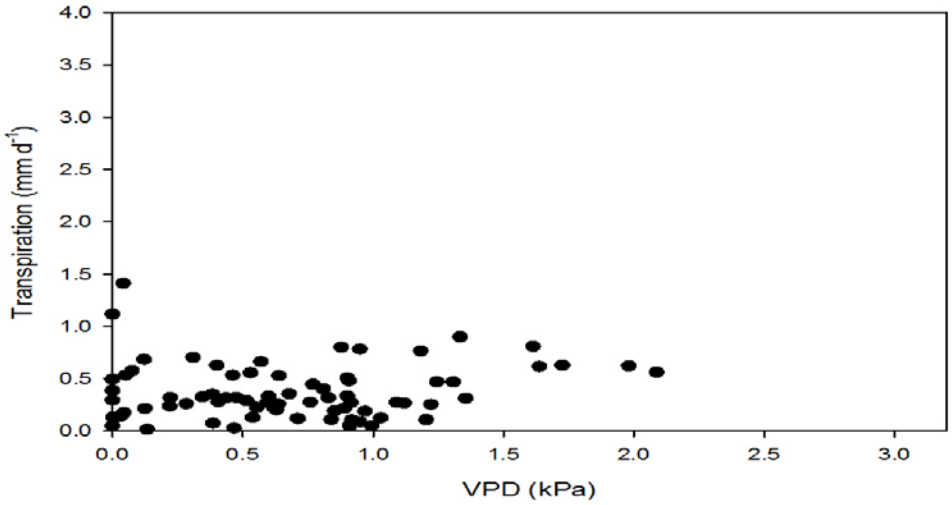

Figure 22: Relationship between *T* (mm d^{-1}) and *VPD* (kPa), Pauciflora fen, Fort McMurray, Alberta, Canada.

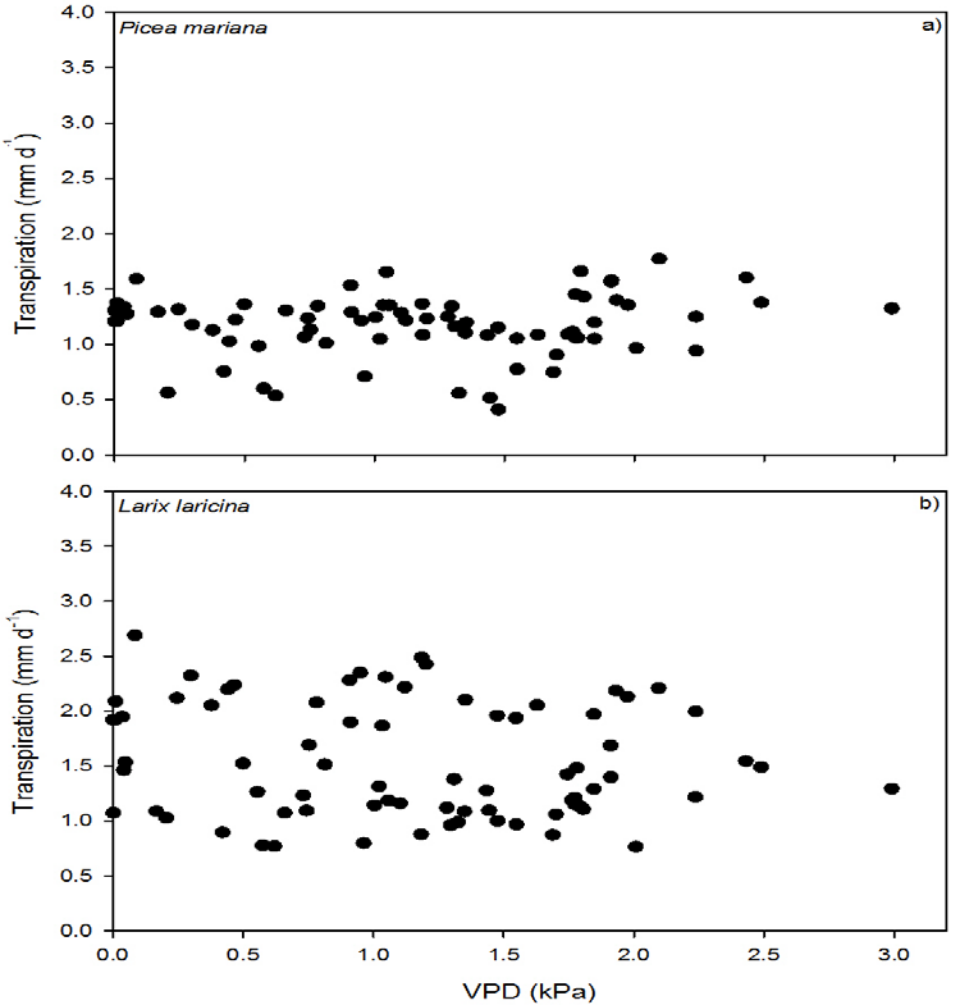

Figure 23: Relationship between (a) *Picea mariana* and (b) *Larix laricina* (mm d^{-1}) against *VPD* (kPa), Poplar fen, Fort McMurray, Alberta, Canada.

4.7 Groundcover Vegetation Captured within Chamber Plots

Pauciflora was dominated by typical poor fen species, including *Rhododendron groenlandicum*, *Oxycoccus microcarpus*, and *Smilacena trifolia* that were equally captured within hummocks and hollows. *Carex aquatilis* was largely present within hollow microforms, while *Rubus chamaemorus, Vaccinium vitis-idaea,* and *Picea mariana* were present only on hummocks (Table 10). The dominant species captured within chamber plots at Poplar included *Equisetum fluviatile* and a variety of sedge species, in which *Carex aquatilis* was the most dominant. Both species were present in both hummock and hollow microforms, however *E. fluviatile* was the only species present within completely flooded plots. *B. pumila*, *S. trifolia* and *Salix* species were strongly correlated with hummock microforms (Table 11).

Microform *LAI* did not vary significantly between microforms at Pauciflora ($U = 30$, $p > 0.05$) (n=16). Hummocks supported a higher mean of *LAI* of 0.76 and hollows just slightly less at 0.70 (Figure 24a). Results were similar when *LAI* was stratified by canopy ($U = 17$, $p > 0.05$) (n=16). Differences in microform *LAI* at Poplar were not significant ($U = 24$, $p > 0.05$) (n=14), with a mean *LAI* of 1.04 and 1.08 between hummocks and hollows, respectively (Figure 24b). However, when *LAI* was separated by canopy cover, differences were significant ($U = 5$, $p < 0.05$) (n=14), supporting a mean *LAI* 0.92 and 1.26 between open and covered plots, respectively. Finally, when surface *LAI* was cumulatively grouped for each fen, results demonstrated a significant difference ($U = 37$, $p = 0.01$) (n=30) between the seasonal mean of 0.73 and 1.06 at Pauciflora and Poplar, respectively.

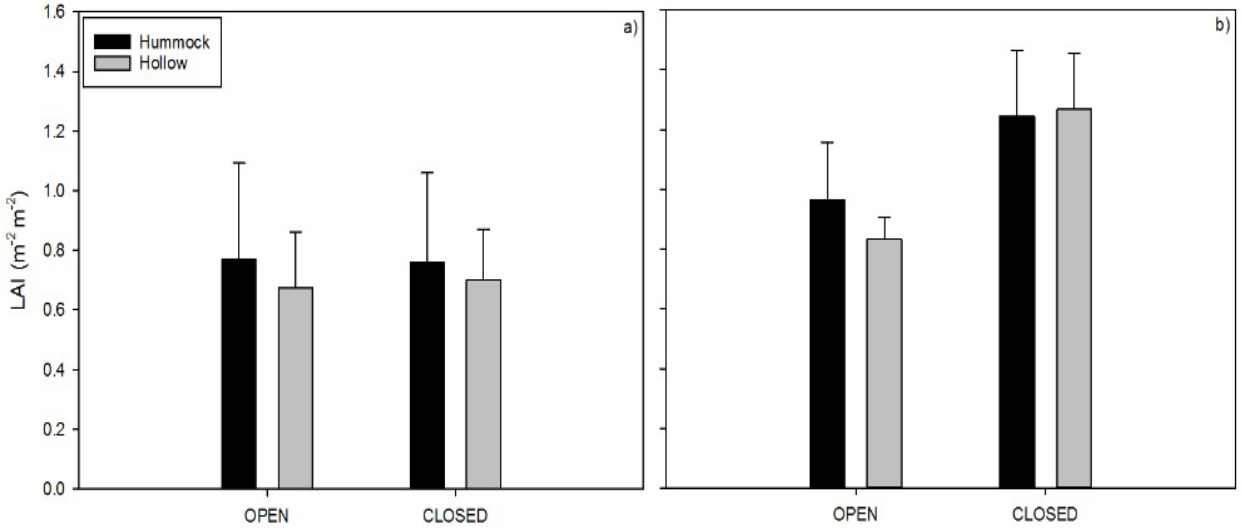

Figure 24: Mean growing season *LAI* (m^{-2} m^{-2}) by canopy cover and microform at (a) Pauciflora and (b) Poplar fen, Fort McMurray, Alberta, Canada, 2013 (Error bars signify standard deviation (S.D.) of variables).

Mean aboveground biomass (*AGB*, g m^{-2}) of hummocks at Pauciflora was significantly higher than hollow *AGB* biomass; with means of 1770 and 930 g m^{-2}, respectively ($U = 12$, $p < 0.05$) (n=16). Belowground biomass (*BGB*, g m^{-2}) measured between microforms at Pauciflora was not significantly different, averaging 84 and 585 g m^{-2} between hummocks and hollows ($U = 23$, $p > 0.05$) (n=16). When results were separated by canopy cover, neither *AGB* ($U = 17$, $p > 0.05$) or *BGB* ($U = 16$, $p > 0.05$) were determined to be significantly different (Figure 25a.c, Table 10). Conversely, there was no significant difference between *AGB* ($U = 13$, $p > 0.05$) or *BGB* ($U = 17$, $p > 0.05$) between microforms at Poplar, averaging *AGB* of ~ 490 and 300 g m^{-2}, and *BGB* of ~ 60 and 80 g m^{-2}, between hummocks and hollows, respectively. Finally, when results were separated by canopy cover, both *AGB* ($U = 14$, $p > 0.05$) and *BGB* ($U = 23$, $p > 0.05$) exhibited consistency between means (Figure 25b.c, Table 11)

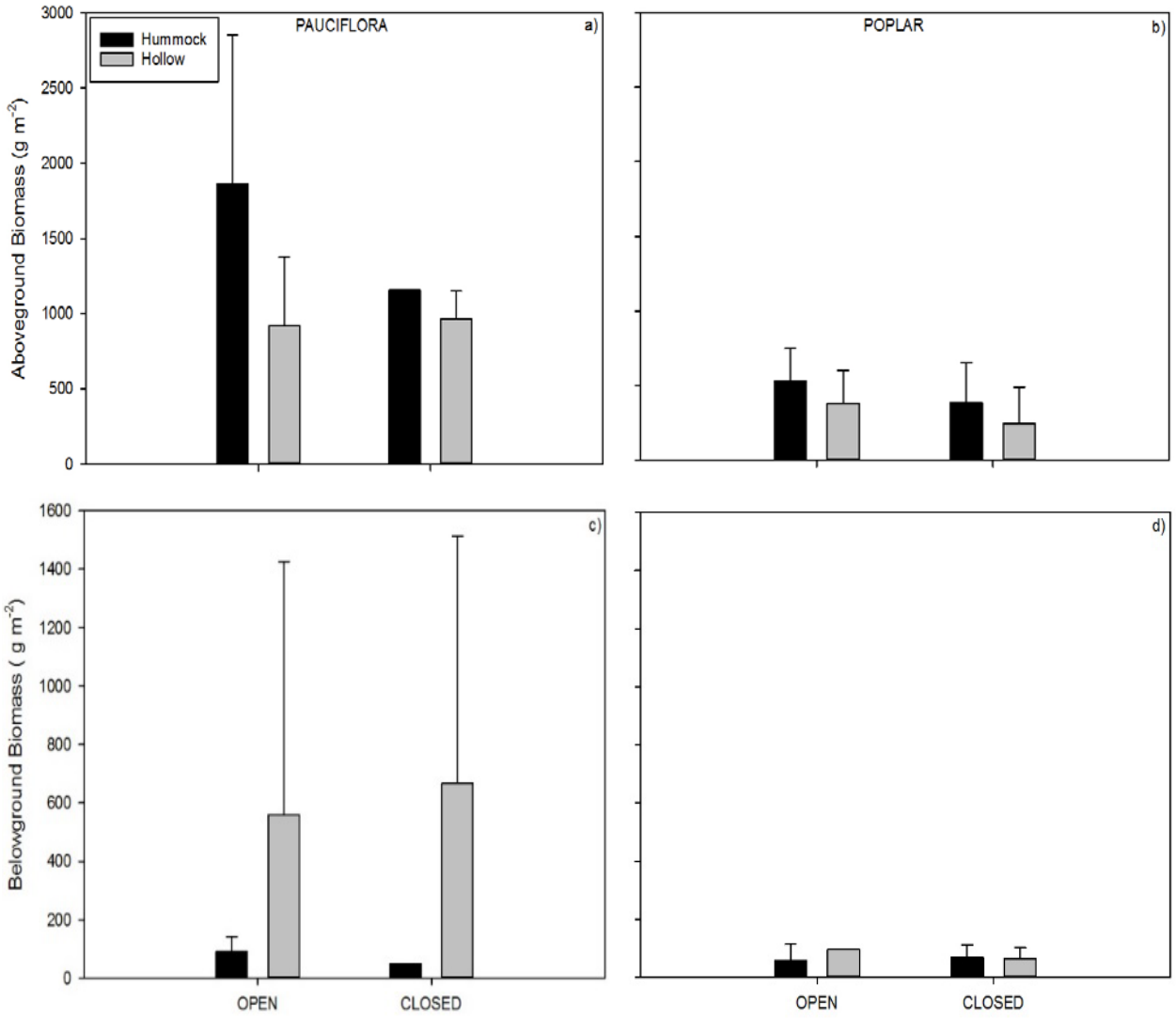

Figure 25: Mean growing season (a)(b) above (*AGB*) and (c)(d) belowground biomass (*BGB*) (g m^{-2}) by canopy cover and microform at Pauciflora and Poplar fen, Fort McMurray, Alberta, Canada, 2013 (Error bars signify standard deviation (S.D.) of variables).

Hummock							Hollow						
			Biomass		*LAI*					Biomass		*LAI*	
	Canopy Cover	Dominate Vegetation	AB ($g\ m^{-2}$)	BG ($g\ m^{-2}$)	Collar ($m^{-2}\ m^{-2}$)	Tree ($m^{-2}\ m^{-2}$)		Canopy Cover	Dominate Vegetation	AB ($g\ m^{-2}$)	BG ($g\ m^{-2}$)	Collar ($m^2\ m^{-2}$)	Tree ($m^2\ m^{-2}$)
1	OPEN	*Sphagnum sp.* *C. calyculata* *S. trifolia* *R. chamaem.*	2479	171	1.04	-	**2**	OPEN	*Sphagnum sp.* *C. calyculata* *V. vitis-idaea* *L. groenland.*	455	1009	0.90	-
3	OPEN	*Sphagnum sp.* *S. trifolia* *C. calyculata* *O. microcar.*	620	46	0.94	-	**4**	OPEN	*Sphagnum sp.* *S. trifolia* *R. chamaem.* *Carex sp.*	535	2148	0.68	-
5	OPEN	*Sphagnum sp.* *L. groenland.* *O. microcar.* *R. chamaem*	3580	23	0.48	-	**6**	OPEN	*Sphagnum* *C. calyculata* *S. trifolia*	1108	24	0.53	-
7	OPEN	*C. calyculata* *C. pauciflora* *V. vitis-idaea* *O. microcar.*	1784	113	0.73	-	**8**	COVERED	*Sphagnum sp.* *C. calyculata* *O. microcar.* *Carex ssp.*	1096	66	0.80	0.45
9	PART COVERED	*Sphagnum sp.* *S. trifolia* *L. groenland.* *C. calyculata* *V. vitis-idaea*	883	110	1.27	0.17	**10**	COVERED	*Sphagnum sp.* *S. trifolia* *C. calyculata* *A. polifolia*	837	1266	0.78	0.17
11	COVERED	*Sphagnum sp.* *Carex sp.* *S. trifolia* *O. microcar.*	1157	48	0.68	0.45	**12**	OPEN	*Sphagnum sp.* *S. trifolia* *O. microcar.* *Carex sp.*	1086	59	0.85	-
13	OPEN	*A. polifolia* *C. calyculata* *S. trifolia*	2059	117	0.45	-	**14**	OPEN	*Sphagnum sp.* *S. trifolia* *C. calyculata* *Carex ssp.*	669	60	0.40	-
15	OPEN	*Sphagnum sp.* *S. trifolia* *C. calyculata* *L. groenland.* *A. polifolia*	1614	46	0.48	-	**16**	OPEN	*Sphagnum sp.* *S. trifolia* *A. polifolia* *O. microcar.* *Carex sp.*	1669	49	0.68	-

Table 10: Dominant vegetation, above and belowground biomass ($g\ m^{-2}$) of community-scale plots, separated between hummock (even) and hollow (odd) microforms and canopy cover, Pauciflora fen, Fort McMurray, Alberta, 2013. OPEN canopy cover, *PAR* > 500 μmol $m^{-2}\ s^{-1}$, COVERED, *PAR* < 500 μmol $m^{-2}\ s^{-1}$.

Hummock							Hollow						
			Biomass		*LAI*					Biomass		*LAI*	
	Canopy Cover	Dominate Vegetation	AB ($g\ m^{-2}$)	BG ($g\ m^{-2}$)	Collar ($m^{-2}\ m^{-2}$)	Tree ($m^{-2}\ m^{-2}$)		Canopy Cover	Dominate Vegetation	AB ($g\ m^{-2}$)	BG ($g\ m^{-2}$)	Collar ($m^2\ m^{-2}$)	Tree ($m^2\ m^{-2}$)
1	OPEN	*S. trifolia* *E. fluviatile* *B. pumila*	310	15	1.04	-	**2**	OPEN	*E. fluviatile*	483	95	0.89	-
3	OPEN	*T. nitens* *E. fluviatile* *B. pumila*	473	152	0.87	-	**4**	OPEN	*E. fluviatile* *Carex ssp.*	133	95	0.75	-
5	OPEN	*T. nitens* *S. trifolia* *Carex ssp.*	707	49	1.10	-	**6**	OPEN	*T. nitens* *S. trifolia* *Carex ssp.*	532	98	0.86	-
7	COVERED	*H. splendens* *S. trifolia* *Carex ssp.*	203	40	1.40	2.12	**8**	COVERED	*E. fluviatile* *Carex ssp.*	114	72	1.38	2.12
9	OPEN	*S. trifolia* *B. pumila* *E. fluviatile*	804	61	0.67	-	**10**	COVERED	*E. fluviatile*	10	103	1.00	2.43
11	OPEN	*S. trifolia* *E. fluviatile* *Salix ssp.*	354	10	1.14	-	**12**	COVERED	*T. nitens* *S. trifolia* *G. trifidum*	565	8	1.27	4.17
13	COVERED	*T. nitens* *E. fluviatile* *Carex ssp.*	574	99	1.09	2.12	**14**	COVERED	*T. nitens* *S. trifolia* *Carex ssp.*	297	64	1.42	2.12

Table 11: Dominant vegetation, above and belowground biomass ($g\ m^{-2}$) of community-scale plots, separated between hummock (even) and hollow (odd) microforms and canopy cover, Poplar fen, Fort McMurray, Alberta, 2013. OPEN canopy cover, *PAR* > 300 $\mu mol\ m^{-2}\ s^{-1}$, COVERED, *PAR* < 300 $\mu mol\ m^{-2}\ s^{-1}$.

In general, Pauciflora's *Picea mariana* produced a low canopy cover that permitted an understory that was dominated by *Sphagnum,* whereas Poplar's *Larix laricina* produced a dense cover that was dominated by *Tomenthypnum nitens* and feather moss species regardless of topographic position. To access potential differences in understory species, specifically whether certain species favoured open or covered canopy conditions, plots were stratified based on moss and vascular percent cover. Generally, plots were classified as *Sphagnum* dominant if they comprised < 20% vascular species, whereas plots were classified as mixed if they consisted of at least > 20% vascular plant cover. A comparison of *LAI*, *AGB* and *BGB* exhibited no significant difference (U =27, 26, 14, $p > 0.05$) between *Sphagnum* and vascular dominated plots. However, when plots were stratified by both canopy cover and dominant understory, the aforementioned variables were generally lower in *Sphagnum* dominant plots, while vascular dominant plots demonstrated lower *LAI* and *AGB* values, but higher *BGB* (Table 10). Conversely, plots at Poplar were generally composed of fewer vascular species, with moss dominated plots supporting < 10% vascular species and mixed plots ranging from 20 – 80% percent cover. A comparison between *LAI, AGB* and *BGB* demonstrated no significant difference (U = 17, 14, 9, $p > 0.05$).Vascular dominant plots typically supported lower averages of the aforementioned with the presence of an overstory. Moss dominant plots generally exhibited a minimal decrease or no change in *AGB* and *BGB* averages, however *LAI* demonstrated a mean increase between open and covered plots (Table 11).

4.8 Temporal and Spatial Variability of Surface ET

To understand the variation in instantaneous *ET* throughout the 2013 snow free growing season, the community-scale measurements were grouped by month. Seasonal mean *ET* at Pauciflora was ≤ 0.1 mm hr^{-1} ($\pm$ 0.05) (Figure 26a). *ET* rates at Pauciflora were not significantly different when compared against microform plots (U = 6490.500, $p > 0.05$); hummocks generally sustained slightly higher rates (Figure 26c). Seasonal mean *ET* at Poplar was comparable ≤ 0.1 mm hr^{-1} (Figure 26b). However, a comparison of seasonal rates measured between microforms was significantly different (U = 4372.500, p = 0.001), with hummocks generally supporting higher rates (Figure 26d).

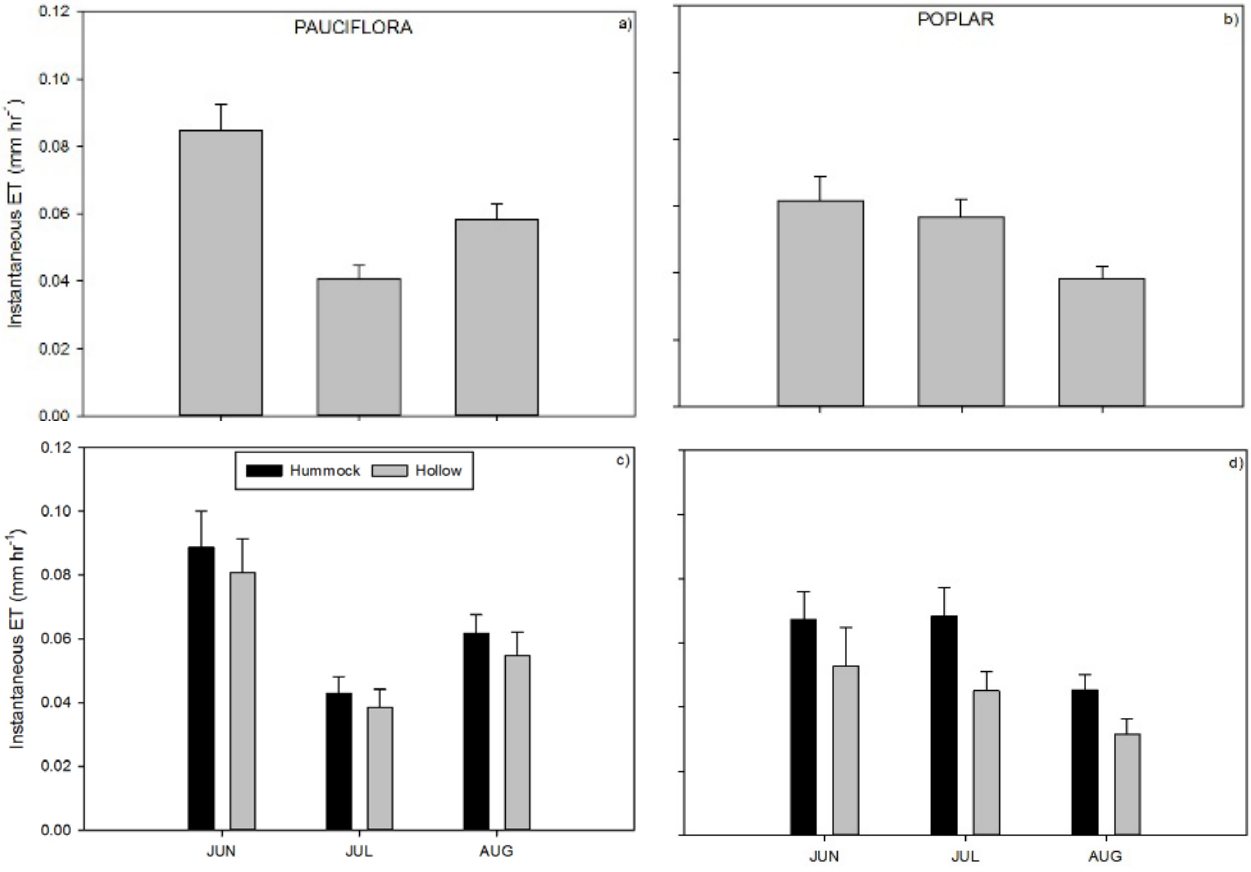

Figure 26: Period averages *ET* (mm hr^{-1}) by (a)(b) month, and by (c)(d) microform, at Pauciflora and Poplar fen, Fort McMurray, Alberta, Canada, 2013 (Error bars signify standard deviation (S.D.) of variables).

A comparison of *ET* when stratified by canopy cover demonstrated no significant difference at either fen ($U = 3702.000$, $p > 0.05$) ($U = 5276.500$, $p > 0.05$), at Pauciflora and Poplar, respectively (Figure 27a.b). Finally, when *ET* rates were further classified by both canopy cover and microform, results displayed that open hummocks maintained the highest rates, while covered hollows generally supported the lowest rates (Figure 27c.d).

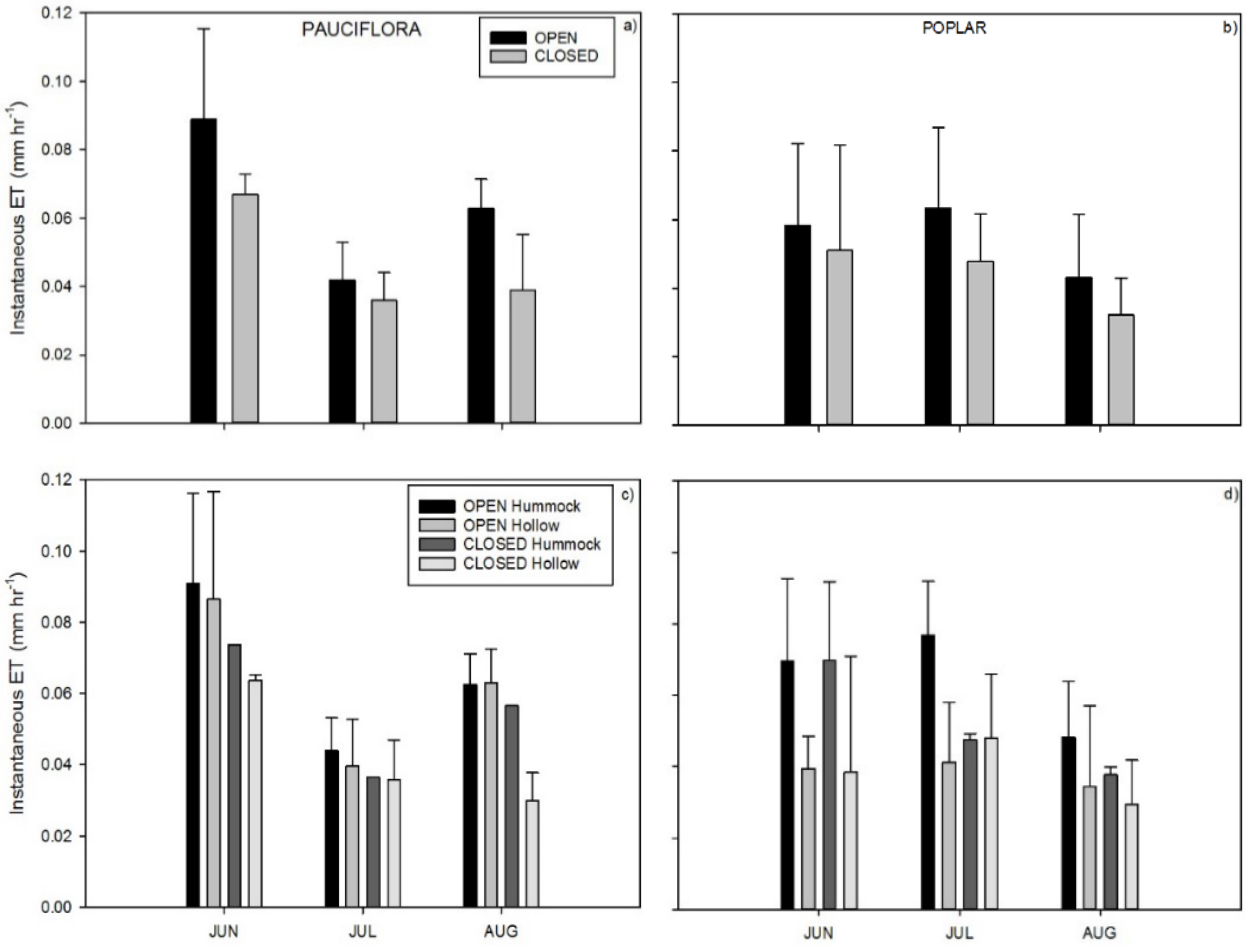

Figure 27: Monthly averaged *ET* (mm hr^{-1}) by (a)(b) canopy cover, and by (c)(d) canopy cover and microform, at Pauciflora and Poplar fen, Fort McMurray, Alberta, Canada, 2013 (Bars signify standard deviation (S.D.) of variables).

4.9 Micro- and hydro-climatic Controls on ET

Microclimatological variables were examined at the same temporal scale as instantaneous *ET* to determine whether there was variation between canopy and microtopographic cover. Pauciflora recorded no significant difference in T_a, (ANOVA ($F(1,238) = 0.718$, $p > 0.05$), *RH* (ANOVA ($F(1,238) = 0.037$, $p > 0.05$), or ice depth ($U = 4296$, $p > 0.05$) when results were grouped by canopy cover (Figure 28). Conversely, open plots reported statistically higher values of *PAR* ($U = 2544.5$, $p < 0.01$) and T_g at 2 cm ($U = 3303$, $p < 0.05$), while covered plots maintained significantly higher *VMC* ($U = 2814$, $p < 0.01$) (Figure 28). A comparison of the same variables when stratified by microtopography reported significant differences in T_g ($U = 4794$, $p < 0.01$), and *VMC* ($U = 515.5$, $p < 0.01$) (data not shown). All subsequent variables, including *PAR* did not display a statistical difference ($p > 0.05$). Conversely, Poplar only displayed significant variation in *PAR* ($U = 3579$, $p < 0.01$) when data were grouped by canopy cover. However, when the same variables were stratified by microtopography, both T_g ($U = 3164.5$, $p < 0.01$) and *VMC* ($U = 2732.5$, $p < 0.01$) exhibited a statistical difference, while remaining variables demonstrated no significant differences ($p > 0.05$) (data not shown). Due to the relative similarity of results, only microclimatic variables stratified by canopy cover are displayed in the following figure (Figure 28).

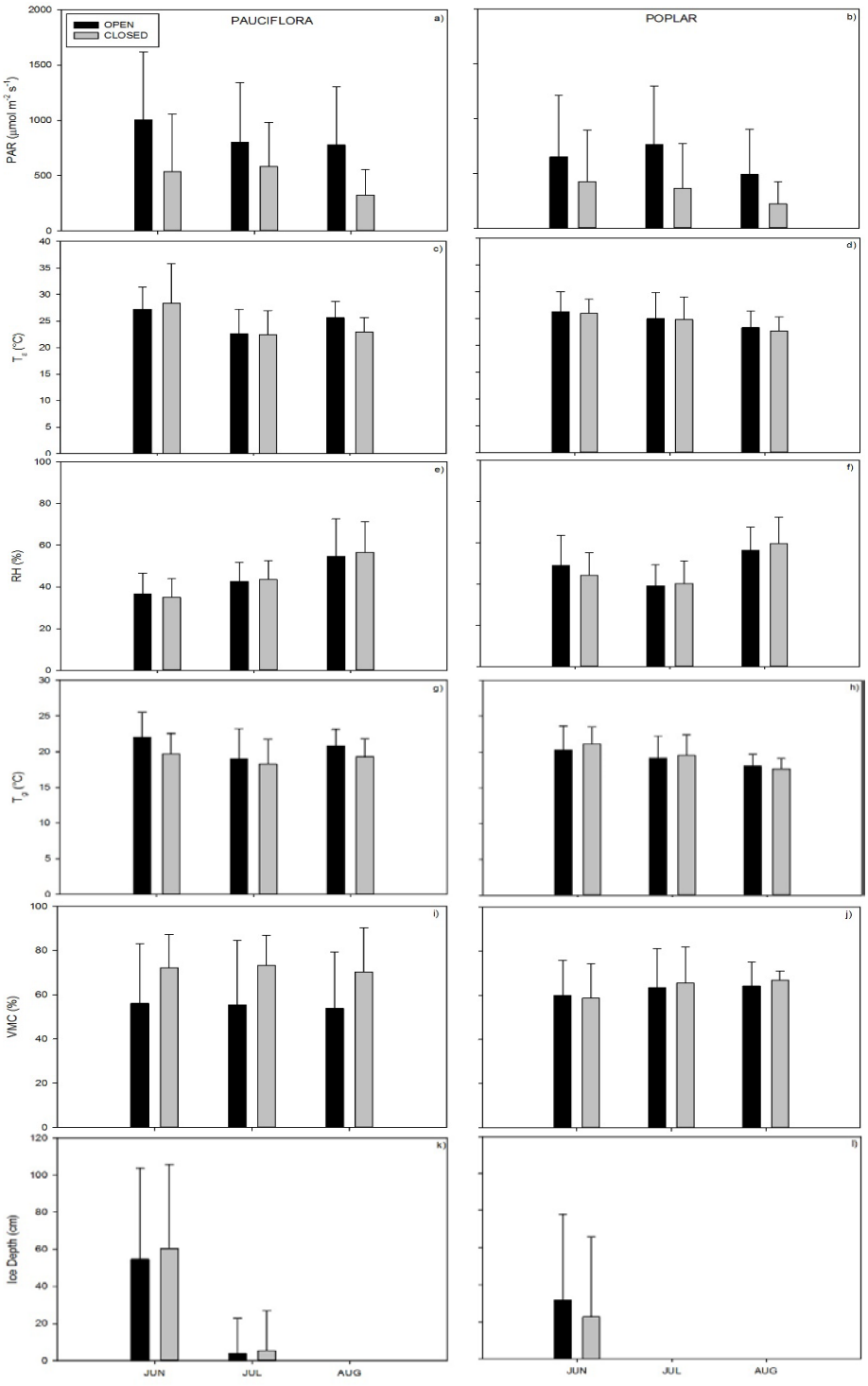

Figure 28: Average seasonal (a)(b) *PAR* (µmol m^{-2} s^{-1}) (c)(d) air temperature (T_a, °C), (e)(f) *RH* (%), (g)(h) soil temperature (T_g, °C), (i)(j) volumetric moisture content (*VMC*, %) and (k)(l) ice depth (cm) partitioned by canopy cover at Pauciflora and Poplar fen, Fort McMurray, Alberta, Canada, 2013 (Error bars signify standard deviation (S.D.) of variables).

PAR reached maxima in the early to mid-season within open plots, averaging > 1000 μmol m^{-2} s^{-1}, and > 700 μmol m^{-2} s^{-1}, at Pauciflora and Poplar, respectively. Both T_a and T_g at Pauciflora displayed similar seasonality, and were generally higher in open plots, reaching maxima of ~ 25 °C (± 4.5) and 20 °C (± 3.7), respectively. Conversely, Poplar demonstrated less seasonal and spatial variation in the aforementioned variables, with seasonal means of ~ 25 °C (± 3.9) and 20 °C (± 2.8). *RH* increased through the study period at both sites. *VMC* was consistently higher within covered plots at Pauciflora, averaging 72%, while open plots averaged 55%. Seasonal mean *VMC* at Poplar was consistent between open and covered plots, with a mean of 63%. Ice depth was prevalent early in the season, averaging ~ 56 cm and ~ 28 cm, at Pauciflora and Poplar, respectively.

An analysis of microclimatic variables against instantaneous *ET* at Pauciflora exhibited a significant, positive correlation between T_a and T_g ($p < 0.01$), and a significant, negative correlation with *RH* ($p < 0.01$). Poplar demonstrated analogous results with the addition of *PAR*, forming a positive correlation with *ET* ($p < 0.01$) and *VMC* that produced a negative correlation ($p < 0.01$). A multiple regression analysis of the aforementioned variables (excluding depth to ice) provided a weak to moderate explanation for changes in *ET* at Pauciflora ($F(5,232) = 33.776$, $p < 0.01$, $R^2 = 0.42$) and Poplar ($F(5, 187) = 28.561$, $p < 0.01$, $R^2 = 0.43$); without distinguishing between the spatial variability of plots. When the same variables were separated by canopy cover, the multiple regression reasonably explained changes in *ET* in open canopy conditions ($F(5,8) = 5.213$, $p < 0.05$, $R^2 = 0.77$) ($F(5,8) = 5.333$, $p < 0.05$, $R^2 = 0.77$), at Pauciflora and Poplar, respectively (Figure 29). Conversely, covered canopy *ET* at Pauciflora demonstrated a weak response when regressed against covered canopy conditions ($F(5,8) = 0.900$, $p > 0.05$, $R^2 = 0.39$), whereas Poplar's covered microclimate provided a strong prediction for changes in *ET* ($F(5,8) = 12.507$, $p = 0.001$, $R^2 =$

0.89) (Figure 29). The presence of an overstory, significantly reduced mean *PAR* and $T_{g,}$ ($p < 0.05$) while significantly increasing *VMC* ($p < 0.01$) at Pauciflora; producing a cool, saturated microclimatic. Whereas, differences in canopy cover at Poplar significantly reduced *PAR* ($p < 0.01$), while remaining variables remained fairly consistent. However, despite distinct differences in canopy structure between the two fens, a comparison of surface *ET* was not statistically different between the two sites ($U = 23938$, $p > 0.05$).

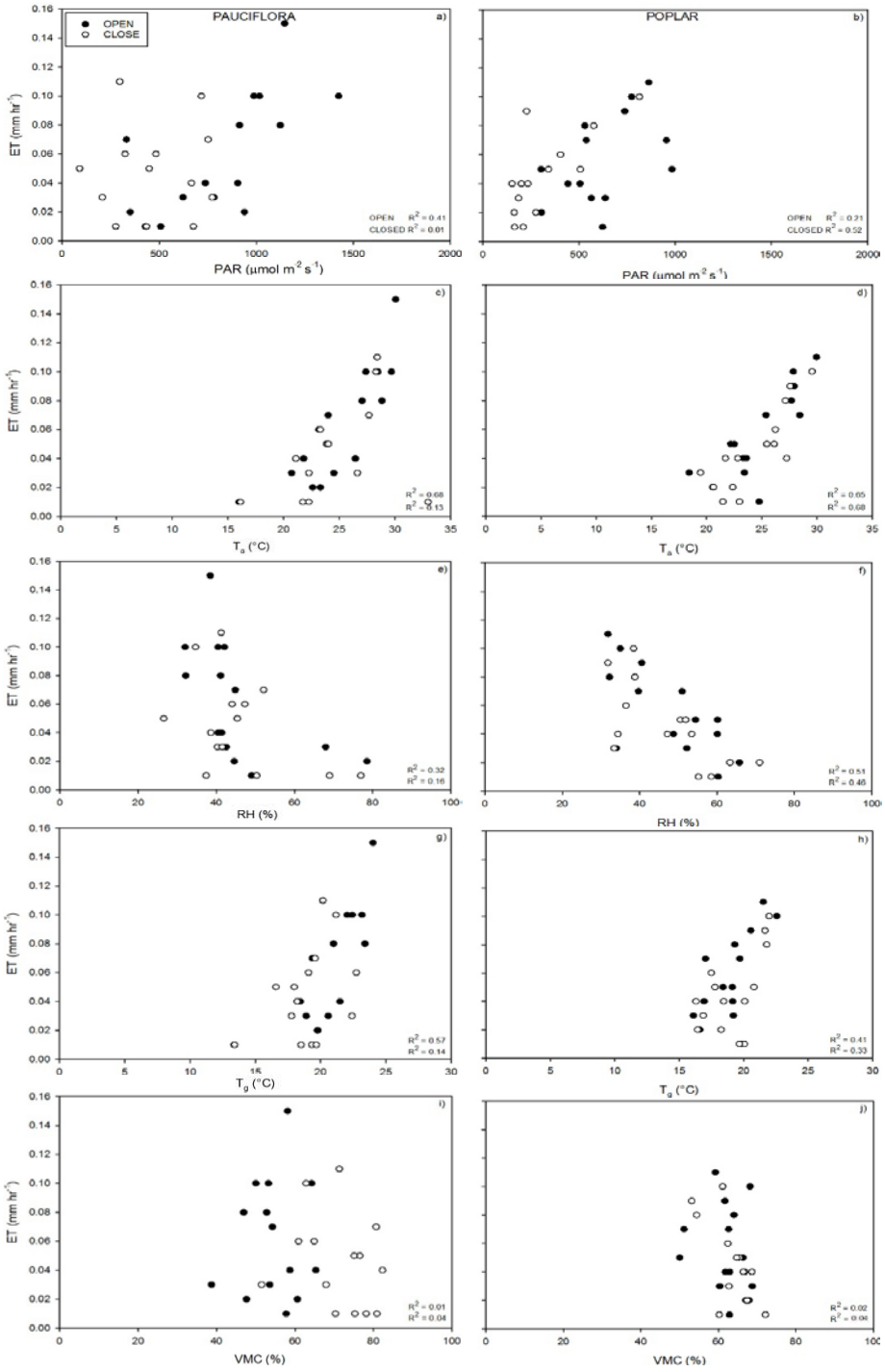

Figure 29: Relationship between *ET* (mm hr^{-1}) and (a)(b) *PAR* (µmol m^{-2} s^{-1}) (c)(d) air temperature (T_a, °C), (e)(f) *RH* (%), (g)(h) soil temperature (T_g, °C), (i)(j) and volumetric moisture content (*VMC*, %) partitioned by canopy cover at Pauciflora and Poplar fen, Fort McMurray, Alberta, Canada, 2013 (Error bars signify standard deviation (S.D.) of variables).

4.10 Vertical Partitioning of ET

The seasonal mean classified ET_{surf} at Pauciflora was 0.8 mm d^{-1}, and 0.5 m d^{-1} at Poplar. A comparison of hourly total fen *ET*, *T* and ET_{surf} (chamber) exhibited differences in each variable's contribution to the total *ET* budget. On average, Pauciflora *T* accounted for < 20% of fen *ET*, while ET_{surf} (chamber) vegetation generally exceeded *T*, often contributing > 80%. Conversely, Poplar *T* accounted for > 80% of fen *ET*, while surface vegetation contributed only < 20% to the total *ET* flux.

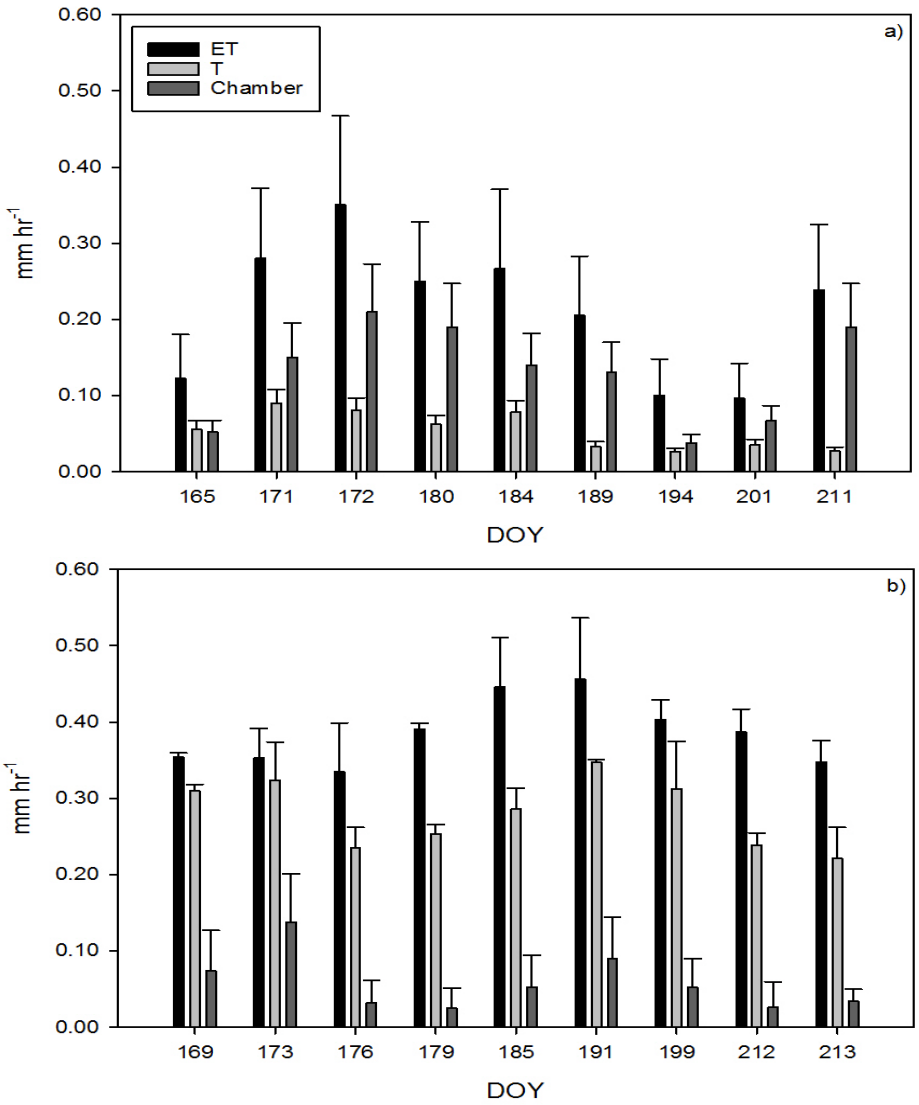

Figure 30: A comparison of hourly Fen *ET*, *T* and Surface (Chamber) *ET* scaled within the MET tower footprint, recorded over the 2013 growing season, (a) Pauciflora and (b) Poplar fen, Fort McMurray, Alberta, Canada. (Error bars signify standard deviation (S.D.) of variables).

4.11 Statistical Error Analysis

EC error was determined using methods by Kroon *et al.* (2010). Results are comparable with studies applying the described and other methods (Kroon *et al*., 2010; Litt *et al*., 2015; Wand *et al*., 2015), suggesting normalized sampling error can range 10-12% (Litt *et al.*, 2015; Wang *et al*., 2015) from sensible heat and 20-30% for trace gases (Finkelstein and Sims, 2001). The accuracy of the SHB gauge design and measurement resolution has been analyzed in detail (Sakuratani, 1981, 1982; Baker and Nieber, 1989; Ham and Heilman, 1990; Groot and King, 1992) and it has been reported at ± 10-15% (Groot and King, 1992). However, it has been recognized that the fundamental steady-state assumption produces decreased accuracy in both high and low flow rate conditions, the later condition is more common in conifer seedlings (Groot and King, 1992). Groot and King (1992) reported inaccuracies of ≤ 48% in low flow rate conditions of conifer seedlings when heat storage was not included in the sapflow calculation, while Steinberg *et al*. (1982) and Grime *et al*. (1995) suggest an error of ≤ 10%. Heat storage was not included in the sapflow calculation, however, measurements were rejected when ΔT was ≤ 0.5 °C. Groot and King (1992) suggested a similar technique using ΔT threshold of 2.5 °C. Additionally, high flow rates were excluded from the sapflow calculation when a maximum velocity was surpassed, specified by the manufacturer (Dynamax Inc., 2007). Deviations from the stead-state condition is more problematic in larger stems (Perämäki *et al*., 2001), in which Shackel *et al*. (1992) reported significant error when the SHB method was applied to stems 60 mm in diameter, while Grime and Sinclair (1999) concluded significant error with 35 mm stems. Grime and Sinclair (1999) suggest an ideal gauge range within 10-30 g hr^{-1}, of which 50-90% of measurements from each of the monitored stems in this study generally fell within this range. Recognizing the combined effects of error inherent to the system and error introduced from environmental variables (monitored trees ± 2 S.D. from fen

mean), Perämäki *et al*. (2001) concluded that the SHB method is satisfactory despite deviations from the basic steady-state assumption. Total SHB error estimated for this study was 15-30% (Shackel *et al*., 1992). Finally, the use of ventilated chambers to measure *ET* has been criticized on the basis that *Q** and microclimate within the chamber may not be representative of ambient conditions (McLeod *et al*., 2004). Previous studies have estimated *Q** in the chamber at approximately 95% of conditions outside the chamber (Greenwood and Beresford, 1979), while others have reported a reduction of 8-10% (Reicosky *et al*., 1983). It has been concluded that changes to *Q** and the microclimate within the chamber only produced a minimal error on absolute *ET* (Reicosky *et al*., 1983), which for this study has been estimated at ≤ 7% (Hamel *et al*., 2015).

Flux Contribution	**Method**	**Description**	**Root Mean Square Error (%)**	**Reference**
ET	EC	One-point Uncertainty	8.3	Kroon *et al*. 210
T	SHB	System measurement resolution, Steady-state assumption, Heat-storage error	15.0	Groot and King, 1992 Shackel *et al.*, 1992 Grime *et al*., 1995 Perämäki *et al*., 2001
ET_{surf}	Chamber	Lower *Q**, Altered Microclimate	6.6	Reicosky *et al*., 1983 McLeod *et al*., 2004 Hamel *et al*., 2015

Table 12: Overview of error and uncertainties of flux measurements. (See Appendix IV for specific equations)

Chapter Five
Discussion

5.1 ET and Energy Balance Components

5.1.1 Fen ET and Energy Balance Components

Fen *ET* generally exhibited "typical" seasonal variability by which peaks in *ET* are generally coupled with the warmest temperatures in July (Rouse, 2000; Brown *et al*., 2010; Runkle *et al*., 2014). *ET* was fairly consistent throughout the growing season, averaging 2.3 mm d^{-1} and 3.5 mm d^{-1} at Pauciflora and Poplar, comparable to results displayed in similar studies (Petrone *et al*., 2003; Wu *et al*., 2010; Brümmer *et al*., 2012; Kettridge *et al*., 2013). Over the four-month growing season, Q_E was the dominant flux at both fens which has been commonly demonstrated by other studies that have examined northern peatlands and peat swap forest environments (Rouse, 2000; Wu *et al*., 2010; Clulow *et al*., 2013; Runkle *et al*., 2014). It is not uncommon for peatlands to exhibit a dominance in Q_H in the pre- and early growing season, as exhibited at Poplar (Table 8), and during plant senescence (Brown *et al*., 2010; Petrone *et al*., 2000; Petrone *et al*., 2004; Admiral and Lafleur, 2007). However, once the vegetation has reached adequate growth, the plant's physiological processes become the dominant energy consumers driving Q_E. Q^* was highest in the first half of the study period (mid-May through early July) and remained distinctly higher at Poplar (Figure 12). Q_G was considerably smaller than the major terms of the surface energy balance (Brutsaert, 1982), accounting for ~3% of Q^* at Pauciflora and ~1% at Poplar. Q_G was the largest in May when the ice-rich ground was rapidly thawing, ~ 9 and 3 W m^{-2} at Pauciflora and Poplar, respectively.

5.1.2 Surface ET

The average range in growing season instantaneous ET_{surf} averaged < 0.1 mm hr^{-1} (± 0.05) between both fens. Although fluxes represent short duration (2-minute) period midday fluxes, inferred daily

fluxes fell within the ranges detailed in other studies (Brown *et al*., 2010, Brümmer *et al*., 2012; Kettridge *et al.,* 2013, Limpens *et al*., 2014) (Figure 30), conducted within similar climatic and/or peatland ecosystems. ET_{surf} patterns do not follow the 'typical' seasonal variability as depicted by previous studies (Rouse, 2000), in which peak *ET* rates are coupled with the warmest temperatures (July). Deviations from the predicted state is especially evident at Pauciflora that exhibited a notable peak early in the season (Figure 26). Brown *et al*. (2010) similarly reported early season *ET* peaks that was attributed to the persistence of an early season ice layer that acts as an impermeable layer to moisture close to the surface. This impermeable layer acts to prevent infiltration of incoming precipitation events, thus creating a moisture-rich environment that fosters early season *ET* peaks (Petrone *et al*., 2006). As the ice begins to melt, it competes against ET_{surf}, consuming a significant portion of Q^*-Q_g, and this period is often characterized by lower ET_{surf} rates.

5.2 Understanding Canopy T and ET_{surf}

The results from this study demonstrate the contribution of *T* within a treed peatland that increase with a higher tree density (Clulow *et al*., 2013). Poplar *T* was the principal contributor to *ET* compared to that at Pauciflora where *T* accounted for < 20% of *ET*, common of *Picea mariana* dominated peatlands. Due to Pauciflora's sparse canopy that permitted incoming radiation to reach the surface, the major contributors to *ET* were the understory species, peat and standing water that was present as a result of the elevated water table. The understory generally paralleled the seasonal trends exhibited by *ET* and *T* at both sites (Figure 30). Surface *ET* peaked on DOY 180 at ~ 0.3 mm hr^{-1}, during the *G* period at Pauciflora, whereas Poplar peaked earlier in the season on DOY 169 at < 0.1 mm hr^{-1}. Figure 30 exhibits substantially low surface *ET* fluxes recorded at Pauciflora on DOY 165, 194 and 201, these measurements days were characterized by high *P* events, high

RH and cool T_a. This highlights the immediate response of the surface to changes in microclimate. Furthermore, the late season conditions that was characterized by lower Q^* and higher *RH*, proved unfavourable for *T*, did not have the same negative impact on surface *ET*. Pauciflora exhibits a typical response of an open canopy, *Picea mariana* dominated peatland in which surface *ET* is the primary contributor to the ecosystem flux exchange (Petrone *et al*. 2011). The dense canopy at Poplar inhibits incoming solar radiation from reaching the peat surface and therefore reduces the surface *ET* flux contribution. The remaining portion of *ET* that was not accounted for is likely attributed to vascular plants present within the subcanopy, which has been recognized as providing an important component to the *ET* flux within forested peatlands (Lafleur and Schreader, 1994; Heijmans *et al*., 2004; Thompson, 2012).

5.3 Environmental Controls on T and ET_{surf}

5.3.1 Environmental Controls on T

Despite the proximity of the two sites, each fen is subjected to unique differences in climate. Pauciflora is distinctly cooler and has historically received greater *P*, producing wetter and more humid conditions, whereas Poplar is generally warmer, receiving higher Q^* and T_a. As such, conditions at Poplar are more favourable for higher *T*, compared to Pauciflora that supported a lower *T* (Figure 17). Additionally, T_g was significantly cooler at Pauciflora compared to Poplar. Cold soil can significantly increase the root resistance to water uptake (Lopushinsky and Kaufmann, 1984), further inhibiting *T* rates. External regulation of *T* has been attributed to numerous variables including the radiative transfer of solar energy through the canopy (Clulow *et al*., 2013), canopy atmospheric turbulence and *VPD* (Dang *et al.*, 1997; Mahrt *et al.*, 2002), intercepted precipitation (Ahrends and Penne, 2010), water availability (Oren *et al*., 1999), as well as canopy structure and associated leaf area (Granier *et al*., 2000). However, it has been determined

that trees can have several mechanisms of internal regulation related to specific morphology and physiology that is partially uncoupled from external conditions (Zweifel *et al*., 2002), that have not been examined within this study. Nevertheless, in most trees with actively transpiring leaves and readily available soil moisture, a diurnal pattern of *T* results from a combination on internal and external conditions, which determines how the canopy contributes to *ET*. Common trends exhibited between both sites demonstrate maximized *T*, exhibited mid-season during the *G* period of plant growth, rates in conditions of high *Q**, T_a and moderate to high *VPD*, that coincides with lower *RH* and moderate *u* (Table 9).

A separate analysis of *VPD* on sapflow within conditions of unrestricted water access has been previously described by Oren *et al*. (1999), reporting that half-hourly water uptake was linearly related to *VPD* at < 0.6 kPa. The evaporation from needle surfaces is proportional to the gradient of vapour pressure between stomatal cavities and the air and, therefore, the vapour pressure deficit of the air. Additionally, *VPD* and its interaction with T_a strongly impacts stomatal conductance to water vapour (Dang *et al*., 1997). Although *T* was not significantly correlated with *VPD* at either fen, attributed to the low stomatal sensitivity of conifers to *VPD* (Dang *et al*., 1997), however the water vapour flux generally becomes limited when *VPD* exceeds approximately 1.0 kPa (Dang *et al*., 1997; Mahrt *et al*., 2002). The stomata partially close with large vapour pressure deficits in order to maintain a constant flow of water within the limits of water availability. As a result, *T* exhibits minimal variation beyond a certain *VPD* threshold. Pauciflora *T* is more responsive to changes in *VPD* compared to Poplar, generally increasing with increasing *VPD* until the threshold of approximately 1.5 kPa was surpassed (Figure 22). Poplar's *Picea mariana* displayed a negligible response to changes in *VPD*, whereas *Larix laricina* not only exhibited greater variability but seem to peak in conditions of nearly 0 kPa, suggesting a log normal curve

(*T* was negatively correlated with *VPD*). *Larix laricina T* became limited once an approximate value of 0.5 kPa was surpassed (Figure 23). Results would suggest that tree water-use at Poplar increases with no constraints imposed by *VMC*, coupled with warmer T_a that encourages a higher saturated vapour pressure. Conversely, tree water-use at Pauciflora is limited by either an environmental or physiological control.

5.3.2 Environmental Controls on ET_{surf}

The study demonstrates that the interaction of *P*, T_a, T_g and vegetation type in controlling ET_{surf} and their variable influence on the amount and temporal distribution of *ET* (Brummer *et al*., 2012). The seasonal course of ET_{surf} was strongly influenced by *P* distribution and the length of the growing season; T_a and *PAR*. ET_{surf} was maximized in favourable conditions following high *P* events that paralleled high *PAR* and T_a; but plateaued with excess *P*. Surplus *P* would likely contribute to higher *VMC* or runoff, rather than being used by surface vegetation. For example, there was a notable decline in ET_{surf} in July at Pauciflora (Figure 26), during which a number of measurement days were characterized by high *P* events, high *RH* and cool T_a. This highlights the immediate response of the surface to changes in microclimate.

Previous studies that have examined inter-annual *ET* variability, have observed significant differences in fluxes between canopy cover, and microtopography (Admiral and Lafleur, 2007; Kettridge *et al*., 2013; Wang *et al*., 2015). Although, Pauciflora's open canopy permitted a greater degree of *PAR* to reach the surface, favourable for the establishment of *Sphagnum* moss, cooler climates of the high altitude fen limited seasonal *ET* across the entire site. Conversely, aside from limiting *PAR*, Poplar's dense canopy created a microclimate that was not statistically different between open and covered plots, which is typical of a dense canopy (Kettridge *et al.*, 2011). The dense canopy was favourable for the establishment of brown and feathermoss.

5.4 Vegetation Controls on ET_{surf} Dynamics

The presence of a dense tree and/or shrub canopy directly impedes incoming radiation, which has been widely recognized to modify the underlying vegetation composition (Petrone *et al*., 2011; Waddington *et al*., 2014), and localized soil moisture regimes (Solondz *et al*., 2008). Pronounced differences in groundcover between the two fens equally demonstrated the ability of shade-tolerant brown and feathermosses to out-compete *Sphagnum* moss under low-light conditions (Marschall and Proctor, 2004; Hájek *et al*., 2009). Additionally, *Sphagnum* mosses exist within a less wet moisture regime, compared to brown and feathermosses that have the ability to thrive in moisture rich environments. Despite drier conditions, *Sphagnum* have been previously recognized for their ability to support higher *ET* rates compared to feather mosses, as a result of their morphological structure and ability to retain moisture (Price, 1997). However, Goetz and Price (2015) compared *ET* rates of *Sphagnum* and *Tomenthypnum* and reported that the active-water conducting structures of the two species were similar.

In *Sphagnum,* water is transported by an external wicking system and adsorption along the stem and leaf surfaces (Nichols and Brown, 1980). Such transport mechanism is lacking within feathermoss (Callaghan *et al*., 1978). As such, it is expected that an open canopy, *Sphagnum* dominant fen would sustain significantly higher surface *ET* rates compared to a covered canopy, feathermoss dominant fen. However, *ET* rates were not statistically different between the two fens. This was partially explained by differences in climate, but it could also be attributed to the establishment of *Tomenthypnum* at Poplar. Despite the ability of *Sphagnum* to retain a large amount of water, Goetz and Price (2015) reported similarity in the active water-conducting structure of *Sphagnum* and *Tomenthypnum,* when the latter species has access to a high water table. Analyzing physiological differences between the two species is beyond the scope of this paper,

however, it may further explain why there did not exist a statistically significant difference in *ET* fluxes between the two fens, despite the dominance of *Sphagnum* at Pauciflora.

5.5 Tree Density Effect

It has been well documented that the presence of a dense canopy will increase the degree of shading on the peat surface and in turn, diffuse radiation reaching the surface (Kettridge *et al*., 2013). However, diffused radiation cannot be considered in isolation as it induces a range of additional feedback mechanisms that regulate *ET* losses. Variations in the density and spatial arrangement of trees also impacts the aerodynamic properties of the subsurface, modifying aerodynamic resistance to *ET*. For example, the surface roughness of a treeless poor fen in Sweden and a treed fen in Central Alberta, were equal to 0.02 m (Mölder and Kellner, 2002) and 0.22 m (Thompson, 2012), respectively. Comparable results were exemplified by the differences in $u*$ from 0.002 to 0.24 m s^{-1} between Pauciflora and Poplar. A higher tree density generally produces a smoother aerodynamic surface as the tree canopy fills in, reducing surface roughness, this additionally raises the displacement height, which is equal to zero in a treeless peatland (Mölder and Kellner, 2002), and therefore increases the resistance from the subcanopy to *ET* (Niu and Yang, 2004). The aforementioned variables were favourable for higher surface *ET* at Pauciflora within the limits of Pauciflora's cooler climate. The impact of environmental conditions coupled with associated differences in understory species, Poplar's dense canopy was more favourable for the establishment of feathermoss which is generally more resistant to *ET* (Kettridge *et al*., 2013) compared to Pauciflora's dominant *Sphagnum* moss, cumulatively controlled understory *ET*. Correspondingly, surface *ET* at Pauciflora contributed > 80% to the total *ET* flux whereas at Poplar it contributed < 20%.

5.6 Microclimate and Canopy Cover on ET_{surf} Flux Dynamics

Both the microtopography and the spatial organization of trees has been shown to produce a fundamental control on *ET.* Although neither fen exhibited statistically significant differences in microclimate between canopy or microtopographic relief elements, covered plots and hollow microforms were generally cooler and wetter at both sites, and generally sustained lower *ET* (Figure 3.5.7). *Sphagnum* hummocks at Pauciflora maintained higher flux rates compared to *Sphagnum* hollows. Petrone *et al.* (2011) reported similar results, again suggesting that *Sphagnum* are better suited for more moderate moisture conditions, generally growing in a lower degree of canopy closure. Differences in *ET* were more pronounced when plots were separated by canopy closure; open plots continually supported higher flux rates (Figure 27). Finally, when fluxes were grouped by microtopography and canopy, open hummocks and hollows generally maintained higher *ET* compared to covered conditions; suggesting a dominance of *Sphagnum* to the flux budget within those locations. Goetz and Price (2015) reported similar trends as Petrone *et al.* (2011), concluding that *Tomenthypnum* and feathermosses are poorly suited for open conditions due to the species poor water transport structure, attributed to stressed induced by drying, as such, conditions at Poplar were more favourable for the establishment of these mosses.

Poplar demonstrated similar differences in *ET* that appeared to vary according to microtopography. Hummocks maintained higher *ET*, however unlike Pauciflora, numerous hollows at Poplar were under flooded conditions for the entire study period. Consequently, lower *ET* rates could be attributed to flood stress reported in other studies (Phillips, 2014) (Figure 26). Once more, when fluxes were separated by microtopography and canopy, both open and covered hummock microforms sustained higher *ET*, compared to open and covered hollows; suggesting the hummock microclimate was more favourable for underlying moss species (Figure 27).

Chapter Six
Conclusions and Implications for Climate and Land-use Change

The WBP is a region that encompasses a high density of wetlands, in particular peatlands (Woynillowicz *et al*., 2005), which continually sustains moisture deficit conditions. As such, these systems are already at a hydrological risk to future climate change scenarios and land use change (Petrone *et al*., 2011), which has implications for carbon sink status. It is well documented that the hydrological response of peatlands represent a first order response to the fate of future carbon storage (Billett *et al*., 2004; Couwenberg and Joosten, 2005; Limpens *et al*., 2008). Understanding the controls on the partitioning of *ET* within typical WBP peatlands is essential to interpreting the influences of climate change on water flux components. Potential increases in global temperatures through climate change is considered to directly impact boreal peatlands through water-level drawdown due to higher tree density (Laine *et al*., 1995; Laiho *et al*., 2003). It has been predicted that future, drier systems could increase canopy cover, therefore reducing or furthermore inhibiting the underlying peat surface from incoming solar radiant energy. It is anticipated that this shift could limit the potential for these peatland ecosystems to dissipate energy via $Q_{H,}$ in favour of Q_E (Worrall *et al*., 2015). Furthermore, this shift has not only been predicted to reduce surface ET_{surf}, but Kettridge *et al.* (2013) suggest a total reduction in *ET* across the entire peatland system that cannot be offset by increased *T*, associated with higher stem density. This not only threatens the future stability and functioning of peatland systems, but it directly threatens carbon stores, providing a positive feedback to atmospheric CO_2 concentrations (Flanagan and Syed, 2011). This is of particular concern for the low density of *P. mariana* dominated peatlands that, at present, allow incoming solar radiation to reach the underlying surface, often dominated by *Sphagnum*, and recognized for its contribution in regulating atmospheric CO_2 (Petrone *et al.*, 2011).

This research emphasized differences in *ET* and *ET* partitioning with respect to peatland type, climate and vegetation cover. The results indicate that the seasonal pattern of *ET* was closely linked with growing season Q^*, T_a and precipitation (*P*) events, as well, *VPD* represented a key factor in controlling fluxes. Seasonal mean *T* rates demonstrated little change across Pauciflora's open canopy, averaging 0.3 mm d^{-1}, while Poplar exhibited greater diversity and a higher contribution of *T* to the *ET* flux, averaging 2.7 mm d^{-1}. Both *ET* and *T* reached maxima in conditions of high Q^* and T_a, moderate to high *VPD*, that coincided with low *RH* and moderate windspeed (*u*). Poplar's dense canopy limited the contribution of understory species to < 20%, compared to Pauciflora that maintained surface ET_{surf} at > 80% contribution.

The presence of an overstory did not produce a microclimate that was significantly different between the two fens, however, Poplar's dense canopy generally supported a more-wet understory. Subsequently, surface vegetation at Pauciflora was dominated by *Sphagnum* moss, while Poplar was composed of a variety of feather moss and the brown moss, *Tomenthypnum nitens*. Both T_a and T_g formed strong, positive correlations with ET_{surf}, while *RH* formed a strong, negative correlation. Despite the dominance of *Sphagnum* at Pauciflora, ET_{surf} was limited by cooler T_a, whereas warmer T_a, coupled with the establishment of *Tomenthypnum* at Poplar largely diminished differences in ET_{surf} fluxes between the two fens. As such, ET_{surf} was not significantly different between the two fens despite distinct differences in canopy structure.

Despite the dominance of high water tables at both sites, the analysis begins to highlight the impacts induced from disturbance, in particular, climate-mediated warming that, in its most basic terms, has been predicted to increase canopy cover, maintained warmer T_a, and alter precipitation patterns. Both *ET* and *T* were the most significantly correlated with Q^*, T_a and *P* events.. Higher Q^* and T_a supported higher *ET* rates at Poplar, compared to Pauciflora which

supported lower seasonal mean Q^* and T_a. However, it is important to recognize that this represents a small component of the complex response of peatlands to disturbance.

The ultimate goal of this research was to accurately assess the partitioning of *ET* within two typical peatland systems with divergent tree canopies. It is essential to quantify energy balance and flux components within typically occurring peatlands to provide a better understanding of potential feedbacks induced by disturbance. The region of Fort McMurray, Alberta is not only subjected to disturbance from resource extraction but climate-mediated warming has been predicted to be the most pronounced within northern peatlands. Current multidisciplinary research within Fort McMurray has focused on landscape reclamation to create fen ecosystems on post oil sands mine sites, which further necessitates a better understanding of the dominant processes that sustained the pre-disturbed system. It is evident that any disruption to climate and moisture regimes has to potential to disrupt the natural functioning of these systems, altering *ET*.

Industrial pressures will play a significant role in altering local hydrological cycles, for example, corridor creation to access prime regions for the extraction of timber, oil and gas exploration may cause enhanced aerobic soil respiration due to the lowering of water tables and higher peat temperatures due to canopy removal (Devito *et al*., 2005; Petrone *et al*., 2005), causing the release of stored carbon to the atmosphere. Climate-mediated warming has the potential to further intensify drought conditions that will perpetuate the shift to a tree-dominated state, and can further increase water level draw-down (Heijmans *et al*., 2013), and permanently alter peatland functioning. This research highlights the role of climate and tree density within treed peatlands, and how changes in either variable can produce strong influences on *ET*. However, further research is necessary to understand and assess these changes over a longer period of time. To understand the potential feedback mechanisms, it is necessary to account for increased tree biomass and the

direct influence on radiation received at the peat surface, potential shifts of the underlying microclimate and controls regulating the *Sphagnum*-feathermoss transition.

Chapter Seven
References

Acreman, M.C., Harding, R.J., Lloyd, C.R., McNeil, D.D. 2003. Evaporation characteristics of wetlands: experience from a wet grassland and a reedbed using eddy correlation measurements. *Hydrology and Earth system Sciences*, **7**(1): 11-21.

Admiral, S.W., Lafleur, P.M., Roulet, N. 2006. Controls on latent heat flux and energy partitioning at a peat bog in eastern Canada. *Agricultural and Forest Meteorology*, **140**: 308-321.

Admiral, S.W., Lafleur, P.M. 2007. Modelling of latent heat partitioning at a bog peatland. *Agricultural and Forest Meteorology*, **144**: 213-229.

Admiral, S.W., Lafleur, P.M. 2007. Partitioning of latent heat flux at a northern peatland. *Aquatic Botany*, **86**: 107-116.

Ahrends, B., Penne, C. 2010. Modeling the impact of canopy structure on the spatial variability of net forest precipitation and interception loss in scots pine stands. *The Open Geography Journal*, **3**: 15-124.

Alberta Environment. 2008. Guideline for wetland establishment on reclaimed oil sands leases (eds). Prepared by Harris, M.L. of Lorax Environmental for the Wetlands and Aquatics Subgroup of the Reclamation Working Group of the Cumulative Environmental Management Association, Fort McMurray, AB.

Allen, R., Pereira, L.S., Raes, D., Smith, M. 1998. Crop evapotranspiration – Guidelines for computing crop water requirements. FAO Irrigation and drainage paper 56.

Asbjornsen, H., Goldsmith, G.R., Alvarado-Barrientos, M.S., Rebel, K., Van Osch, F.P. Rietkerk, M., Chen, J., Gotsch, S., Tobón, C., Geissert, D.R., Gómez-Tagle, A., Vache, K., Dawson, T.E. 2011. Ecohydrological advances and applications in plant-water relations research: a review. *Journal of Plant Ecology*, **4**: 3-22.

Aurela, M., Riutta, T., Laurila, T., Tuovinen, J.-P., Vesala, T., Tuittila, E.-S., Rinne, J., Haapanala, S., Laine, J. 2007. CO_2 exchange of a sedge fen in southern Finland-The impact of drought period. *Tellus Series B*, **59**(5): 826-837.

Baker, B.L., Nieber, J.L. 1989. An analysis of the steady-state heat balance method measuring sap flow in plants. *Agricultural and Forest Meteorology*, **48**: 93-109.

Baker, J.M., van Bavel, C.H.M. 1987. Measurement of mass flow of water in stems of herbaceous plants. *Plant, Cell & Environment*, **10**: 777-782.

Barr, A.G., King, K.M., Gillespie, T.J., den Hartog, G., Neumann, H.H. 1994. A comparison of Bowen ratio and eddy correlation sensible and latent heat flux measurements above deciduous forest. *Boundary-Layer Meteorology*, **71**: 21-41.

Belyea, L.R. 2009. Nonlinear dynamics of peatlands and potential feedbacks on the climate system, in Carbon Cyling in Northern Peatlands, Geophysical Monograph Series 184. American Geophysical Union, Washington; 5-18.

Bisbee, K.E., Gower, S.T., Norman, J.M., Nordheim, E.V. 2001. Environmental controls on ground cover species composition and productivity in a boreal peatland complex. *Oecologia*, **129**: 261-270.

Billet, M.F., Palmer, S.M., Hope, D., Deacon, C., Storeton-West, R., Hargreaves, K.J., Flechard, C., Fowler, D. 2004. Linking land-atmosphere-stream carbon fluxes in a lowland peatland system. *Global Biogeochemical Cycles*, **18**, GB1024.

Blanford, J.H., Gay, L.W. 1992. Tests of a robust eddy correlation system for sensible heat flux. *Theoretical and Applied Climatology*, **46**: 53-60.

Blanken, P.D., Black, T.A., Yang, P.C., Neumann, H.H., Staebler, R., Nesic, Z., den Hartog, G., Novak, M.D., Lee, X. 1997. The energy balance and canopy conductance of a boreal aspen forest: partitioning overstory and understory components. *Journal of Geophysical Research*, **102**: 915-927.

Bocking, E. 2015. Analyzing the impacts of road construction on the development of a poor fen in Northeastern Alberta, Canada. Master's thesis, University of Waterloo, Waterloo, Canada.

Bond-Lamberty, B., Wang, C., Gower, S.T. 2002. Aboveground and belowground biomass and sapwood area allometric equations for six boreal tree species of northern Manitoba. *Canadian Journal of Forest Research*, **32**: 1441-1450.

Botting, R.S., Fredeen, A.L. 2006 Net ecosystem CO_2 exchange for moss and lichen dominated forest floors of old-growth sub-boreal spruce forests in central British Columbia, Canada. *Forest Ecology and Management*, **235**: 240-251.

Bréda, N., Granier, A. 1996. Intra-and interannual variations of transpiration, leaf area index and radial growth of a sessile oak stand *(Quercus petraea). Annals of Forest Science*, **53**: 521-536.

Breeuwer, A., Robroek, B.J.M., Limpens, J., Heijmans, M.M.P.D., Schouten, M.G.C., Berendse, F. 2009. Decreased summer water table depth affects peatland vegetation. *Basic and Applied Ecology*, **10**: 330-339.

Bridgham, S.D., Pastor, J., Updegraff, K., Malterer, T.J., Johnson, K., Harth, C., Chen, J. 1999. Ecosystem Control over Temperature and Energy Flux in Northern Peatlands. *Ecological Applications*, **9**(4): 1345-1358.

Brown, S., Petrone, R., Mendoza, C., Devito, K. 2010. Surface vegetation controls on evapotranspiration from a sub-humid Western Boreal Plain. *Hydrological Processes*, **24**: 1072-1085.

Brown, S.M., Petrone, R.M., Chasmer, L., Mendoza, C., Lazerjan, M.S., Landhäusser, S.M., Silins, U., Leach, J., Devito, K.J. 2014. Atmospheric and soil moisture controls on evapotranspiration from above and within a Western Boreal Plain aspen forest. *Hydrological Processes*, **28**: 4449-4462.

Brümmer. C., Black, T.A., Jassal, R.S., Grant, N.J., Spittlehouse, D.L., Chen, B., Nesic, Z., Amiro, B., Arain, M.A., Barr, A.G., Bourque, C.P.A., Coursolle, C., Dunn, A.L., Flanagan, L.B., Humphreys, E.R., Lafleur, P.M., Margolis, H.A., McCaughey, J.H., Wofsy, S.C. 2012. How climate and vegetation type influence evapotranspiration and water use efficiency in Canadian forest, peatland and grassland ecosystems. *Agricultural and Forest Meteorology*, **153**: 14-30.

Bubier, J., Moore, T. 1994. An ecological perspective on methane emissions from northern wetlands. *Trends in Ecology and Evolution*, **9**: 460-464.

Bubier, J.L., Crill, P.M., Moore, T.R., Savage, K., Varner, R.K. 1998. Seasonal patterns and controls on net ecosystem CO2 exchange in a boreal peatland complex. *Global Biogeochemical Cycles*, **12**: 703-714.

Bubier, J.L., Bhatia, G., Moore, T.R., Roulet, N.T., Lafleur, P.M. 2003. Spatial and temporal variability in growing season net ecosystem carbon dioxide exchange at a large peatland in Ontario, Canada. *Ecosystems*, **6**: 353-367.

Bubier, J.L., Moore, T.R., Crosby, G. 2006. Fine-scale vegetation distribution in a cool temperature peatland. *Canadian Journal of Botany*, **84**: 910-923.

Callaghan, T.V., Collins, N.J., Callaghan, C.H. 1978. Photosynthesis, growth and reproduction of *Hylocomium splendens* and *Polytrichum commune* in Swedish Lapland. *Oikos*, **31**: 73-88.

Canadian Council on Ecological Area. 2006. Ecozones of Canada. *In* Couling, K., Prepas, E.E., Smith, D.W. 2007. Improved estimation of wetland cover in the western Canadian boreal forest. *Lake and Reservoir Management*, **23**: 245-254.

Čermák, J., Kučera, J., Nadezhdina, N. 2004. Sap flow measurement with some thermodynamic methods, flow integration within trees and scaling up from sample trees to entire forest stands. *Trees*, **18**: 529-546.

Chasmer, L., Hopkins, C., Montgomery, J., Petrone, R. 2016.A Physically-based Terrain Morphology and Vegetation Structural Classification for Wetlands of the Boreal Plains, Alberta, Canada. *Canadian Journal of Remote Sensing. (In printing)*

Chuang, Y., Oren, R., Bertozzi, A.L., Phillips, N., Katul, G. 2006. The porous media model for the hydraulic system of a conifer tree: Linking sap flux data to transpiration rate. *Ecological Modelling*, **191**: 447-468.

Chymko, N. 2000. Guideline for wetland establishment on reclaimed oil sands leases. Oil Sands Wetlands Working Group, Alberta Environment, Environmental Service, Edmonton, Canada, Report #ESD/LM/00-1, T/517.

Cleugh, H.A., Leuning, R., Mu, Q., Running, S.W. 2007. Regional evaporation estimates from flux tower and MODIS satellite data. *Remote Sensing of Environment*, **106**: 285-304.

Clulow, A.D., Everson, C.S., Price, J.S., Jewitt, G.P.W., Scott-Shaw, B.C. 2013. Water-use dynamics of a peat swamp forest and a dune forest in Maputaland, South Africa. *Hydrology and Earth System Sciences*, **17**: 2053-2067.

Comer, N.T., Lafleur, P.M., Roulet, N.T., Letts, M.G., Skarupa, M., Verseghy, D. 2000. A test of the Canadian Land Surface Scheme (CLASS) for a variety of wetland types. *Atmosphere-Ocean*, **38**: 161-179.

Couwenberg, J., Joosten, H. 2005. Self-organization in raised bog patterning: the origin of microtope zonation and mesotope diversity. *Journal of Ecology*, **93**: 1238-1248.

Cumming, S.G., Drever, C.R., Houle, M., Cosco, J., Racine, P., Bayne, E., Schmiegelow, F.K.A. 2015. A gap analysis of tree species representation in the protected areas of the Canadian boreal forest: applying a new assemblage of digital Forest Resource Inventory data. *Canadian Journal of Forest* Research, **45**: 163-173.

Currie, D.J., Paquin, V. 1987. Large-scale biogeographical patterns of species richness of trees. *Nature*, **329**(6137): 326-327.

Dang,Q., Margolis, H., Coyea, M., Sy, M., Collatz,G. 1997. Regulation of branch-level gas exchange of boreal trees: roles of shoot water potential and vapour pressure difference. *Tree Physiology*, **17**: 521-535.

Daum, C.R. 1967. A method for determining water transport in trees. *Ecology*, **48**: 425-431.

Devito, K., Creed, I., Gan, T., Mendoza, C., Petrone, R., Silins, U., Smerdon, B. 2005a. A framework for broad-scale classification of hydrologic response units on the Boreal Plain: is topography the last thing to consider? *Hydrological Processes*, **19**: 1705-1714.

Devito, K., Mendoza, C. 2007. Maintenance and dynamics of natural wetlands in western boreal forests: synthesis of current understanding from the Utikuma study area. *In* Appendices to the guideline for wetland establishment on reclaimed oil sands leases (eds). Lorax Environmental for the Wetlands and Aquatics Subgroup of the Reclamation Working Group of the Cumulative Environmental Management Association, Fort McMurray, Alberta, Canada.

Drexler, J.Z., Snyder, R.L., Spano, D., Kyaw, T.P.U. 2004. A review of models and micrometeorological methods used to estimate wetland evapotranspiration. *Hydrological Processes*, **18**: 2071-2101.

Dynamax Inc., 2007. Dynagage Manual. Dynamax Inc., Houston, TX, USA.

Dynamax Inc. 2007. Flow32-1K Manual. Dynamax Inc., Houston, TX, USA.

Eaton, A.K., Rouse, W.R., Lafleur, P., Marsh, P., Blanken, P. 2001. Surface energy balance of the Western and Central Canadian subarctic: variations in the energy balance among five major terrain types. *Journal of Climate*, **14**: 3692-3703.

Environment Canada. 2015. *Canadian Climate Normals*. Retrieved from http://climate.weather.gc.ca/climate_normals/index_e.html

Falge, E., Baldocchi, D., Olson, R., Anthoni, P., Aubinet, M., Bernhofer, D., Burba, G., Ceulemans, R., Clement, R., Dolman, H., Granier, A., Gross, P., Grünwald, T., Hollinger, D., Jensen, N., Katul, G., Keronen, P., Kowalski, A., Lai, C.T., Law, B.E., Meyers, T., Moncrieff, J., Moors, E., Munger, J.W., Pilegaard, K., Rannik, Ü., Rebmann, C., Suyker, A., Tenhunen, J., Tu, K., Verma, S., Vesala, T., Wilson, K., Wofsy, S. 2001. Gap filling strategies for defensible annual sums of net ecosystem exchange. *Agricultural and Forest Meteorology*, **107**: 43-69.

Ferone, J.M., Devito, K.J. 2004. Shallow groundwater-surface water interactions in pond-peatland complexes along a Boreal Plains topographic gradient. *Journal of Hydrology*, **292**: 75-95.,

Flanagan, L.B., Syed, K.H. 2011. Stimulation of both photosynthesis and respiration in response to warmer and drier conditions in a boreal peatland ecosystem. *Global Change Biology*, **17**: 2271-2287.

Finkelstein, P.L., Sims, P.F. 2001. Sampling error in eddy correlation flux measurements. *Jounral of Geophysical Research*, **106**(4): 3503-3509.

Ford, C.R., Hubbard, R.M., Kloeppel, B.D., Vose, J.M. 2007. A comparison of sap flux based evapotranspiration estimates within catchment-scale water balance. *Agricultural and Forest Meteorology*, **145**: 16-185.

Fraser, C.J.-D., Roulet, N.T., Lafleur, P.M. 2001. Groundwater flow patterns in a large peatland. *Journal of Hydrology*, **246**: 142-154.

Fritts, H.C. 1976. Tree rings and climate. Academic Press, New York, NY, 567 pp.

Fraver, S., Bradford, J.B., Palik, B.J. 2011. Improving Tree Age Estimates Derived from Increment Cores: A Case Study of Red Pine. *Forest Science*, **57**(2): 164-170.

Frolking, S., Roulet, N., Fuglestvedt, J. 2006. How northern peatlands influence the Earth's radiative budget: sustained methane emission versus sustained carbon sequestration. *Journal Geophysical Research*, **111**, G01008.

Goetz, J.D., Price, J.S. 2015. Role of morphological structure and layering of *Sphagnum* and *Tomenthypnum* mosses on moss productivity and evaporation rates. *Canadian Journal of Soil Science*, **95**: 109-124.

Goulden, M.L., Daube, B.C., Fan, S.M., Sutton, D.J., Bazzaz, A.M., Munger, J.W., Wolfsy, S.C. 1997. Physiological responses of a black spruce forest to weather. *Journal of Geophysical Resources*, **102**: 28987-28996.

Gower, S.T., Kucharik, C.J., Norman, J.M.1999. Direct and Indirect Estimation of Leaf Area Index, f_{APAR}, and Net Primary Production of Terrestrial Ecosystems. *Remote Sensing of Environment*, **70**: 29-51.

Granier, A. 1985. Une nouvelle méthode pour la mesure du flux de sève brute dans le tronc des arbres. *Annals of Forest Science*, **42**: 193-200.

Granier, A., Loustau, D., Bréda, N. A generic model of forest canopy conductance dependent on climate, soil water availability and leaf area index. *Annals of Forest Science*, **57**: 247-260.

Grant, J., Dryer, S., Woynillowicz, D. 2008. Fact or Fiction: Oil Sands Reclamation. The Pembina Institute.

Greenwood, E.A.N., Beresford, J.D. 1979. Evaporation from vegetation in landscapes developing secondary salinity using the ventilated chamber technique. I. Comparative transpiration from juvenile *Eucalyptus* above saline groundwater seeps. *Journal of Hydrology*, **42**: 369-382.

Groot, A., King, K.M. 1992.Measurement of sap flow by heat balance method: numerical analysis and application to coniferous seedlings. *Agricultural and Forest Meteorology*, **59**: 289-308.

Grime, V.L., Morrison, J.I.L., Simmonds, L.P. 1995a. Including heat storage term in sap flow measurements with the heat storage method. *Agricultural and Forest Meteorology*, **74**: 1-25.

Grime, V.L., Sinclair, F.L. 1999. Sources of error in stem heat balance sap flow measurements. *Agricultural and Forest Meteorology*, **94**: 103-121.

Gao, Y., Markkanen, T., Backman, L., Henttonen, H.M., Pietikäinen,J.P., Mäkelä, H.M., Laaksonen, A. 2014. Biogeophysical impacts of peatland forestation on regional climate changes in Finland. *Biogeosciences*, **11**: 7251-7267.

Guo, Y., Sun, L. 2012. Surface energy fluxes and control of evaporation from a Carex lasiocarpa mire in the Sanjiang Plain, Northeast China. *International Journal of Biometeorology*, **56**: 221-232.

Hájek, T., Tuittila E-S, Ilomets, M., Laiho, R. 2009. Light responses of mire mosses – a key to survival after water-level drawdown? *Oikos*, **118:** 240-250.

Ham, J.M., Heilman, J.L., 1990. Dynamics of a heat balance steam flow gauge during high flow. *Agronomy Jounral*, **82**: 147-152.

Hamel, P., Mchugh, I., Coutts, A., Daly, E., Beringer, J., Fletcher, T.D. 2015. Automated Chamber System to Measure Field Evapotranspiration Rates. *Journal of Hydrologic Engineering*, **20**(2): 04014037.

Harper, K.A., Bereron, Y., Drapeau, P., Gautheir, S., De Grandpre, L. 2006. Changes in spatial pattern of trees and snags during structural development in *Picea mariana* boreal forests. *Journal of Vegetation Science*, **17**: 625-636.

Hatton, T.J., Wu, H.I. 1995. Scaling theory to extrapolate individual tree water use to stand water use. *Hydrological Processes*, **9**: 527-540.

Heijmans, M., Arp, W.J., Berendse, F. 2001. Effects of elevated CO_2 on vascular plants on evapotranspiration in bog vegetation. *Global Change Biology*, **7**: 817-827.

Heijmans, M., Arp, W.J., Chapin, F.S. III. 2004 Carbon dioxide and water vapour exchange from understory species in boreal forest. *Agricultural and Forest Meteorology*, **123**: 135-147.

Heijmans, M.M.P.D., Arp., W.J., Chapin F.S. III. 2004. Controls on moss evaporation in boreal black spruce forest. *Global Biogeochemical Cycles*, **18**: GB2004.

Heijmans, M.P.D., Van der Knaap, Y.A.M., Holmgren, M., Limpens, J. 2013. Persistent versus transient tree encroachment of temperate peat bogs: effects of climate warming and drought events. *Global Change Biology*, **19**: 2240-2250.

Hillebrand, H. 2004. On the generality of the latitudinal diversity gradient. *The American Naturalist*, **163**(2): 192-211.

Hillman, G.R., Roberts, J.J. 2006. Early growth response in trees following peatland drainage, *Information Report NOR-X-408*, Natural Resources Canada., Canadian Forestry Service, Northern Forestry Centre, Edmonton, Canada.

Hollinger, D.Y., Richardson, A.D. 2005. Uncertainty in eddy co-variance measurements and its application to physiological models. *Tree Physiology*, **25**: 873-885.

Husch, B., Miller, C.I., Beers, T.W. 1972. Forest mensuration 2nd edition. The Ronald Press Company, New York, USA.

Integral Ecology Group. 2014. COSIA, WECF, Forest Mensuration 2014.

Jarvis, P.G., McNaughton, K.G. 1986. Stomatal control of transpiration: scaling from lead to region. *Advances in Ecology Research*, **15**: 1-49.

Johnson, E.A., Miyanishi, K. 2008. Creating new landscapes and ecosystems the Alberta oil sands. *Annals New York Academy of Sciences*, **1134**: 120-145.

Kellner, E. 2001. Surface energy fluxes and control of evaporation from a Swedish *Sphagnum* mire. *Agricultural and Forest Meteorology*, **110**: 101-123.

Kettridge, N., Thompson, D.K., Bombonato, L., Turetsky, M.R., Benscoter, B.W., Waddington, J.M. 2013. The ecohydrology of forested peatlands: Simulating the effects of tree shading on moss evaporation and species composition. *Journal of Geophysical Research, Biogeosciences*, **118**: 422-435.

Kim, J., Verma, S.B. 1996. Surface exchange of water vapour between an open Sphagnum fen and the atmosphere. *Boundary-Layer Meteorology*, **79**: 234-264.

Kjelgaard, J.F., Sogachev, A. 2006. Flux footprint simulation downwind of a forest edge. *Boundary-Layer Meteorology*, **121**: 459-473.

Köstner, B., Granier, A., Čermák, J. 1998. Sapflow measurements in forest stands: methods and uncertainties. *Annals of Forest Science*, **55**: 13-27.

Kramer, P.J., Kozlowski, T.T. 1979. Physiology of woody plants. Academic Press, New York.

Kroon, P.S., Hensen, A., Jonker, H.J.J., Ouwersloot. H.G., Vermeulen, A.T., Bosveld, F.C. 2010. Uncertainties in eddy covariance flux measurements assessed from CH_4 and N_2O observations. *Agricultural and Forest Meteorology*, **150**: 806-816.

Kuhry, P., Nicholson, B., Gignac, L., Vitt, D., Bayley, S. 1992. Development of Sphagnum-dominated peatlands in Boreal continental Canada. *Canadian Journal of Botany*, **71**: 10-22.

Kutscha, N.P., Sachs, I.B. 1962. Colour Tests for Differentiating Heartwood and Sapwood in Certain Softwood Tree Species. Forest Products Laboratory, Forest Service U.S. Department of Agriculture.

Lafleur, P., Rouse, W. 1988. The influence of surface cover and climate on energy partitioning and evaporation in a subarctic wetland. *Boundary-Layer Meteorology*, **44**: 327-347.

Lafleur, P.M. 1990. Evaporation from wetlands. In: Roulet, N.T. (Ed.), Focus: Aspects of Physical Geography of Wetlands. Canadian Geography, **34**, 79-82.

Lafleur, P.M., Schreader, C.P. 1994. Water loss from the floor of a sub-arctic forest. *Arctic Alpine Research*, **26**: 152-158.

Lafleur, P.M., Roulet, N.T., Bubier, J.L., Frolking, S.E., Moore, T.R. 2003. Interannual variability in evapotranspiration and water table at a shrub-covered bog in southern Ontario, Canada. *Hydrological Processes*, **19**(18): 3533-3550.

Lafleur, P.M., Hember, R.A., Admiral, S.W., Roulet, N.T. 2005. Annual and seasonal variability in evapotranspiration and water table at a srub-covered bog in southern Ontario, Canada. *Hydrological Processes*, **19**: 3533-3550.

Lafleur, P. 2008. Connecting Atmospheric and Wetland: Energy and Water Vapour Exchange. *Geography Compass*, **2**(4): 1027-1057.

Laiho, R., Vasander, H., Penttilä, T., Laine, J. 2003. Dynamics of plant-mediated organic matter and nutrient cycling following water-level drawdown in boreal peatlands. *Global Biogeochemical Cycles*, **17**, 1053, DOI: 10.1029/2002GB002015.

Laine, J., Vasander, H., Laiho, R. 1995. Long-term effects of water level drawdown on the vegetation of drained pine mires in southern Finland. *Journal of Applied Ecology*, **32**: 785-802.

LeCain, D.R., Morgan, J.A., Schuman, G.E., Reeder, J.D., Hart, R.H. 2002. Carbon exchange and species composition of grazed pastures and exclosures in shortgrass steppe of Colorado. *Agriculture, Ecosystems and Environment*, **93**: 421-435.

Leuning, R., Judd, M.J. 1996. The relative merits of open and closed path analyzers for measurements if eddy fluxes. *Global Change Biology*, **2**: 241-253.

Lieffers, V.J., Macdonald, S.E. 1990. Growth of foliar nutrient status of black spruce and tamarack in relation to depth of water table in some Alberta peatlands. *Canadian Journal of Forest Research*, **20**: 805-809.

Limpens, J., Berendse, F., Blodau, C., Canadell, J.G., Freeman, C., Holden, J., Roulet, N., Rydin, H., Schaepman-Strub, G. 2008. Peatlands and the carbon cycle: from local processes to global implications-a synthesis. *Biogeosciences*, **5**: 1475-1491.

Limpens, J., Holmgren, M., Jacobs, C.M.J., Van der Zee, S.E.A.T.M., Karofeld, E., Berendse, F. 2014. How does tree density affect water loss of peatlands? A mesocosm experiment. *Public Library of Science*, **9**(3): e91748.

Limpens, J., van Egmond, E., Li, B., Holmgren, M. 2014. Do plant traits explain tree seedling survival in bogs? *Functional Ecology*, **28**: 283-290.

Litt, M. Sicart, J.-E., Helgason, W. 2015. A study of turbulent fluxes and their measurement errors for different wind regimes over the tropical Zongo Glacier (16°S) during the dry season. *Atmospheric Measurement Techniques*, **8**: 3229-3250.

Lopushinsky, W., Kaufmann, M.R. 1984. Effects of cold soil on water relationship and spring growth of Douglas-fir seedling. *Forestry Science*, **30**(3): 628-634.

MacDonald, S.E., Yin, F. 1999. Factors influencing size inequality in peatland black spruce and tamarack evidence from post drainage release growth. *Journal of Ecology*, **87**: 404-412.

Maguire, D.A., Hann, D.W. 1987. Equations for predicting sapwood area at crown base in southwestern Oregon Douglas-fir. *Canadian Journal of Forest Research*, **17**: 236-241.

Mahrt, L., Vickers, D. 2002. Relationship of area-averaged carbon dioxide and water vapour fluxes to atmospheric variables. *Agricultural and Forest Meteorology*, **112**: 195-202.

Mann, J., Lenschow, D.H. 1994. Errors in airborne flux measurements. *Journal in Geophysical Research*, **99**(7): 14519-14526.

Marschall, M., Proctor, M.C.F. 2004. Are bryophytes shade plants? Photosynthetic light responses and proportions of chlorophyll a, chlorophyll b and total carotenoids. *Annals of Botany*, **94**: 593-603.

Margolis, H., Flanagan, L., Amiro, B. 2006. The Fluxnet-Canada Research Network: Influence of climate and disturbance on carbon cycling in forests and peatlands. *Agriculture and Forest Meteorology*, **140**: 1-5.

Martin, T.A., Hinckley, T.M., Meinzer, F.C., Sprugel, D.G. 1999. Boundary layer conductance, leaf temperature and transpiration of *Abies amabilis* branches. *Tree Physiology*, **19**: 435-443.

Matsumoto, K., Ohta, T., Nakai, T., Kuwada, T., Daikoku, T., Iida, S., Yabuki, H., Kononov, A.V., van der Molen, M.K., Kodama, Y., Maximov, T.C., Dolman, A.J., Hattori, S. 2008. Energy consumption and evapotranspiration at small scale. *Agricultural Water Management*, **148**: 1978-1989.

McGuire, A.D., Melillo, J.M., Kicklighter, D.W., Joyce, L.A. 1995. Equilibrium responses of soil carbon to climate change: Empirical and process based estimates. *Journal of Biogeography*, **22**: 785-796.

McLeod, M.K., Daniel, H., Faulkner, R. Murison, R. 2004. Evaluation of an enclosed portable chamber to measure crop and pasture actual evapotranspiration at small scale. *Agricultural Water Management*, **67**: 15-34.

McNeil, P., Waddington, J.M. 2003. Eco-hydrology controls on Sphagnum growth and CO_2 exchange on a cutover bog surface. *Journal of Applied Ecology*, **40**: 354-367.

Mölder, M., Kellner, E. 2002. Excess resistance of bog surfaces in central Sweden. *Agriculture and Forest Meteorology*, **112**: 23-30.

Monteith, J.L., Unsworth, M.H. 1990. Principles of environmental physics. Edward Arnold, New York.

Moore, T.R., Roulet, N.T., Waddington, J.M. 1998. Uncertainty in predicting the effect of climate change upon the carbon cycling of Canadian peatlands. *Climate Change*, **40**: 229-245.

Moore, T.R., Bubier, J.L., Frolking, S.E., Lafleur, P.M., Roulet, N.T. 2002. Plant biomass and production and CO_2 exchange in an ombrotrophic bog. *Journal of Ecology*, **90**: 25-36.

Morris, P., Baird, A.J., Belyea, L.R. 2012. The DigiBog model of peatland development s: ecohydrological simulations in 2-D. *Ecohydrology*, **5**: 256-268.

National Wetlands Working Group. 1988. Wetlands of Canada, ecological land classification Series No. 24, Ottawa.

Nichols, D.S., Brown, J.M. 1980. Evaporation from a *Sphagnum* moss surface. *Journal of Hydrology*, **48**: 289-302.

Niu, G.-Y., Yang, Z.L. (2004). Effects of vegetation canopy processes on snow surface energy and mass balances. *Journal of Geophysical Research*, **109**: D23111.

Nobel, P.S. 1991. Physiochemical and environmental plant physiology. Academic Press, San Diego.

Oechel, W.C., Van Cleve, K. 1986. The role of bryophytes in nutrient cycling in the taiga. *In* Forest Ecosystems in the Alaskan Taiga, Van Cleve, K., Chapman III, F.S., Flanagan, P., Viereck, L.A., Dryness, C.T. (eds). Springer-Verlag, New York; 121-37.

Oke, T.R. Boundary Layer Climates 2nd Edition. University Press, Cambridge, 1987.

Oren, R., Phillips, N., Ewers, B.E., Pataki, D.E., Megonigal, J.P. 1999. Sap-flux-scaled transpiration responses to light, vapor pressure deficit, and leaf area reduction in a flooded Taxodium distichum forest. *Tree Physiology*, **19**: 337-347.

Overgaard, J., Rosbjerg, D., Butts, M.B. 2006. Land-surface modeling in hydrological perspective-a review. *Biogeosciences*, **3**: 229-241.

Peixoto, J.P., Oort, A.H. 1992. Physics of Climate Change. American Institute of Physics, New York.

Perämäki, M., Vesala, T., Nikinmaa, E. 2001. Analyzing the applicability of the heat balance method for estimating sap flow in boreal forest conditions. *Boreal Environment Research*, **6**: 29-43.

Petrone, R.M., Rouse, W.R., Marsh, P. 2000. Comparative surface energy budgets in western and central subarctic regions of Canada. *International Journal of Climatology*, **20**: 1131-1148.

Petrone, R.M., Waddingtion, J.M., Price, J.S. 2001. Ecosystem-scale flux of CO2 from restored vacuum peatland. *Wetlands Ecology and Management*, **11**(6): 419-432.

Petrone, R.M., Waddington, J.M., Price, J.S. 2003. Ecosystem-scale flux of CO_2 from a restored vacuum harvested petland. *Wetlands Ecology and Management*, **11**: 419-432.

Petrone, R.M., Silins, U., Devito, K.J. 2007. Dynamics of evapotranspiration from riparian pond complex in the Western Boreal Forest, Alberta, Canada. *Hydrological Processes*, **21**(11): 1391-1401.

Petrone, R.M., Devito, K.J., Silins, U., Mendoza, C., Brown, S., Kaufman, S.C., Price, J.S. 2008. Transient peat properties in two pond-peatland complexes in the sub-humid Western Boreal Plain, Canada. *Mires and Peat*, **3**: Article 05.

Petrone, R.M., Solondz, D.S., Macrae, M.L., Gignac, D., Devito, K.J. 2011. Microtopographical and canopy cover controls on moss carbon dioxide exchange in a western Boreal Plain peatland. *Ecohydrology*, **4**: 115-129.

Phillips, T. 2014. Quantifying and Characterizing Evapotranspiration in a Natural Saline Fen within the Western Boreal Plain, Fort McMurray, Alberta, Canada. Master's thesis, Wilfrid Laurier University, Waterloo, Canada.

Pickard, W.F., Puccia, C.J. 1972. A theory of steady-state heat step method of measuring water flux in woody plant stems. *Mathematical Biosciences*, **14**: 1-15.

Price, J.S., Maloney, D.A. 1994. Hydrology of a patterned bog-fen complex in southeastern Labrador, Canada. *Nordic Hydrology*, **25**: 313-330.

Price, J.S. 1997. Soil moisture, water tension, and water table relationships in a managed cutover bog. *Journal of Hydrology*: **202**: 21-32.

Price, J.S., Branfireun, B., Waddington, J.M., Devito, K. 2005. Advances in Canadian wetland hydrology, 1999-2003. *Hydrological Processes*, **18**: 201-214.

Price, J.S., Rochefort, F., Rezanezhad, F., Andersen, R., Pouliot, R. 2011. Fen creation in the Athabasca oil sands region, Final Report and Implications, Suncor Energy Inc.

Quiñonez-Piñón, M. 2007. Improved Techniques for Measuring and Estimating Scaling Factors Used to Aggregate Forests Transpiration. Dissertation, University of Calgary, Calgary, Alberta.

Raddatz, R.L., Papakyriakou, T.N., Swystun, K.A., Tenuta, M. 2009. Evapotranspiration from a wetland tundra sedge fen: surface resistance of peat for land-surface schemes. *Agriculture and Forest Meteorology*, **149**: 851-861.

Raupach, M.R., Finnigan, J.J. 1997. The influence of topography on metrological variables and surface-atmosphere interactions. *Journal of Hydrology*, **190**: 182-213.

Reicosky, D.C., Sharratt, B.S., Ljungkull, J.E., Baker, D.G. 1982. Comparison of Alfalfa Evapotranspiration Measured By A Weighing Lysimeter And A Portable Chamber. *Agricultural Meteorology*, **28**: 205-211.

Renger, M., Wessolek, G., Schwärzel, K., Sauerbrey, R., Devito, K. 2005. Aspects of peat conservation and water management. *Journal of Plant Nutrition and Soil Science*, **165**(4): 487-493.

Restrepo, N.C., Arain, M.A. 2005. Energy and water exchanges from a temperate pine plantation forest. *Hydrological Processes*, **19**: 27-49.

Robroek, B.J.M., Schouten, M.G.C., Limpens, J., Berendse, F., Poorter, H. 2009. Interactive effects of water table and precipitation on net CO_2 assimilation of three co-occuring *Sphagnum* mosses differing in distribution above the water table. *Global Change Biology*, **15**: 680-691.

Rosenberg, N.J., Blad, B.L., Verma, S.B. 1983. Microclimate: The Biological Environment. Wiley, New York; 495.

Roulet, N.T., Munro, D.S., Mortsch, L. 1997. Wetlands, in *The Surface Climates of Canada*, edited by Bailey, W.G., Oke, T.R., Rouse, W.R., McGill-Queen's University Press, Montreal, Quebec, Canada.

Rouse, W. 2000. The energy and water balance of high-latitude wetlands: controls and extrapolation. *Global Change Biology*, **6**: 59-68.

Runkle, B.R.K., Willie, C., Gažovič, Wilmking, M., Kutzback, L. 2014. The surface energy balance and its drivers in a boreal peatland fen of northwest Russia. *Journal of Hydrology*, **511**: 359-373.

Ryan, M.G. 1989. Sapwood volume for three subalpine conifers: predictive equations and ecological implications. *Canadian Journal of Forest Research*, **19**: 1397-1401.

Sakuratani, T. 1979. Apparent thermal conductivity of rice stem in relation to transpiration stream. *Journal of Agricultural Meteorology*, **34**: 177-187.

Sakuratani, T. 1981. A heat balance method for measuring water flux in the stem of intact plants. *Journal of Agricultural Meteorology*, **37**: 9-17.

Sakuratani, T. 1982. Two thermic methods for measuring water flux in the stem of intact plants and their applications. *Japanese Journal of Crop Science*, **29**: 47-121.

Sakuratani, T. 1984. Improvement of the probe for measuring water flow rate in intact plants with the stem heat balance method. *Journal of Agricultural Meteorology*, **40**: 273-277.

Schuepp, P.H., Leclerc, M.Y., MacPherson, J.I., Desjardins, R.L. 1990. Footprint prediction of scaler fluxes from analytical solutions of the diffusion equation. *Boundary-Layer Meteorology*, **50**: 355-373.

Schuepp, P.H. 1993. Leaf boundary layers: Tansley Review No. 59. *New Phytologist*, **125**: 477-507.

Sellers, P.J., Hall, F., Margolis, H., Kelly, B., Baldocchi, D., den Hartog, G., Cihlar, J., Ryan, M.G., Goodison, B., Crill, P., Ranson, K.J., Lettenmaier, D., Wickland, D.E. 1995a. The Boreal Ecosystem-Atmoshpere Study (BOREAS): An overview and early results from the 1994 field year. *Bulletin of the American Meteorological Society*, **76**: 1549-1577.

Shackel, K.A., Johnson, R.S., Medawar, C.K. 1992. Substantial Errors in Estimates of Sap Flow Using the Heat Balance Technique on Woody Stems under Field Conditions. *Journal of the American Society for Horticultural Science*, **117**(2): 351-356.

Shaver, G.R., Canadell, J., Chapin III, F.S., Gurevitch, J., Harte, J., Henry, G., Ineson, P., Jonasson, S., Melillo, J., Pitelka, L., Rustad, L. 2002. Estimating carbon accumulation rates of undrained mires in Finland-application to boreal and subarctic regions. *The Holocene*, **12**: 69-80.

Shurpali, N.J., Verma, S.B., Kim, J., Arkebauer. 1995. Carbon dioxide exchange in peatland ecosystem. *Journal of Geophysical Research*, **100**(D7), 14: 319-314.

Sims, P.H. Bradford, J.A. 2001. Carbon dioxide fluxes in a southern plains prairie. *Agricultural and Forest Meteorology*, **50**: 355-374.

Smerdon, B.D., Devito, K.J., Mendoza, C.A. 2005. Interaction of groundwater and shallow lakes on outwash sediments in the sub-humid Boreal Plains regions. *Journal of Hydrology*, **314**: 246-262.

Smerdon, B.D., Mendoza, C.A., Devito, K.J. 2007. Simulations of fully coupled lake-groundwater exchange in a subhumid climate with an integrated hydrological model. *Water Resource Research*, **43**, W01416.

Smith, D.M., Allen, S.J. 1996. Measurement of sap flow in plant stems. *Journal of Experimental Biology*, **47**: 1833-1844.

Smith, W.B., Brand, G.J. 1983. Allometric equations for 98 species of herbs, shrubs, and trees. USDA Forest Service Research Note NC-299.

Solondz, D.S., Petrone, R.M., Devito, K.J. 2008. Forest floor carbon dioxide fluxes within an upland-peatland complex in the Western Boreal Plain, Canada. *Ecohydrology*, **1(4)**: 361-376.

Sonnentag, O., Talbot, J., Chen, J.M., Roulet, N.T. 2007. Using direct and indirect measurements of leaf area index to characterize the shrub canopy in an ombrotrophic peatland. *Agricultural and Forest Meteorology*, **144**: 200-212.

Souch, C., Wolfe, C.P., Grimmtind, C.S.B. 1996. Wetland evaporation and energy partitioning: Indiana Dunes National Lakeshores. *Journal of Hydrology*, **184**: 189-208.

Stagnitti, F., Parlange, J.Y., Rose, C.W. 1989. Hydrology of a small wet catchment. *Hydrological Processes*, **3**: 137-150.

Stannard, D.I. 1988. Use of a hemispherical chamber for measurement of evapotranspiration. Open file-File Report 88-452. United Stare Geological Survey, Denver, CO.

Steinburg, S., van Bavel, C.H.M., McFarland, M.J. 1989. A gauge to measure mass flow rate of sap in stems and trunks of woody plants. *Journal of the American Society for Horticultural Science*, **114**(3): 466-472.

Steinburg, S.L., van Bavel, C.H.M., McFarland, M.J. 1990b. Improved sap flow gauge for woody and herbaceous plants. *Agronomy Journal*, **82**: 851-854.

Strack, M., Waddington, J.M., Tuittila, E.-S. 2004. Effect of water table drawdown on northern peatland methane dynamics: Implications for climate change. *Global Biogeochemical Cycles*, **18**, GB4003.

Strack, M., Kellner, E., Waddington, J.M. 2006. Effect of entrapped gas on peatland surface level fluctuations. *Hydrological Processes*, **20**: 3611-3622.

Sutherland, G., Chasmer, L.E., Petrone, R.M., Kljun, N., Devito, K.J. 2014. Evaluating the use of spatially varying versus bulk average 3D vegetation structural inputs to modelled evapotranspiration within heterogeneous land cover types. *Ecohydrology*, DOI: 10.1002/eco. 1477.

Swanson, R.V. Flanagan, L.B. 2001. Carbon regulation of carbon dioxide exchange at the forest floor in a boreal black spruce ecosystem. *Agricultural and Forestry Meteorology*, **108**: 165-181.

Tan, C.S., Black, T.A., Nnyamah, J.U. 1978. A simple diffusion model of transpiration applied to a thinned Douglas-fir stand. *Ecology*, **59**: 1221-1229.

Taylor, A.M., Brooks, J.R., Lachenbruch, B., Morrell, J.J. 2007. Radial patterns of carbon isotopes in the xylem extractives and cellulose of Douglas-fir. *Tree Physiology*, **27**: 921-927.

Thompson, D.K. 2012. Wildfire impacts on peatland ecohydrology. PhD Thesis, McMaster University, Hamilton, Ontario, Canada.

Thompson, D.K., Baisley, A.S., Waddington, J.M. 2015. Seasonal variation in albedo and radiation exchange between a burned and unburned forested peatland: implications for peatland evaporation. *Hydrological Processes*: **29**, 3227-3225.

Trites, M., Bailey, S.E. 2009. Vegetation communities in continental boreal wetlands along a salinity gradient: Implications for oil sands mining reclamation. *Aquatic Botany*, **91**: 27-39.

Turetsky, M.R., Donahue, W.F., Benscoter, B.W. 2011. Experimental drying intensifies burning and carbon losses in a northern peatland. *Nature Communications*, **2**, 514.

Turunen, J., Tomppo, E., Tolonen, K., Reinikainen, A. 2002. Estimating carbon accumulation rates of undrained mires in Finland-application to boreal and subarctic regions. *The Holocene*, **12**: 69-80.

Twine, T.E., Kustas, W.P., Norman, J.M., Cook, D.R., Houser, P.R., Meyers, T.P., Prueger, J.H., Starks, P.J., Wesely, M.L. 2000. Correcting eddy-covariance flux underestimates over a grassland. *Agricultural and Forest Meteorology*, **103**: 279-300.

Valancogne, C., Nasr, Z. 1989. Measuring sap flow in stems of small trees by a heat balance method. *Horticultural Science*, **24**: 383-385.

Vertessy, R.A., Benyon, R.G., O'Sullivan, S.K., Gribben, P.R. 1995. Relationship between stem diameter, sapwood area, leaf area and transpiration in a young mountain ash forest. *Tree Physiology*, **15**: 559-567.

Vieweg, G.H., Ziegler, H. 1960. Thermoelektrische Registrierung der Geschwindigkeit des Transpirationsstromes. *Berichte der Deutschen Botanischen Gesellschaft*, **73**: 221-226.

Vitt, D., Chee, W. 1989. The vegetation, surface water chemistry and peat chemistry of moderate-rich fens in central Alberta, Canada. *Wetlands*, **9**: 227-261.

Vitt, D.H. 1990. Growth and production dynamics of boreal mosses over climatic, chemical, and topographic gradients. *Botanical Journal of the Linnean Society*, **104**: 35-59.

Vitt, D.H., Halsey, L., Bray, J., Kinser, A. 2003. Patterns of Bryophyte Richness in a Complex Boreal Landscape: Identifying Key Habitats at McClelland Lake Wetland. *The Bryologist*, **106**(3): 372-382.

Vitt, D.H. 2006. Functional characteristics and indicators of boreal peatlands. *In* Weider, R.K., Vitt, D.H. (eds). Boreal Peatland Ecosystems. Springer-Verlag, Berlin-Heidelburg-New York.

Vötter, D. 2005. Splintholzerkennung mittels Computertomographie und Färbeverfahren an Fichte und Buche. Ein Methodenvergleich. Diploma thesis, TU Munich, MWW-DA 146, 151 pp.
Waddington, J.M., Griffis, T.J., Rouse, W.R. 1998. Northern Canadian wetlands: net ecosystem CO_2 exchange and climate change. *Climatic Change*, **40**: 267-275.

Waddington, J.M., Price, J.S. 2000. Effect of peatland drainage, harvesting, and restoration on atmospheric water and carbon exchange. *Physical Geography*, **21**: 433-451.

Waddington, J.M., Roulet, N.T. 2000. Carbon balance of boreal patterned peatland. *Global Change Biology*, **6**: 87-97.

Waddington, J.M., Morris, P.J., Kettridge, N., Granath, G., Thompson, D.K., Moore, P.A. 2014. Hydrological feedbacks in northern peatlands. *Ecohydrology*, **8**: 113-127.

Walter, H. 1973. Vegetation of the earth, first English edition. Springer, Berlin-Heidelburg-New York.

Wang, J., Zhuang, J., Wang, W., Liu, S., Xu, Z. 2015. Assessment of Uncertainties in Eddy Covariance Flux Measurement Based on Intensive Flux Matrix of HiWATER-MUSOEXE. *IEEE Geoscience and Remote Sensing Letters*, **12**(2): 259-263.

Wang, S., Pan, M., Qiaozhen, M., Xiaoying, S., Mao, J., Brümmer, C., Jassal, R., Krishnan, P., Li, J., Black, A. 2015. Comparing Evapotranspiration from Eddy Covariance Measurements, Water Budgets, Remote Sensing, and Land Surface Models over Canada. *Journal of Hydrometeorology*, **16**: 1540-1560.

Watson, R.T., Noble, I.R., Bolin, B., Ravindranath, N.H., Verardo, D.J., Dokken, D.J. 2000. Intergovernmental Panel on Climate Change Special Report. Summary for Policymakers: Land Use, Land-Use Change, and Forestry. IPCC Plenary XVI, Montreal, Canada. WMO & UNEP, Geneva.

Webb, E.K., Pearman, G.I., Leuning, R. 1980. Correction for flux measurements for density effects due to heat and water vapour transfer. *Quarterly Journal of the Royal Meteorological Society*, **106**: 85-100.

Weibel, F.P., Boersma, K. 1995. An improved stem heat balance method using analog heat control. *Agricultural and Forest Meteorology*, **75**: 191-208.

Weltzin, J.F., Harth, C., Bridgham, S.D., Pastor, J., Vonderharr, M. 2001. Production and microtopography of bog bryophytes: response to warming and water-table manipulations. *Oecologia*, **128**: 557-565.

Wieder, R.K., Kamminga, S.K., Vile, M.A., Vitt, D.H., Bone, T., Xu, B., Benscoter, B.W., Bhatti, J. 2009. Post-fire carbon balance in boreal bogs of Alberta Canada. *Global Change Biology*, **15**: 63-81.

Williams, T.G., Flanagan, L.B. 1996. Effects of changes in water content on photosynthesis, transpiration and discrimination against 13C02 and C18O16O in *Pleurozium* and *Sphagnum*. *Oecologia*, **108**: 38-46.

Worrall, F., Burt, T.P., Clay, G.D., Moody, C.S. 2015. A 19-year long energy budget of an upland peat bog, northern England. *Journal of Hydrology*, **520**: 17-29.

Woynillowicz, D., Severson-Baker, C., Raynolds, M. 2005. Oil Sands Fever: The environmental implications of Canada's oil sands rush. The Pembina Institute, Drayton Valley, Alberta.

Wu, J., Kutzbach, L., Jager, D., Willie, C., Wilmking, M. 2010. Evapotranspiration dynamics in boreal peatland and its impact on the water and energy balance. *Journal of Geophysical Research*, **115**, G04038.

Wullschleger, S.D., Meinzer, F.C., Vertessy, R.A. 1998. A review of whole-plant water use studies in trees. *Tree Physiology*, **18**: 499-512.

Yu, Z.C. 2012. Northern peatland carbon stocks and dynamics: a review. *Biogeosciences*, **9**: 4071-4085.

Zweifel, R., Zimmerman, L., Newbery, D.M. 2005. Modeling tree water deficit from microclimate: an approach to quantify drought stress. *Tree Physiology*, **25**: 147-156.

Appendix I

PAUCIFLORA ***Picea mariana***			
DOY	Daily Regression Model	**DOY**	Daily Regression Model
159	y=1336x-17080	**195**	y=966.6x-12441
160	y=-2122x+29930	**196**	y=944.6x-12064
161	y=859.1x - 9500	**197**	y=996x-12807
162	y= 3840.2x - 48930	**198**	y=1080.2x-13816
163	y=4872x-62204	**199**	y=920.8x-11603
164	y=2512.6x-32976	**200**	y=873.6x-11070
165	y=1957.2x-25421	**201**	y=1238.8x-15960
166	y=1738.4x-22556	**202**	y=744x-9431
167	y =1882x - 24468	**203**	y=1099x-14034
168	y=2209.8x-28721	**204**	y=33.2x-285.72
169	y=1774.6x-22959	**205**	y=1124.8x-14684
170	y=2696x-34980	**206**	y=950.2x-12219
171	y=3159.4x-40903	**207**	y=908.2x-11500
172	y=2839x-36734	**208**	y=1235.6x-15961
173	y=2809.8x-36352	**209**	y=455.6x-5852.8
174	y=2323x-30025	**210**	y=481.4x-6232.6
175	y=1881.2x-24409	**211**	y = 945.64x - 12217
176	y=1687.2x - 21860	**212**	y=1133.6x-14661
177	y=2022.4x-26205	**213**	y=765.8x-9797.7
178	y=746.68x - 9657.8	**214**	y=1168.2x-15044
179	y=889x-11510	**215**	y=1637.4x-21169
180	y=2183.6x-28313	**216**	y=1111.8x-14349
181	y=1556.6x-20100	**217**	y=691x-8833
182	y=1979.8x-25720	**218**	y=1129.4x-14664
183	y=2202.8x-28532	**219**	y=764.2x-9652
184	y=2764x-35957	**220**	y=641.4x-8138.5
185	y=2160x-27926	**221**	y=639x-7937.9
186	y=2410.8x-31291	**222**	y=405x-4906.9
187	y = 520.08x - 6750.2	**223**	y=407.6x-4846.1
188	y=616.4x-8008.9	**224**	y=141x-1578.1
189	y=1143.8x - 14610	**225**	y=378.6x-4597.7
190	y=1388.6x-17756	**226**	y=345.8x-4300.8
191	y=1633.8x-21055	**227**	y=120.8x-1128.1
192	y=1836.2x-23649	**228**	y=40x-62
193	y=816x-10360	**229**	y=290.2x-3607.4
194	y=905.8x-11662	**230**	y=345x-4202.3

231	y=352.4x-4310
232	y=399x-4991.4
233	y=225.2x-2629.2
234	y = 412.94x - 5188.3
235	y=508x-6401.2
236	y=357.6x-4295.3
237	y=306.2x-3473
238	y=333.22x - 3855.2
239	y=387.2x-4465.5
240	y=499.6x-6365.3
241	y=475.6x-5828.3
242	y=323.2x-3790.7
243	y=404.84x - 4930.2

Appendix I: Daily regression modelled for *Picea mariana* at Pauciflora fen.

Appendix II

POPLAR *Larix laricina*			
DOY	Daily Regression Model	**DOY**	Daily Regression Model
159	y = 362.92x - 680.73	**195**	y = 278.9x + 2342.6
160	y = 347.26x - 953.35	**196**	y = 199.79x + 2656.9
161	y = 347.26x - 953.35	**197**	y = 319.08x + 1675.9
162	y = 483.92x - 1271.6	**198**	y = 251.06x + 2471.7
163	y = 196.42x - 764.74	**199**	y = 212.98x + 2791
164	y = 309.66x - 933.45	**200**	y = 343.04x + 1332.8
165	y = 340.52x - 875.82	**201**	y = -1051x + 20891
166	y = 355.18x - 1033.9	**202**	y = -1286.8x + 23987
167	y = 336.01x - 886.99	**203**	y = -1933.7x + 33444
168	y = 383.26x - 1203.9	**204**	y = -1331.3x + 24494
169	y = 352.31x - 921.99	**205**	y = -927.08x + 18282
170	y = 357.93x - 1006.2	**206**	y = -1220.9x + 23260
171	y = 361.18x - 989.02	**207**	y = -1404.1x + 25823
172	y = 405.2x - 1319.8	**208**	y = -1259.1x + 23413
173	y = 285.57x - 376.31	**209**	y = -1259.1x + 23413
174	y = 411.29x - 1099.1	**210**	y = -1236.1x + 23185
175	y = 252.03x - 154.77	**211**	y = -1529.8x + 27023
176	y = 201.33x + 76.43	**212**	y = -1689x + 29580
177	y = 246.57x - 63.542	**213**	y = -792.35x + 15955
178	y = 235.61x - 31.037	**214**	y = 262.9x - 614.11
179	y = 219.74x + 29.426	**215**	y = 65.72x + 1367.8
180	y = 180.26x + 352.35	**216**	y = 177.63x + 128.52
181	y = 167.01x + 553.6	**217**	y = 96.222x + 756.23
182	y = 195.36x + 285.72	**218**	y = 224.7x - 828.64
183	y = 245.12x + 55.294	**219**	y = 324.95x - 1979.7
184	y = 211.15x + 301.47	**220**	y = 227.53x - 808.95
185	y = 236.06x + 55.97	**221**	y = 297.09x - 1657.8
186	y = 292.3x + 1137.5	**222**	y = 250.94x - 1059.1
187	y = 246.44x + 1983.8	**223**	y = 247.87x - 895.64
188	y = 310.52x + 1001.4	**224**	y = 157.81x - 65.933
189	y = 288.77x + 1154.3	**225**	y = 226.1x - 690.11
190	y = 357.12x + 310.59	**226**	y = 182.15x - 297.37
191	y = 297.92x + 1047.5	**227**	y = 137.61x + 141.19
192	y = 276.47x + 1889.8	**228**	y = 149.62x - 601.87
193	y = 259x + 2717.9	**229**	y = 281.32x - 2547
194	y = 266.35x + 2221.5	**230**	y = 218.71x - 1895.2

231	y = 264.82x - 2514.7
232	y = 254.95x - 2319
233	y = 201.13x - 1869

Appendix II: Daily regression modelled for *Larix laricina* at Poplar fen.

Appendix III

POPLAR *Picea mariana*			
DOY	Daily Regression Model	**DOY**	Daily Regression Model
159	y = 362.92x - 680.73	**195**	y = 278.9x + 2342.6
160	y = 347.26x - 953.35	**196**	y = 199.79x + 2656.9
161	y = 347.26x - 953.35	**197**	y = 319.08x + 1675.9
162	y = 483.92x - 1271.6	**198**	y = 251.06x + 2471.7
163	y = 196.42x - 764.74	**199**	y = 212.98x + 2791
164	y = 309.66x - 933.45	**200**	y = 343.04x + 1332.8
165	y = 340.52x - 875.82	**201**	y = -1051x + 20891
166	y = 355.18x - 1033.9	**202**	y = -1286.8x + 23987
167	y = 336.01x - 886.99	**203**	y = -1933.7x + 33444
168	y = 383.26x - 1203.9	**204**	y = -1331.3x + 24494
169	y = 352.31x - 921.99	**205**	y = -927.08x + 18282
170	y = 357.93x - 1006.2	**206**	y = -1220.9x + 23260
171	y = 361.18x - 989.02	**207**	y = -1404.1x + 25823
172	y = 405.2x - 1319.8	**208**	y = -1259.1x + 23413
173	y = 285.57x - 376.31	**209**	y = -1259.1x + 23413
174	y = 411.29x - 1099.1	**210**	y = -1236.1x + 23185
175	y = 252.03x - 154.77	**211**	y = -1529.8x + 27023
176	y = 201.33x + 76.43	**212**	y = -1689x + 29580
177	y = 246.57x - 63.542	**213**	y = -792.35x + 15955
178	y = 235.61x - 31.037	**214**	y = 262.9x - 614.11
179	y = 219.74x + 29.426	**215**	y = 65.72x + 1367.8
180	y = 180.26x + 352.35	**216**	y = 177.63x + 128.52
181	y = 167.01x + 553.6	**217**	y = 96.222x + 756.23
182	y = 195.36x + 285.72	**218**	y = 224.7x - 828.64
183	y = 245.12x + 55.294	**219**	y = 324.95x - 1979.7
184	y = 211.15x + 301.47	**220**	y = 227.53x - 808.95
185	y = 236.06x + 55.97	**221**	y = 297.09x - 1657.8
186	y = 292.3x + 1137.5	**222**	y = 250.94x - 1059.1
187	y = 246.44x + 1983.8	**223**	y = 247.87x - 895.64
188	y = 310.52x + 1001.4	**224**	y = 157.81x - 65.933
189	y = 288.77x + 1154.3	**225**	y = 226.1x - 690.11
190	y = 357.12x + 310.59	**226**	y = 182.15x - 297.37
191	y = 297.92x + 1047.5	**227**	y = 137.61x + 141.19
192	y = 276.47x + 1889.8	**228**	y = 149.62x - 601.87
193	y = 259x + 2717.9	**229**	y = 281.32x - 2547
194	y = 266.35x + 2221.5	**230**	y = 218.71x - 1895.2

231	y = 264.82x - 2514.7
232	y = 254.95x - 2319
233	y = 201.13x - 1869

Appendix III: Daily regression modelled for *Picea mariana* at Poplar fen.

Appendix IV

Fen	Parameter	Equation
		= √(2/Mσ)^(*w*ˈ*c*ˈ) M represents the number of independent measurements of *w*ˈ*c*ˈ
PFLORA	**EC**	= √(2/3670)^(0.0842)
POPLAR	**EC**	= √92/2194)^(0.0657)

Method	Parameter	Error Percent (%)	Mean Error (%)	Root Mean Square Error	Reference
SHB	Measurement resolution	10.0	17.0	4.1	Groot and King, 1992 Shackel *et al.*, 1992 Grime *et al*., 1995 Perämäki *et al*., 2001
	Steady-state Assumption	30.0			
	Heat Storage	10.0			
Chamber	Reduced *Q**	10.0	6.7	3.0	Reicosky *et al*., 1983 McLeod *et al*., 2004 Hamel *et al*., 2015
		10.0			

Appendix IV: Specific equations used to determine error for each parameter